Soft soil reinforcement by rigid vertical inclusions : numerical modeling under static and dynamic loading

Amar Alyaman

Université de Lille

THÈSE DE DOCTORAT DE L'UNIVERSITÉ DE LILLE

École doctorale n°632 : Sciences de l'Ingénierie et des Systèmes – ENGSYS

Laboratoire de Génie Civil et Géo-Environnement – LGCgE ULR4515

'Renforcement des sols compressibles par inclusions rigides verticales - Modélisation numérique du comportement sous sollicitation statique et dynamique'

'Soft soil reinforcement by rigid vertical inclusions - Numerical modeling under static and dynamic loading'

Thèse soutenue publiquement le **26/10/2023**, par

Amar ALYAMAN

pour obtenir le grade de
DOCTEUR en Génie Civil de L'UNIVERSITE DE LILLE

Devant le jury composé de :

LOPEZ-CABALLERO Fernando, Professeur, Université Paris Saclay, ENS	Président
BREUL Pierre, Professeur, Université Clermont Auvergne	Rapporteur
FAHJAN Yasin, Professeur, Istanbul Technical University	Rapporteur
ROSIN-PAUMIER Sandrine, Maitresse de conférences, université de Lorraine	Examinatrice
MROUEH Hussein, Professeur, Université de Lille	Directeur de thèse
DIAS Daniel, Professeur, Université Grenoble Alpes	Co-directeur de thèse
SADEK Marwan, Maitre de conférences, Université de Lille	Membre invité
ANTOINET Eric, Directeur technique, Antea Group	Membre invité

Laboratoire de Génie Civil et géo-Environnement

ABSTRACT

This work examines the seismic performance of soils reinforced with rigid inclusions, considering the soil-mattress-inclusion interaction. The analysis consists of 3D numerical modelling using the finite element method with Aster code and the finite difference method with Flac3D code. The study is divided into four chapters.

The first chapter outlines the context and objectives of this thesis.

The second chapter presents a literature review on the behaviour of rigid inclusions in seismic zones. It first provides an overview of the reinforcement technology and applications of rigid inclusion. Then it presents different approaches used to analyse soil-structure interaction under seismic loading, including a comparison between pile groups and rigid inclusions in analysing soil-structure interaction under seismic loading.

Moving on, chapter three delves into an analysis of the various models for rigid inclusion modelling. Following this analysis, we employed the most suitable approach to study the kinematic interaction of the soil-mattress-inclusion system using a three-dimensional model of 25 inclusions. This investigation explores the impact of various parameters like the mattress and soil properties, length and diameter of inclusions, and their location on the system's response.

The fourth chapter examines the impact of soil non-linearities, mattress non-linearities, and the combined effects of both on system response. Additionally, it analyses the effect of raft foundations on the response. The chapter scrutinises the impact of various parameters, including the cover ratio and the overload applied on the raft. A three-dimensional numerical model employing the finite difference method was developed for this purpose. The chapter also focuses on the impact of various parameters, including the cover ratio and the overload applied on the raft.

Keywords: rigid inclusion; numerical modelling; dynamic analysis; kinematic interaction; Inertial interaction.

RESUME

Ce travail examine le comportement sismique des sols renforcés par des inclusions rigides, en tenant compte de l'interaction sol-matelas-inclusion. L'analyse consiste en une modélisation numérique 3D utilisant la méthode des éléments finis avec le code Aster et la méthode des différences finies avec le code Flac3D. L'étude est divisée en quatre chapitres.

Le premier chapitre présente le contexte et les objectifs de cette thèse.

Le deuxième chapitre présente une synthèse bibliographique sur le comportement des inclusions rigides dans les zones sismiques. Il donne d'abord un aperçu de la technologie de renforcement et des applications des inclusions rigides. Ensuite, il présente différentes approches utilisées pour analyser l'interaction sol-structure sous charge sismique, y compris une comparaison entre les groupes de pieux et les inclusions rigides dans l'analyse de l'interaction sol-structure sous charge sismique.

Le chapitre 3 analyse les différents modèles de modélisation des inclusions rigides. Suite à cette analyse, nous avons utilisé l'approche la plus appropriée pour étudier l'interaction cinématique du système sol-matelas-inclusion à l'aide d'un modèle tridimensionnel de 25 inclusions. Cette étude explore l'impact de divers paramètres tels que les propriétés du matelas et du sol, la longueur et le diamètre des inclusions, et leur emplacement sur la réponse du système.

Le quatrième chapitre examine l'impact des non-linéarités du sol, des non-linéarités du matelas et des effets combinés des deux sur la réponse du système. De plus, il analyse l'effet des fondations des radier sur la réponse. Le chapitre examine l'impact de divers paramètres, y compris le taux de couverture et la surcharge appliquée sur le radier. Un modèle numérique tridimensionnel utilisant la méthode des différences finies a été développé à cette fin. Le chapitre se concentre également sur l'impact de divers paramètres, notamment le taux de couverture et la surcharge appliquée sur le radier.

Mots-clés : inclusion rigide; modélisation numérique; analyse dynamique; interaction cinématique ; interaction inertielle.

ACKNOWLEDGEMENTS

I take advantage of this page to place a definitive end to this manuscript and to my student journey, and to express my gratitude to everyone who has helped, guided, and encouraged me throughout these three years of doctoral research.

This CIFRE thesis was carried out in collaboration between the Civil Engineering and Geo-Environment Laboratory at the University of Lille and the company “Antea Group”. This PHD takes part in the French National Project ASIRI+ (Amélioration des Sols par Inclusions Rigides).

First and foremost, I want to express my gratitude to Hussein MROUEH and Daniel DIAS, my thesis supervisors, who have given me the exceptional opportunity to work under their guidance. Their deep expertise, enthusiasm for research, and genuine commitment to seeing every student succeed have turned this experience into a truly enriching learning journey. I would like to thank Eric ANTOINET for providing me with the opportunity to carry out this thesis, for his demonstrated confidence in my abilities, and for his consistent encouragement and continuous support.

I extend my sincere gratitude and profound appreciation to my co-supervisors Marwan SADEK and Fernando LOPEZ CABALLERO for guiding my journey throughout this work. Their advice, encouragement, and the welcoming atmosphere of Fernando's team at the University of Paris Saclay have provided me with invaluable and essential support. And the moral support from Marwan, which aided me in surmounting the obstacles of my PhD, will remain etched in my memory. Thank you for your availability whenever I reached out for help.

I want to express my gratitude to Professor Yasin FAHJAN of Istanbul Technical University and Professor Pierre BREUL of the University of Clermont Auvergne for graciously agreeing to be the reviewers of this work.

I would also like to extend my thanks to Madame Sandrine ROSIN from the University of Lorraine for accepting to be a part of my thesis committee.

I wish to express my warm thanks to all my colleagues at Antea Group, LGCgE and LMPS laboratories, for contributing to a great working atmosphere and for the countless enjoyable moments we've had together. I am equally appreciative of my friends from different backgrounds, whose support, assistance, and presence have contributed to the culmination of this work.

I want to express my profound appreciation and endless love to my family, for standing by my side throughout the journey, offering unconditional support and love.

I sincerely express my gratitude to Ibrahim. His unconditional support, love and constant motivation have brought me the serenity, patience, and inner peace necessary for the successful completion of this PhD journey.

And as they say, the best should be saved for last. These expressions of gratitude would be incomplete without a special mention of my first and greatest supporter: my mother. Her presence and encouragement have made me the person who I am today.

My final thanks go to the spirit of my father, who did everything to assist me, who stood by me, and above all, supported me through all circumstances and in everything I undertook. I dedicate my thesis to them.

TABLE OF CONTENTS

LIST OF FIGURES

LIST OF TABLES

CHAPTER 1: INTRODUCTION AND PROBLEM STATEMENT

1.1 General Introduction

Civil engineers have to face a considerable challenge when building embankments and structures on weak compressible soils. Such soils are typically identified by their low bearing capacity, high void ratios, high saturation, and consolidation settlements. The application of external loads can lead to excessive total settlements, differential displacements (foundation rotations), large lateral movements, and slope instability, resulting in damage to the structures. Various techniques have been developed to confront these problems, including preloading and vertical drains, geosynthetic reinforcement, compaction, soil replacement, and the use of lightweight materials. One of them, which is a widely used methods for improving compressible soils is the use of vertical rigid inclusions. This technique offers various advantages such as versatility, cost-effectiveness, and rapid construction, in addition to its technical efficiency in terms of both bearing capacity and reduction of absolute and differential settlements.

This technique involves installing a network of inclusions throughout the compressible soil to transfer the loads to a rigid layer. A load transfer platform is constructed between the inclusions and the reinforced structure. It facilitates the load transfer to the inclusions by forming arches in the granular soil. This mattress allows for the reduction and homogenization of the surface settlements. A geosynthetic layer could be introduced in the platform, contributing to a load transfer through membrane effects. The various elements of the system interact with various soil/structure interaction phenomena.

The use of rigid inclusions in seismic risk regions presents an interesting concept. In terms of seismic loading, this reinforcement system is equivalent to a base isolation system. The load transfer mattress serves as an energy dissipation zone between the structure and the rigid elements, reducing the inertial effect of the superstructure (Dobry et al., 2003; Garnier and Pecker, 1999; Pecker and Salencon, 1999). This type of reinforcement has been implemented for the Rion-Antirion bridge (Pecker and Teyssandier, 1998), and it differs from the pile foundation method by the presence of the load transfer mattress. The seismic behavior of rigid inclusions involves numerous parameters, including soil behavior, the connection conditions between the inclusions, the mattress, and the soil, loading characteristics, the interaction between inclusions, the interaction between inclusions and the mattress, and finally, the

interaction between the entire soil-mattress-inclusions system and the structure. It should be noted that the loading frequency and the frequencies of the structure and the underlying soil mass influence significantly the seismic forces acting on the system.

Previous researches, particularly the National ASIRI Project (Improvement of Soil by Rigid Inclusions), primarily focused on the behavior of compressible soils reinforced with inclusions and subjected to uniform static loads. Hence, little attention was given to the response of soils reinforced with rigid inclusions under complex cyclic and/or dynamic loading. In practice, structures are frequently subjected to dynamic and cyclic loading events, such as wave loading on offshore structures, wind loading on buildings, loading, and unloading of storage tanks, and earthquakes.

For this reason, the new ASIRI+ project aims to study the response of soils reinforced with rigid inclusions under complex cyclic and/or dynamic loading (inertial and kinematic effects). This thesis is part of this project which aims to establish new recommendations concerning this subject.

This thesis represents a contribution to the behavior study of rigid inclusion systems under dynamic loadings and proposes a comprehensive analysis of the problem, performing three-dimensional numerical modeling using finite elements and finite differences, which integrates the soil, inclusions, load transfer platform, and structure. Such a modeling approach allowed to investigate specific aspects of the problem, including the grouping effect, kinematic interaction, inertial interaction, and the influence of different parameters.

1.2 Objectives and motivations

The new ASIRI+ project, comprising a "PN Project" (ASIRI+) and an "ANR Project", is part of a global approach to adapt the land use planning to the requirements of sustainable development. It aims to study the behavior of soft soil reinforced by RI subjected to seismic loadings (inertial and kinematic effects). The project brings together companies and research centers. “Antea Group” is one of the organizations participating in this initiative.

This thesis is conducted under a CIFRE contract, with “Antea Group” to meet the requirements of the project which was elaborated around three main axes. Axis 1, concern the study of load transfer platforms, Axis 2, present the behavior of structures under quasi-static and inclined loads, and Axis 3, study the behavior of structures under dynamic and seismic loads. This thesis is part of the third axis, and the primary objectives of this work are to investigate the seismic behavior of the rigid inclusion system and to evaluate the effects of the different interactions and the different parameters on the system response using three-dimensional numerical models.

More precisely, this research was concentrated on:

- Adopting the direct method, where the entire three-dimensional soil-rigid inclusion systems is modeled with a representation of all the geometrical complexity, the connection between elements, and material properties,
- Evaluating the effect of kinematic interaction due to soil deformation under seismic loading,
- Studying the impact of different rigid inclusions modeling techniques, such as hybrid, linear and volumetric elements on the response of the reinforcement system,
- Evaluating the influence of parameters such as the diameter, depth, and position of inclusions, as well as the mechanical properties of the soil and mattress, and particularly their stiffness,
- Examining the nonlinearity influence using the elastic perfectly plastic model considering the Mohr-Coulomb shear failure criteria for the mattress, the soil and for both, as well as a raft foundation influence on the seismic response of the analyzed system,
- Analyzing the effect of different surcharges, as well as investigating the pile cover ratio impact on the system's response.

1.3 Outline of the thesis

After an introduction of the considered problem, and presenting the motivations and objectives, chapter 2 comprises a literature review of the studies conducted on rigid inclusions and the analysis of their behavior under seismic loadings. The chapter begins by introducing the rigid inclusions reinforcement technology, along with its usage then it proceeds with an overview of the different approaches used for analyzing the soil structure interaction under seismic loadings. Previous studies on the seismic behavior of rigid inclusions are also highlighted after presenting the dynamic behavior of different elements constituting the system.

Chapter 3 focuses on analyzing the kinematic interaction of the soil-rigid inclusion system. A comprehensive approach is used to calculate the response of all the system elements subjected to seismic loadings. This is achieved through a three-dimensional modeling of the reinforcement system using the Finite Element Method. The chapter is divided into three parts. The first part presents various methods for modeling the rigid inclusions, while the second part discusses the numerical model used and includes an analysis of a soil reinforced by a group of 5x5 rigid inclusions. And the third part presents a parametric study that aims to investigate the influence of key parameters on the seismic response of the rigid inclusion group.

Chapter 4 focuses on conducting an analysis using the linear elastic-perfectly plastic constitutive model, which incorporates the Mohr-Coulomb shear failure criterion, utilizing the Finite Difference Method (FDM). The chapter is divided into three parts. The first part discusses the numerical model used, the second part presents the model of the soil reinforced with a group of 3x3 rigid inclusions, and the last part focuses on studying the implications of incorporating the Mohr-Coulomb criterion in both the mattress and the soil, as well as individually in each component, while also examining the influence of a raft foundation on the seismic response of the group. Furthermore, the chapter explores the effects of overload and the cover ratio on the system's response.

CHAPTER 2: LITERATURE REVIEW

2.1 Introduction

This chapter includes a literature review of studies conducted on rigid inclusions and the analysis of their behavior under seismic loadings. The chapter is divided into two main parts, the first presents the rigid inclusions reinforcement technology, along with its application. The second part present an overview of the different approaches used for analyzing the soil structure interaction under seismic loadings including previous studies on the seismic behavior of rigid inclusions and pile systems.

2.2 Rigid Inclusion System

2.2.1 Principle and behavior

The principle of soil reinforcement using rigid inclusions is depicted in (**Erreur ! Source du renvoi introuvable.**). By inserting rigid inclusions into the compressible soil, the loads caused by the weight of the structure can be transferred to the bedrock via the development of peak and frictional forces along the inclusions. Additionally, slabs can be placed at the inclusion heads to increase the load-bearing surface area.

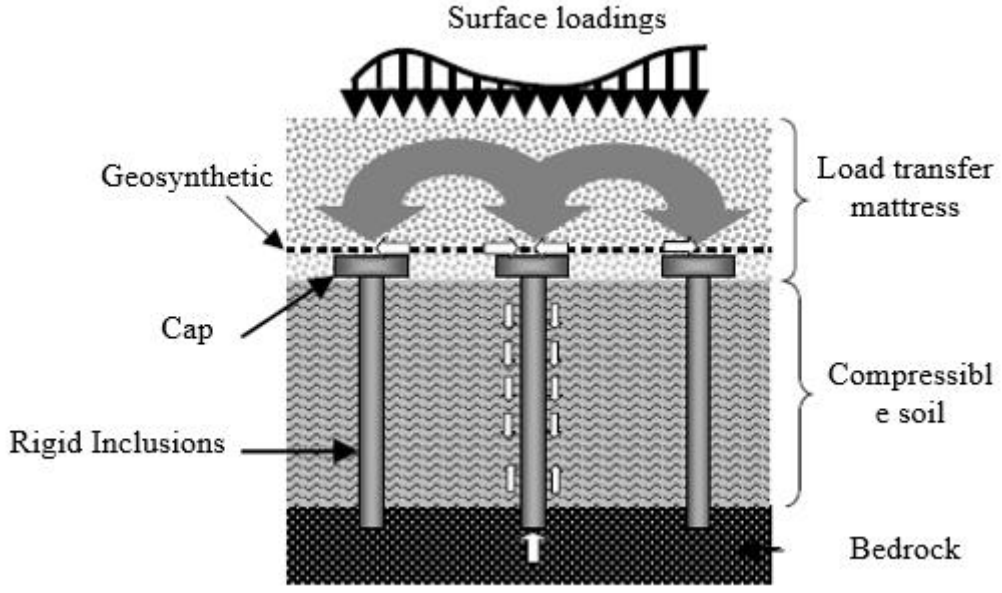

Figure 2.1: Rigid inclusion system

A load transfer platform (LTP) is positioned between the structure and the heads of the rigid

inclusions. This mattress facilitates the distribution of the load applied to the inclusion heads, which in turn reduces and homogenizes settlements under the structure through the development of shear mechanisms. The load transfer mattress can be made of either treated or untreated materials, and its mechanical and geometrical characteristics play a crucial role in the load transfer mechanisms. In addition, horizontal reinforcement layers can be placed above the rigid inclusions to enhance the load transfer towards the inclusion heads. Due to the differential settlement between the inclusion heads and the compressible soil, the reinforcement layer is put under tension and contributes to the load transfer through a membrane effect (Han and Gabr, 2002).

Unlike the pile foundation method, the soil reinforcement technique with rigid inclusions does not require a direct connection between the inclusions and the slab foundation, as shown in (Figure 2.2). This approach offers several advantages, including reduced construction time and costs, increased design flexibility, and improved load transfer mechanisms.

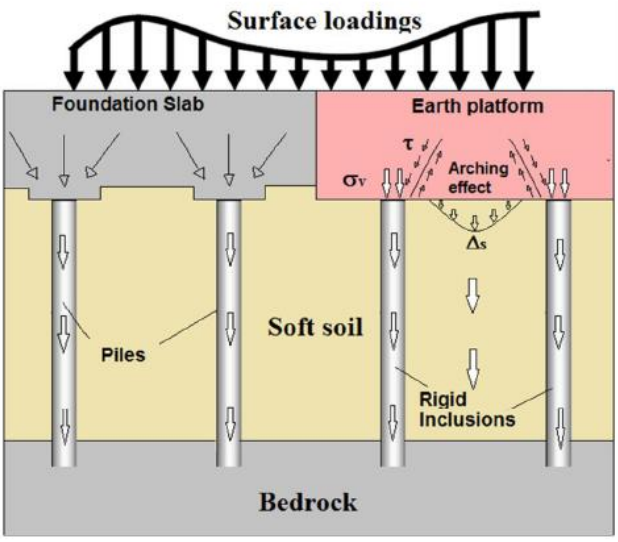

Figure 2.2:Transfer of load in the soil-inclusion-platform-structure system (Briançon et al., 2004; Deb, 2010)

The load transfer mechanisms in the reinforcement system rely on the mobilization of shear forces and frictional forces along the rigid inclusions and the load transfer mattress. The development of shear mechanisms in the mattress facilitates load transfer towards the inclusion heads by promoting arching effects. Meanwhile, the friction along the inclusions also contributes to the load transfer process. Specifically, the upper part of the inclusions is mobilized by negative friction induced by the relative displacement between the ground and the inclusion heads, whereas the lower part experiences positive friction (Berthelot et al., 2003).

The load transfer efficiency is influenced by various factors, including the surcharge, platform thickness, mechanical properties of the load transfer platform, compressibility of the underlying soft soil, and configuration of the rigid inclusion group. Therefore, it is essential to carefully consider these factors during the design and construction of the reinforcement system to ensure optimal load transfer performance. (Figure 2.3) provides an illustration of the load transfer mechanisms in soil reinforced by rigid inclusions subject to negative and positive friction.

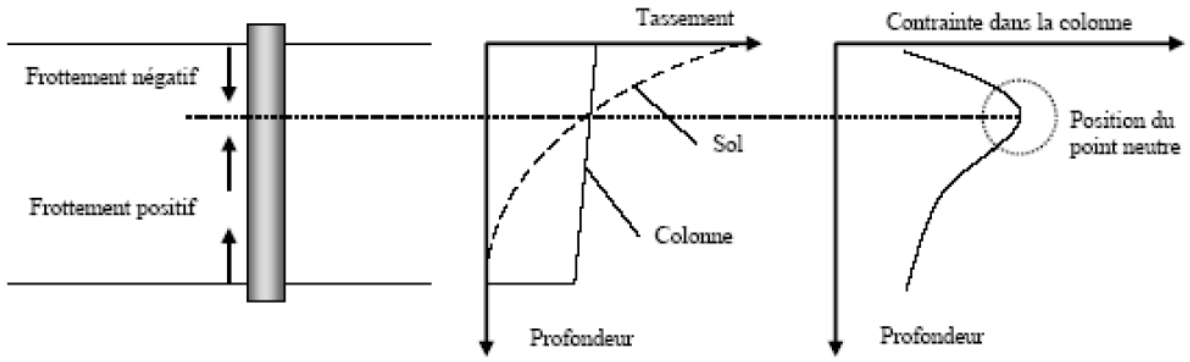

Figure 2.3 :load transfer mechanism (Berthelot et al., 2003)

2.2.2 Rigid inclusion

There are various types of rigid inclusions that can be used depending on the mechanical properties and geometry of the compressible layer. These inclusions can either be prefabricated or made in situ. The deformation modulus of these inclusions can vary greatly, ranging from 20 MPa for soil mixing columns to 200 GPa for metallic piles.

Prefabricated inclusions refer to various types of piles that are driven into the ground without any prior excavation. These piles can be constructed using wood, concrete, or steel, and can be solid or hollow in shape. The speed of pile installation in the ground, the use of manufactured materials, and the controlled material and geometry of their section are the main advantages of using prefabricated piles. Regarding the disadvantages of this technique, the installation process may generate noise or vibrations, and the lateral displacement of soil during installation can potentially affect nearby structures.

There are several types of piles constructed in situ, including drilled piles, cased driven piles (reinforced concrete piles), Vibro Concrete Columns (VCC), Controlled Modulus Columns (CMC), (Liausu and Pezot, 2001), and soil mixing techniques such as jet grouting, Lime Cement Columns, etc (Balfour, 2013). The implementation of these inclusions is described by (Briançon, 2002; Kempfert, 2003). In situ inclusions have more flexibility compared to

prefabricated inclusions, with less soil displacement and a length that can adapt to the geological horizons of the site. Generally, inclusions are constructed until they reach a more rigid substratum, onto which they can rest or be anchored.

2.2.3 Load Transfer Platform

The load transfer platform (LTP), also referred to as an earth platform or mattress, is responsible for facilitating the transfer of loads from the surface to the rigid inclusions. This helps to concentrate the loads on the inclusions, resulting in a reduction and equalization of surface settlements through the arching effect. Consequently, the platform is instrumental in minimizing stress on the system, promoting its durability and proper functioning. The phenomenon of arching in granular soils was first described by (Terzaghi, 1943). Nonetheless, as highlighted by (Briançon et al., 2004), the design methods for load transfer platforms differ significantly. Load transfer platforms are typically composed of a single layer of compacted granular material or materials treated with lime or cement to enhance their mechanical properties (Dano et al., 2004). Alternatively, they may consist of a layer of soil reinforced with horizontal geosynthetic layers.

2.2.4 Reinforcement layers

The granular material that constitutes the load transfer mattress can be reinforced to improve its properties. Various types of reinforcements can be implemented. When a single geosynthetic layer is placed on top of the inclusions, it contributes to the reinforcement by the membrane effect. When multiple layers are implemented within the granular mattress, the membrane effect is complemented by a mattress stiffening effect (Briançon, 2002; Collin, 2004). (Figure 2.4) shows the different arrangements of the layer within the mattress. Reinforcement layers are generally made of either geotextiles or geogrids that allow soil interlocking within the layer.

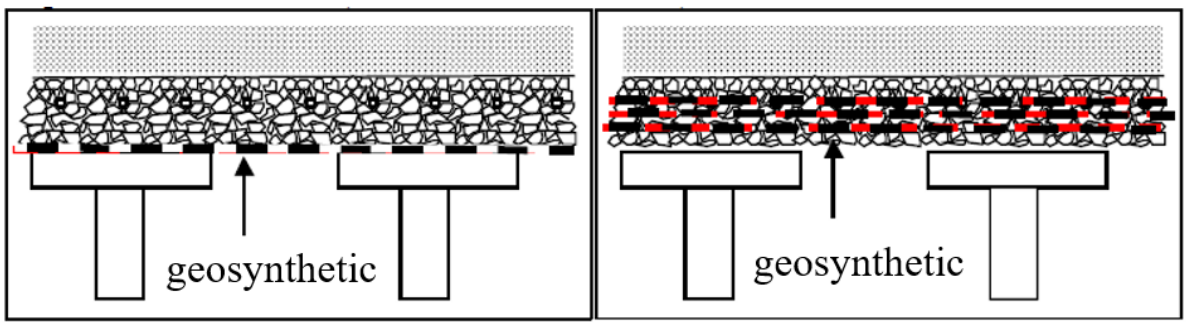

Figure 2.4: Different arrangements of horizontal reinforcement in the load transfer mattress, (Briançon et al., 2004)

2.2.5 Fields of application of the Rigid inclusion Systems

Since the 1970s, the use of vertical rigid inclusions for soil reinforcement has become widespread, particularly in loose soil types like alluvial soils and silts. (Figure 2.5) presents the diverse range of applications for this method, including road and railway embankments (a), access embankments for engineering structures (b), industrial platform foundations (c), and storage tanks (d), among others.

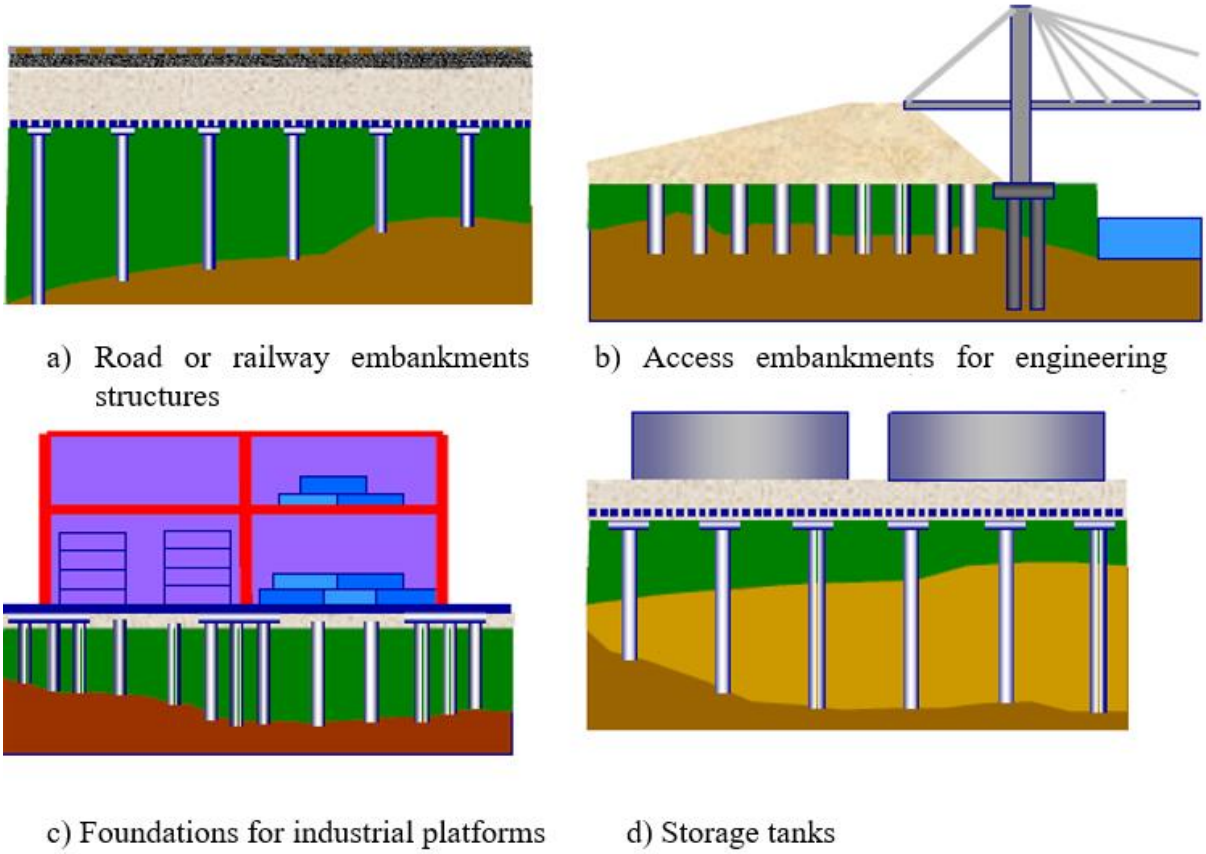

Figure 2.5: Application of Rigid inclusion system

Numerous examples of this technique's application can be found in the literature, within France and abroad. One such example, as shown in (Figure 2.6), is the Rion-Antirion bridge.

Figure 2.6: Soil Reinforcement for an inclusion bridge Rion-Antirion, Greece (Combault and Pecker, 2000).

2.2.6 Comparison of Pile and Rigid Inclusion systems

When dealing with soft soil, the pile foundation technique serves as an effective alternative for supporting structures. The system allows loads from the structure to be carried and transferred to deeper, stiffer soil layers as seen in (Figure 2.7). In instances where tall structures with significant overturning moments are being supported, the pile elements may be required to resist uplift forces. The transfer of surface structure loads to the soil occurs through shearing mechanisms generated along the shaft of the pile (shaft resistance) and normal stresses generated at the base of the pile (base resistance). These two types of pile elements are commonly referred to as floating and end-bearing piles, respectively.

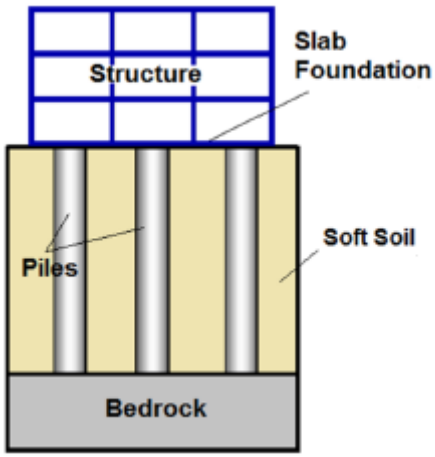

Figure 2.7: Soil pile structure system

The difference between the pile foundation system and the rigid inclusion system lies in the fact that the inclusions are not connected to the slab foundation. Despite this similarity, the behavior of these two systems differs. In the rigid inclusion system, a load transfer platform, is placed

between the compressible layer and the surface structure. The primary advantage of using this reinforcement technique in seismic areas is that the LTP serves as a zone for energy dissipation between the structure and the vertical rigid elements.

2.3 Overview of the Soil Structure Interaction

2.3.1 Concept

Seismic waves during an earthquake result in the deformation of the soil in a soil-foundation-structure system. This deformation is then transferred to the structure, generating inertial forces that create stress at the foundation (Figure 2.8). These stresses are then transmitted to the supporting soil. The soil deposit's characteristics significantly influence the seismic motion experienced at the structure's base. Understanding soil-structure interaction (SSI), is crucial for comprehending the behavior of the system. To understand the behavior of the system, it is essential to study the relative movements and load transfer mechanisms simultaneously.

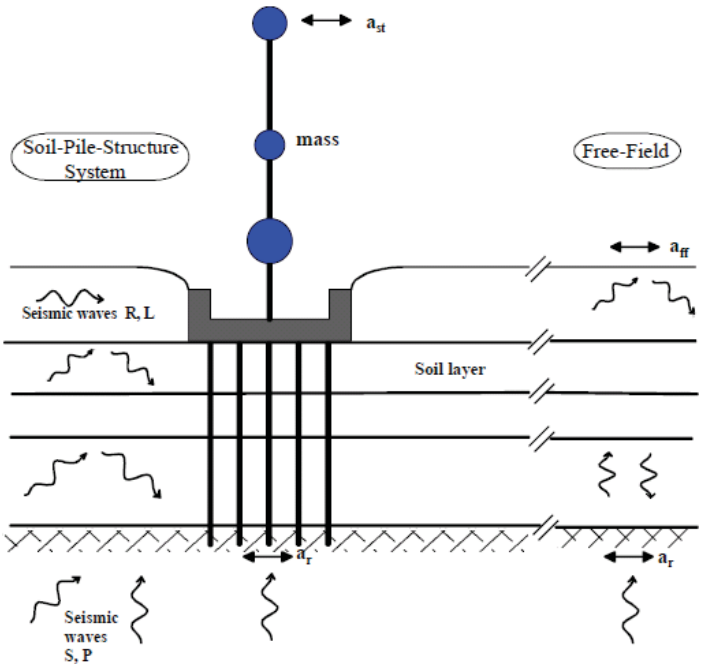

Figure 2.8: Schematic Representation of Soil-Structure Interaction:(Gazetas and Mylonakis, 1998)

Consider two identical structures, one of which is embedded in rock while the other rests on a softer soil. These structures may behave differently under seismic loading. The structure resting on the softer soil, with lower stiffness and lower natural frequencies than the one embedded in rock, may experience more amplified displacements. This indicates that soil properties significantly affect the dynamic behavior of the structure. Conversely, the presence of the

structure may alter the soil behavior, as soil behavior in free field can differ significantly from that in the presence of the structure. The influence of the structure on soil behavior strongly depends on the contrast between their respective stiffness. For example, the structure embedded in rock will have no effect on the behavior of the soil in free field. The stiffness of the rock being infinitely large, the insertion of the structure into the rock has little impact on the stiffness of the soil-structure system. Similarly, the inertial forces generated by the structure have no effect on the very stiff rock.

For structures built on softer soil foundation, we can distinguish between two types of interaction: kinematic interaction and inertial interaction.

- Kinematic interaction arises due to the difference between seismic motion in a free field and that in a field where the excavation and the foundation's inclusion have altered the characteristics. This interaction is entirely caused by the difference in rigidity between the soil and the foundation, which prevents the foundation from following the motions enforced by the soil.

- Inertial interaction arises due to the inertia forces generated by the mass of the structure at its base, and in the soil as a result of the imposed motion on the foundation. The displacement field is also affected by this interaction and not just by the kinematic one.

The interaction of soil and structure is a concurrent process, with both influencing the other at the same time. The soil-structure interaction is caused by both kinematic and inertial interactions. To study the dynamic response of the soil-foundation system under the effect of inertial interaction, a prior kinematic analysis is required to obtain the motion at the base of the structure, which can be used to deduce the inertial forces induced by the superstructure. Several elements impact the behavior of the superstructure, including site parameters, type of loading, soil mechanical properties, and structural and foundation type.

2.3.2 Methods of analysis

To account for the effect of soil-structure interaction, two categories of methods are distinguished: direct methods and substructure methods. These methods are described and detailed in numerous works (Pecker, 1984; Wolf, 1988). In the following, we briefly present each of these types of methods.

2.3.2.1 Substructure method

Unlike direct methods, substructure methods rely on decomposing the global problem into several sub-problems that are simpler to solve before applying the principle of superposition to obtain the overall results. It should be noted that these methods, like any superposition problem, are only applicable to fully linear problems.

The approach, which utilizes the principle of superposition by (Kausel et al., 1978) as illustrated in (Figure 2.9) for the case of rigid foundations, consists of three successive steps.

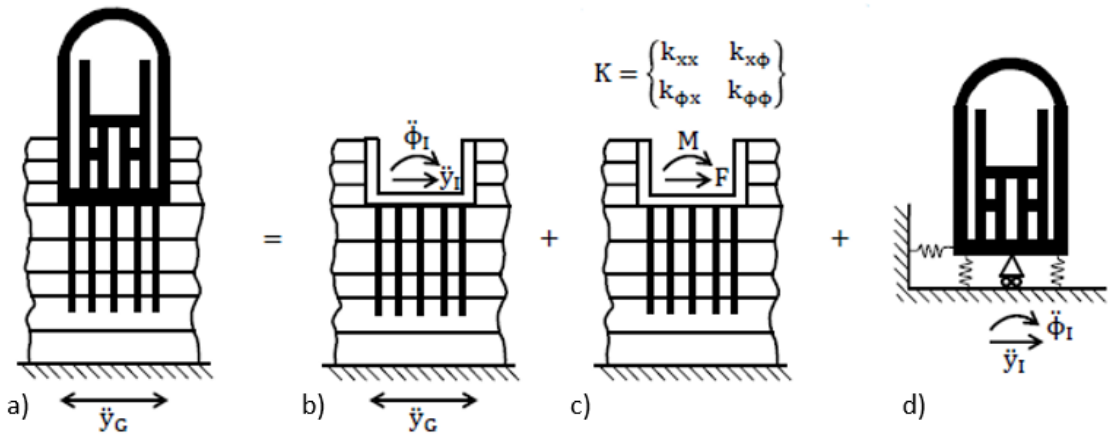

Figure 2.9: Decomposing SSI Problems using Kausel's Superposition Theorem for Structures Supported by Deep Foundations. The SSI problem a) is divided in three steps: b) kinematic interaction, c) dynamic impedances and d) dynamic response considering SSI (modified from*(Kausel et al., 1978)*)

Firstly, a kinematic interaction analysis is carried out, where the substructure consisting of the soil mass and the rigid foundation without mass is considered. The acceleration at the soil-foundation interface is deduced from the seismic motion at the base of the soil mass. In the literature, numerous studies have proposed analytical and numerical methods, including the method of integral equations (Aubry, 1986), to solve this initial problem.

In the second step, an analysis of inertial interaction is carried out to determine the dynamic impedance of the foundation. This impedance characterizes the dynamic forces that act on the rigid foundation without mass when it is subjected to a harmonic excitation of unit amplitude. Complex impedance functions are calculated for each of the six degrees of freedom (three translations and three rotations) of the foundation, and they depend on the frequency of the applied excitation. The real part of the impedance function represents the stiffness of the soil-foundation system, while the imaginary part represents the radiation damping. The literature provides methods and results for determining the dynamic impedance of any type of foundation,

such as those presented in (Gazetas, 1991; Pecker, 1984; Sieffert and Cevaer, 1992).

Next, we proceed to determine the dynamic response of the structure connected to the soil foundation through the impedance springs calculated in the second step, when subjected to the seismic excitation obtained from the first step. The solution of this problem is a conventional approach and commonly employs finite element method.

Several studies have demonstrated that although substructure methods are restricted to linear problems, they provide excellent results (Pitilakis et al., 2008).

2.3.2.2 Direct method

The direct approach involves the modeling and analysis of the complete soil-foundation-structure system accounting for the kinematic and the inertial interaction (Wolf, 1985) in a single step using either time or frequency domain, and it is typically implemented via the finite element method. If solved in the time domain, this technique can incorporate non-linear effects, such as material inelasticity, foundation uplift, and sliding.

The effect of soil pile structure interaction on the structure's behavior using the direct method was studied by several researchers as (Hokmabadi and Fatahi, 2016; Lu et al., 2005; Mánica Malcom et al., 2016; Van Nguyen et al., 2017).
The direct method consists in solving the equation of motion (1) of the soil pile structure system.

$$M.\ddot{u} + C.\dot{u} + K.u = F \qquad (1)$$

Where M, C and K are respectively the mass, damping and stiffness matrices of the system, u is the displacement vector of the system, $\dot{u}$ is its derivative, and F is the load vector applied to the outer boundary of the system.
The direct solution of this system of equations is so complex that the use of numerical methods, such as finite element and finite difference methods, is practically essential.

One of the main advantages of direct methods is their ability to integrate into the numerical model the material heterogeneities of the soil and the structure, the geometrical singularities of the problem, and the constitutive laws well adapted to consider the nonlinearities in the soil or

at the soil-foundation interface of the system. These methods require a more discretization of the soil supporting the foundation to minimize the numerical reflection on the boundary which moves the structure again. The absorbing boundaries can be introduced at the lateral faces of the soil to model the radiation damping which, apart from the internal friction of the materials, dissipates part of the energy of the structure and of the soil, during the propagation of waves towards infinity.

Moreover, the maximum size of the elements is limited to correctly model the propagation of high frequency waves. If a large mesh is employed, it cannot accurately transmit high frequency waves, thereby affecting the accuracy of the results. Consequently, the implementation of these methods remains a generally expensive operation from the numerical point of view, especially for three-dimensional problems.

Various techniques are available for analyzing dynamic soil-pile-structure systems. These include numerical analysis, simplified analytical methods that rely on equivalent soil springs, small-scale tests like the centrifuge and shaking table, as well as full-scale prototypes (Boulanger et al., 1999).

2.3.2.2.1 Analytical methods

In simplified methods for analyzing the behavior of piles, non-linear p-y springs are used to connect the piles to the ground. These methods compute how the piles respond to horizontal ground movement over time, assuming wave propagation in the vertical direction in the free field. The elastic column, p-y, and Winkler approaches are examples of simplified methods. In the Winkler method (Winkler, 1876), a series of unconnected linear springs with stiffness (Es) is used to model the soil as shown in (Figure 2.10), and the behavior of a single pile is analyzed using the equation of an elastic beam supported on an elastic foundation. This equation is represented by the 4th order differential beam bending equation and was first described by (Hetenyi, 1946).

$$E_p I_p \left(\frac{d^4 y}{dx^4}\right) + Q\left(\frac{d^2 y}{dx^2}\right) + E_s(y) = 0 \qquad (2)$$

The equation (2) includes the pile elastic modulus, represented by E_p, the axial load on the pile, represented by Q, and the moment of inertia of the pile's cross section, represented by I_p. Additionally, the equation takes into account the vertical depth, represented by x, and the lateral

deflection of the pile at the specific point x, represented by y.

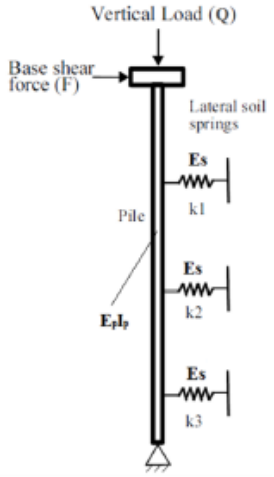

Figure 2.10: Modelling Piles Using the Winkler Approach

The main drawback of this method is the disconnected displacements at each point due to the independent operation of the linear elastic springs.

2.3.2.2.2 Experimental tests

There are two experimental methods commonly used to model soil-structure interaction (SSI) problems under dynamic loading: the shaking table and the centrifuge test.

Shaking table tests involve conducting scale models under gravity force. This approach is well-suited for modeling cohesive soils, which exhibit stress-strain behavior that is independent of the confining pressure. However, a significant drawback of this method is its limited ability to reproduce actual stresses due to the small size of the model used. Additionally, this test is influenced by boundary effects of the testing container, scale modeling techniques, and non-adherence to similitude laws, as noted by (Meymand, 1998).

The centrifuge test is an alternative approach for analyzing soil-foundation-structure problems. This method involves a rotating arm that supports an experimental package fixed to a swivel at one end. By increasing the gravitational force through rotation, the centrifuge test can simulate soil stress-strain conditions similar to those in the actual prototype. This is particularly useful for analyzing cohesionless soils, which exhibit stress-strain behavior that is dependent on the confining pressure. However, some researchers have described challenges associated with this method, such as difficulty in constructing complex prototypes, undesirable vertical motions,

and limited ability to reproduce a range of frequencies similar to those experienced during actual earthquakes (Jakrapiyanun, 2002; Wilson, 1998). Full-scale prototype tests may also be utilized to evaluate the behavior of pile groups under seismic loads (Lu et al., 2004).

2.3.2.2.3 Numerical methods

Due to the development of computing technology, numerical analysis has become a valuable tool in engineering design and research in soil mechanics and geotechnical engineering. Numerical models allow for the description of soil behavior and failure mechanisms, as well as pre-existing stress states, anisotropy, and time-dependent behavior due to creep and plastic deformations. These models can also generate 3D simulations and do dynamic analysis. Incorporating hydraulic processes into soil mechanics analysis poses a significant challenge.

2.3.3 Previous analysis considering SSI under dynamic loading

2.3.3.1 Pile-reinforced system

Extensive literature on the seismic behavior of piles is very beneficial for the analysis of Rigid inclusion in seismic sites. Various studies have shown that the calculation of piles under seismic loading is a very complex problem. This is due to the interaction between soil-pile, pile-pile, pile-cap, pile-cap-soil system with the superstructure and the frequency involved, such as the frequency of the load and its interaction with the frequency of the soil and the frequency of the structure.

A significant number of analytical and numerical studies have been conducted on the seismic behavior of pile (Cai et al., 2000; Kaynia, 1982; Maheshwari et al., 2004; Shahrour et al., 2000). Similarly, piles have been extensively studied experimentally, with the shaking table technique (Dou and Byrne, 1996; Liu and Chen, 1991; Meymand, 1998; Sreerama, 1993), and the centrifuge tests which allow for a closer approximation to field conditions (Barton and Pande, 1982; Boulanger et al., 1999; chang and Kutter, 1998).

Post-earthquake observations and analyses indicate that the interaction between soil, foundation and superstructure plays a decisive role in the seismic damage of piles and structures (Boulanger et al., 1999; Miura, 2002). A synthesis of experimental work carried out on a centrifuge, along with numerical modeling, is very useful in understanding the mechanism of

soil-pile-superstructure interaction. Two important phenomena arise when considering seismic excitation. First, as the soil moves, piles are forced to follow and resist the movement through their rigidity. As a result, wave reflection and diffusion occur, and the pile displacement may differ from the free field one. The second phenomenon is that the movement of the foundation induces vibrations in the superstructure that generate inertial forces. These dynamic forces are transmitted to the piles and the soil in contact with them.

Several authors (Gazetas, 1984; Wu and Finn, 1997) have studied the dynamic behavior of soil-pile-structure interaction. (Chung, 2000) create a 2D and 3D finite element model, to study the effect of inertial interaction on the seismic response of soil-pile-structure. The investigation is centered on the linear viscoelastic response of one and a group of piles, (Figure 2.11) depicts the mesh used for an isolated pile. Several variables have been investigated, including the characteristics of the superstructure and its frequency, the number of piles, the spacing between them, and the distribution of piles within the group. The behavior of soil-pile-structure system is considered linear elastic with Rayleigh damping. The superstructure is represented as a single-degree-of-freedom system consisting of a mass concentrated at the head of a column. The results show that 2D modeling ensures the rigidity of the soil-pile system, indicating the need for tridimensional modeling to properly handle the soil-pile-structure interaction under seismic loading.

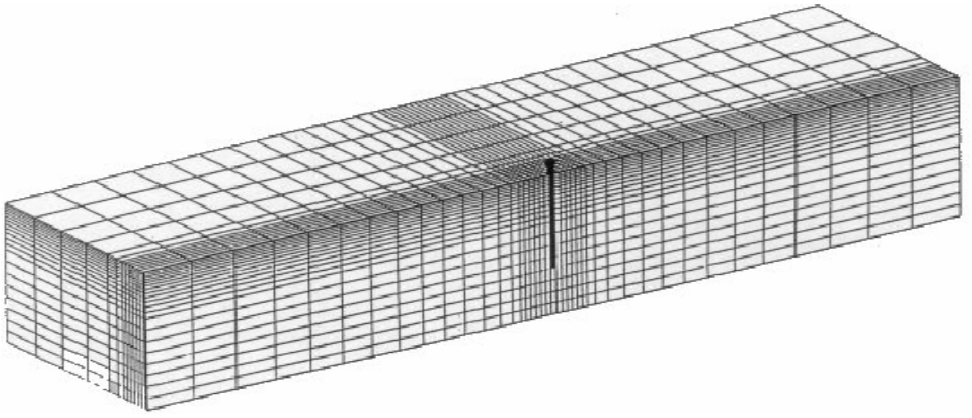

Figure 2.11: Meshing approach for investigating the inertial response of an isolated pile, as proposed by (Chung, 2000)

Other authors used numerical models to study the interaction considering one single pile. (Rovithis et al., 2009) investigated the seismic response of a single-pile, one-degree-of-freedom structure resting on a viscoelastic soil layer supported by a stiff rock (Figure 2.12). The researchers determined that flexible and slender piles experience substantial bending moments

on their upper part as a result of structural vibrations. In contrast, the kinematic interaction dominates the pile bending moment at great depths with short and rigid piles.

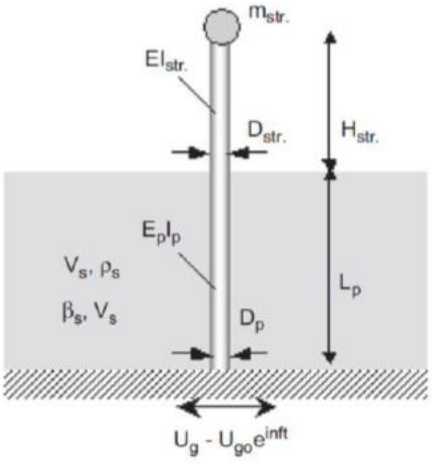

Figure 2.12: Characteristic of the soil-pile-structure considered in(Rovithis et al., 2009) study

(Chu and Truman, 2004) studied the seismic response of a soil-pile model using a 3D finite element method and various pile configurations. Soft clay was considered with a Young's modulus of 20 MPa and a Poisson's ratio of 0.3. The soil nonlinearity was investigated using the Drucker-Prager soil plasticity model. To illustrate the piles, volumetric elements were used. The model was validated using experimental data and current numerical analysis results. The study highlighted that soil characteristics have a significant impact on pile head response (acceleration and displacement).

To study the effect of foundation type and size on the seismic response of mid-rise buildings, a 3D finite element numerical model was created (Van Nguyen et al., 2017) for a 15-story moment-resisting frame building that is supported by both end bearing and floating pile foundations (Figure 2.13). Interface elements between soil and pile were considered. The soil is a soft clayey soil with a unit weight of 14.42 kN/m³, a shear velocity of 150 m/s and an undrained shear strength of 50 kPa. An equivalent linear method was used. Pile elements were modeled using volumetric elements. The results of the study revealed that the lateral deflection of the structure is made up of two factors, the rocking, and the structural distortion. Support mechanisms impact the way shear forces are absorbed by the structure and distributed along the pile elements.

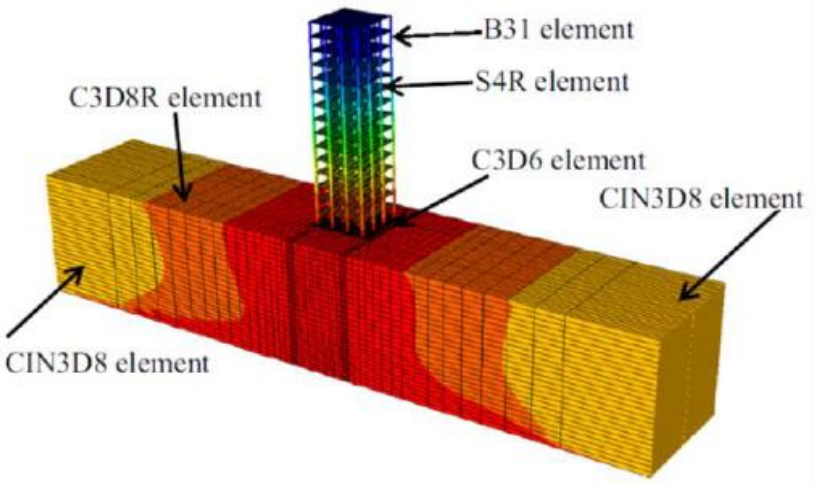

Figure 2.13: Soil-pile-structure 3D models (Van Nguyen et al., 2017)

Another study was done by (Nghiem and Nien-Yin, 2008) to evaluate the seismic response of a 33-story building using a 3D finite element system. The different elements of the system: pile, soil, and cap were modeled using volumetric elements. The building is supported by sandy clay soil. It is assumed that the soil behaves in a linear elastic perfectly plastic way with the Mohr-Coulomb failure criterion. To explore the changes in soil-structure interaction (SSI) effects, two types of analysis were conducted: one assuming a rigid base soil, and the other assuming a flexible base soil. The results indicated that the shearing of the flexible base is less than that of the rigid base it also revealed that the shape irregularity of the building has a notable effect on the top deflection of the building.

(Sadek, 2003) discovered that embedding vertical micropiles in a hard bedrock promotes dynamic amplification in a 2x2 micropile group supporting a superstructure. The embedding causes large loads at the pile heads and at the embedding level in the stiff layer. This suggests that the embedment zone is a key zone in shear and bending.

2.3.3.2 Rigid inclusion system

Even though there are no real failure cases of rigid inclusions, studies have shown that these elements are vulnerable to damage and failure, like pile elements except the failure mechanism due to the connection with the slab foundation. Hence the need to understand their behavior under seismic loading. Their behavior specially the kinematic effect appears to be identical to that of piles. The difference in their behavior under seismic loading is due to the inertial effect. Inertial forces are transmitted to the piles through the embedded heads. However, in the case of

rigid inclusions the inertial forces are transmitted through the load transfer mattress. Due to the energy dissipation that took place between the structure and the rigid elements, their heads experience a decrease in the actual dynamic load applied to them. Numerous studies have been done aiming to understand the seismic behavior of the complex rigid inclusion system.

(Mayoral, 2006) used a two-dimensional model to analyze the dynamic response of a single inclusion embedded in a soil mass exposed to geotechnical conditions in Mexico City. They discovered that the existence of LTP and inclusion reinforcement is mostly responsible for the decrease in surface acceleration. Another study using 2D finite element numerical model was created by (Rangel-Núñez et al., 2008) on a soft soil (typical clay of Mexico City) deposit reinforced with a group of rigid inclusions, to investigate its seismic response taking into account the rigid inclusion's construction stages and various types of fixity conditions. The soil is modeled as a linear elastic material without considering the water table. The study also examined the formulation of Rayleigh damping. The inclusions were modeled using linear beams. The findings revealed that the pile support conditions had a significant impact on the dynamic response. (Mánica Malcom et al., 2016) investigated how inclusions embedded in Mexico City's soft clay layers affect seismic ground response (Figure 2.14). Soil was simulated using a linear elastic constitutive model. To account for energy dissipation, Rayleigh damping was used. The inclusions were represented by solid zones. It was demonstrated by the results that the dynamic characteristic of the structure has a significant effect on the system's ground response. This response varies slightly due to support conditions, inclusion length, and inclusion spacing. Shear forces and bending moments in inclusions rise in zones where soil stiffness varies significantly.

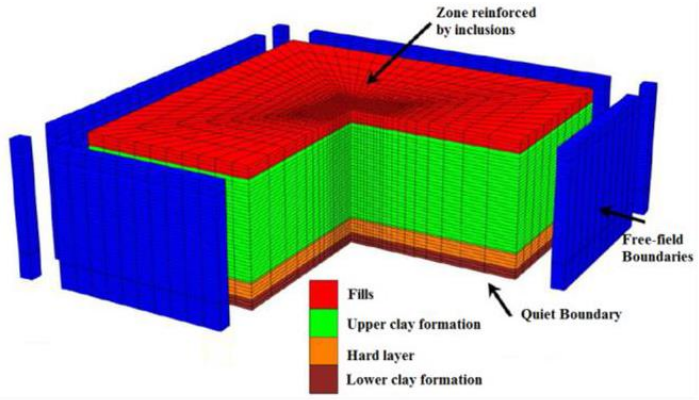

Figure 2.14 : Rigid inclusion system, (Mánica Malcom et al., 2016)

In (Hatem, 2009) thesis, a 3D numerical model study was conducted on the kinematic effect and the coupling of kinematic and inertial effects in the soil reinforced by rigid inclusion with the granular mattress. A group of four inclusions (2x2) resting on a stiff clay layer has been modelled. A footing is embedded in the granulated mattress. The parameters of the soft soil (Young modulus of 6 MPa, Poisson's ratio of 0.3, and density of 1700 kg/m3). The soil behavior is considered to be linear-elastic perfectly plastic with Mohr-Coulomb shear failure criteria.
The superstructure is represented by a 1000kN mass rigidly fixed to the footing through a column for the study of the coupled kinematic and inertial interaction. The seismic loading applied to the base of the soil is modeled by the Tabas earthquake in Iran (Figure 2.15). The parametric study assessed the impact of numerous factors on the behavior of IR.

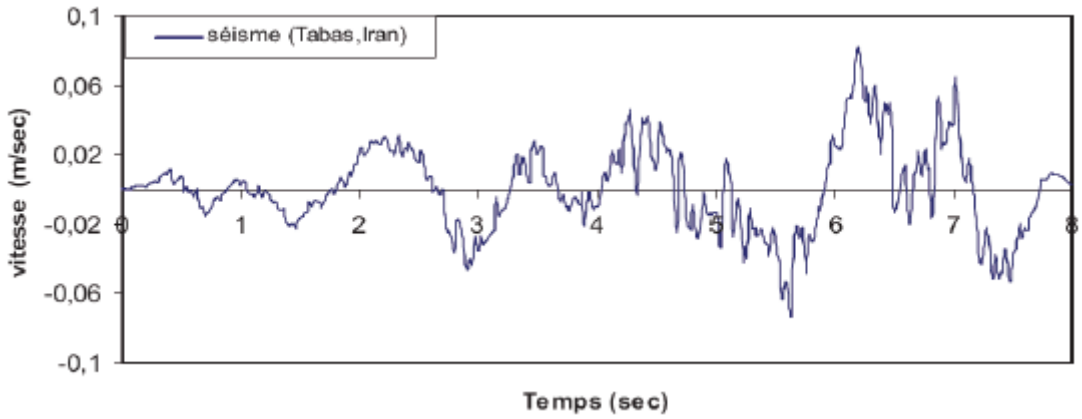

Figure 2.15: Seismic recording of the Tabas earthquake in Iran (Hatem, 2009)

The analysis of the kinematic effect shows a significant amplification of surface responses and in the heads of inclusions. A positive group effect is observed with a reduction in internal inclusion efforts of 20% for bending moment in comparison to an isolated inclusion (Figure 2.16). The increase in thickness of the mattress allows for a reduction in the flexural moment in the inclusions. (Hatem, 2009) found that forces and bending moments are higher in the piles due to a dynamic amplification compared to the inclusion system.

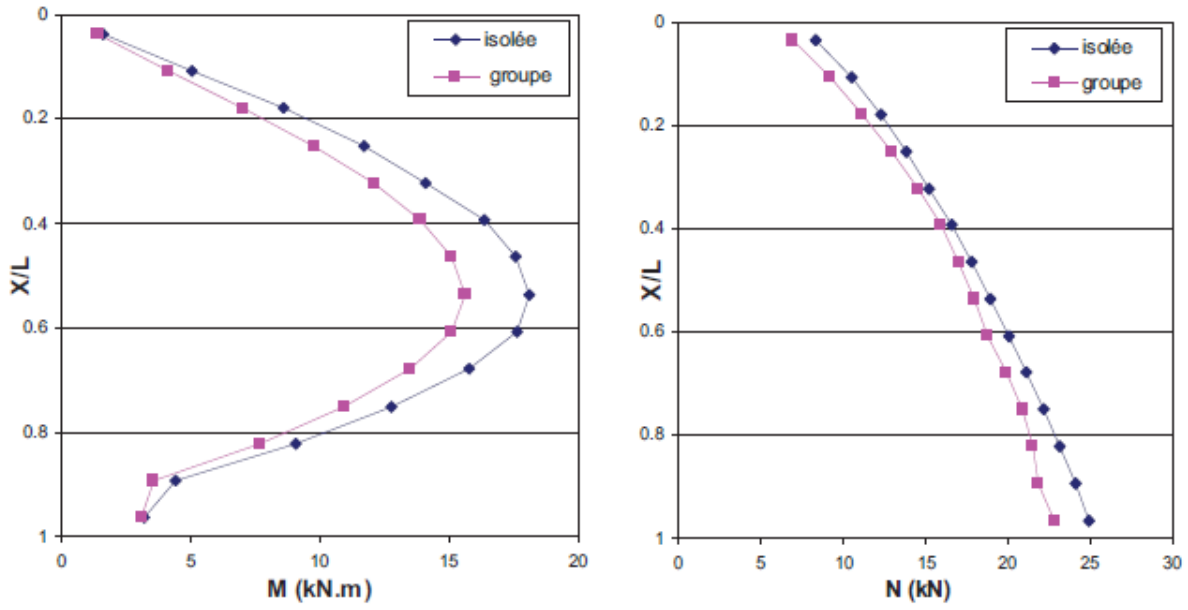

Figure 2.16: internal forces comparison in single inclusion and a group of 2x2 inclusions (Hatem, 2009)

The evaluations of the combined kinematic and inertial interaction reveal the significant influence of the inertial effect on inclusion responses, with for example, a bending moment twice as large as that mobilized by the kinematic interaction (Figure 2.17).

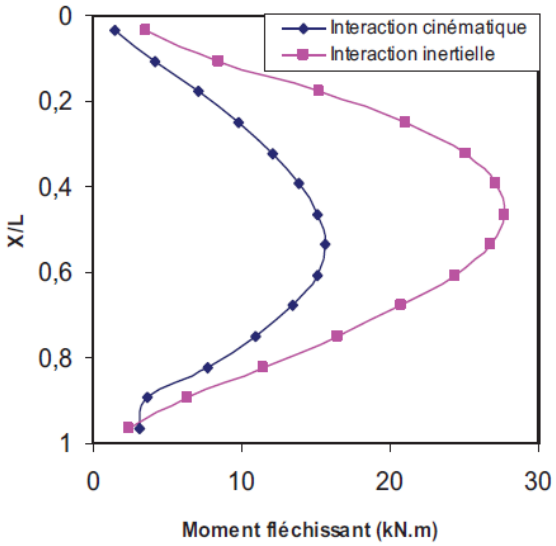

Figure 2.17:Influence of the presence of the structure on the bending moment in inclusions

(Lopez Jimenez, 2019), created a three-dimensional numerical model (Figure 2.18) to study the influence of different parameters on the response of soil-platform-inclusions-structure systems under dynamic loading using tridimensional finite difference (Flac3D) analyses. In this study,

the soil was modeled, using typical values of soft soil properties and assuming drained conditions. The linear elastic and the elastic-perfectly plastic constitutive model were used, incorporating a Mohr-Coulomb criterion to account for possible plasticity and shear failure in soil components, to represent soil behavior.

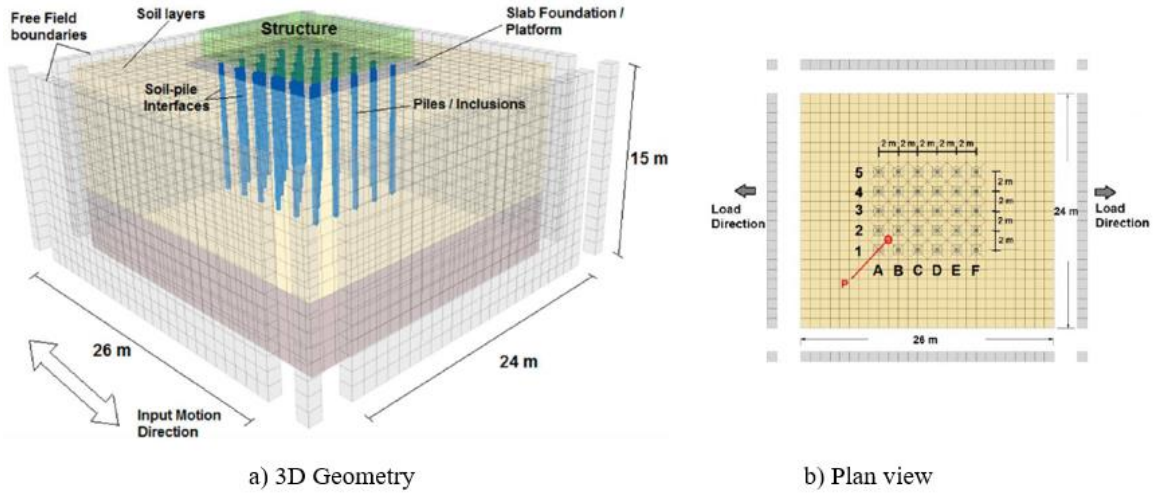

Figure 2.18: Geometry of the numerical model (Lopez Jimenez, 2019)

The study showed that, the characteristics of the soil, structure, and foundation significantly alter the movement experienced at the base of the structure. The spectral accelerations observed at the ground surface (the base of the structure) are higher than those of the input motion (the bottom of the model). The analysis indicated that considering the nonlinearity of the soil reduce the amplitude of the peaks of the spectra compared to the linear elastic model. The plasticity of soil results in reduction in the energy transmitted to the superstructure which leads to a decrease in the internal forces transmitted to the rigid elements when elasto-plastic soil conditions are considered, as opposed to elastic calculations. And when considering embedment in a hard soil, the result indicates that the system is significantly impacted by the lateral deformation surrounding the soil which lead to additional kinematic forces in the elements. Moreover, stiffer rigid elements are subjected to higher efforts and displacements.

2.4 Seismic behavior

2.4.1 Dynamic loading

To model the seismic loading, two approaches can be defined. The first one is a temporal approach, which gives the temporal variation of the solicitations from the recordings or from the modeling. The second one is a spectral approach, which gives the spectral characteristics of

the seismic movements.

The seismic motion is defined by its three components: two orthogonal horizontal components, independent and represented by the same spectrum, and a vertical component, which can be represented by the spectrum of the horizontal component, but with an intensity equal to 70% of the horizontal component. Seismic motion undergoes spatial and temporal variations during its propagation. Spatial and temporal changes in seismic motion can have amplifying or attenuating effects on motion. The greatest accelerations of Loma Prieta's 1989 earthquake observed on rocky sites in San Francisco, for example, are twice or three times larger than those reported on alluvial regions.

There are multiple variables that can generate dynamic forces on a structure, such as blast loads, wind, wave action, traffic, industry, and earthquakes. The force exerted might be created by different sources. (Figure 2.19) present different sorts of loads dependent on their source.

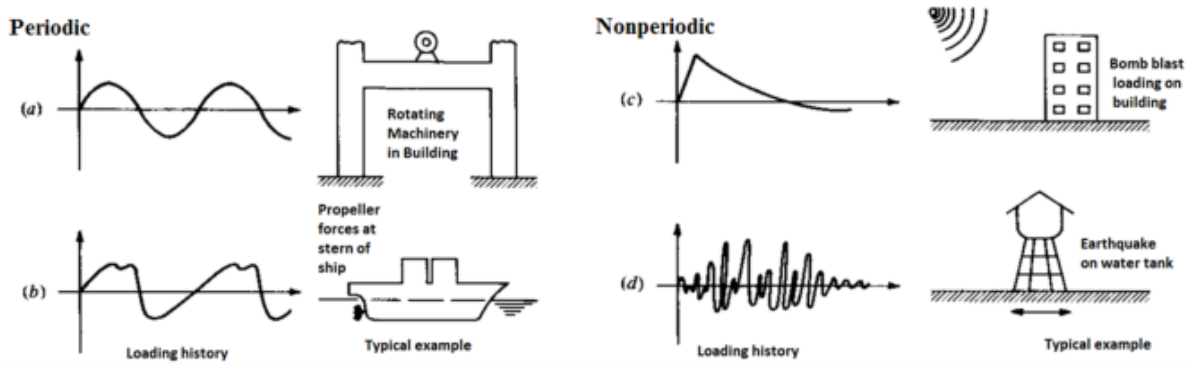

Figure 2.19 : Sources and characteristics of dynamic loadings: a) Harmonic load, b) Complex periodic load, c) Transient load, d) Earthquake load (Clough and Penzien, 1975).

2.4.2 Soil dynamic behavior and important aspects to be considered

2.4.2.1 Soil behavior

The seismic waves (Figure 2.20) resulting from the earthquake impose movements in the soil. These movements can harm and damage the structures present in the shaking area. There is an important relation between the seismic waves and the soil, each one affects the other. The propagation of the shear waves induces shear stresses which are the main interest in the geotechnical earthquake engineering. Usually, the relationship between the shear stress and shear strain describes the soil response which is too important under dynamic and cycling

loading (Ishihara, 1996).

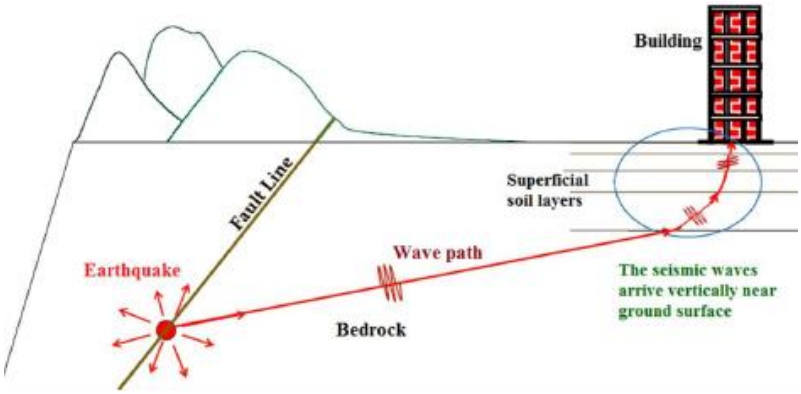

Figure 2.20: Seismic waves propagation in the soil (Lopez Jimenez, 2019)

The most important ground motion parameters are the amplitude of motion (peak velocity, peak acceleration, and peak displacement), frequency content (bandwidth, response spectra, Fourier spectra, predominant period) and duration. These parameters can be impacted by three significant factors: source effects, path effects, and site effects.

2.4.2.2 Soil stiffness and damping ratio

The dynamic analysis of geotechnical structures requires an important study of the parameters involved in dynamic loading. Solving these problems requires the description of the behavior of soils under dynamic loading. Shear modulus (G) and material damping ratio (D) are the main properties that need to be characterized (Barani et al., 2013; Darendeli, 2001; Phillips and Hashash, 2009). These parameters are important input data for modeling or for the calibration of constitutive laws used to solve engineering problems such as seismic behavior studies, and vibration analysis of piles.

The shear modulus, G, characterizes the shear stiffness of the soil, it is a secant deformation modulus. It is defined as the slope of the curve relating shear stress (τ) and shear strain (γ).

$$G = \frac{\tau}{\gamma} \tag{3}$$

This parameter should not be confused with the tangent modulus, which represents the slope of the tangent line associating axial stress and axial strain.

The greatest value of shear modulus for extremely small stresses may be attributed to the shear wave velocity Vs moving through the soil using equation (4) (Kramer, 1996).

$$G_{max} = \rho * V_s^2 \quad (4)$$

ρ: is the bulk density of the soil.

The soil's shear modulus is not constant and varies with strain magnitude because of the non-linear stress-strain relationship. The path of stress and strain depicted in (Figure 2.21) is known as the hysteresis loop. The damping factor D measures the amount of energy that dissipates in the loop relative to the maximum elastic energy obtained during a given cycle.

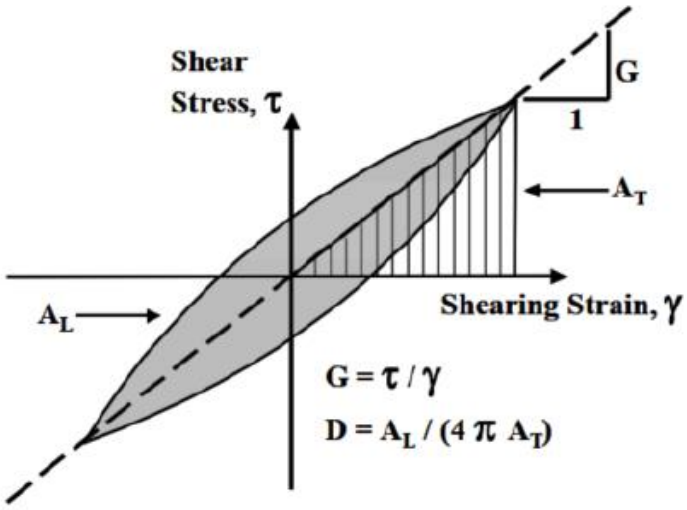

Figure 2.21: Estimation of shear modulus and damping ratio during cyclic loading

The energy dissipated over one loading cycle is represented by the gray area (AL) of the hysteresis loop, and the maximum retained strain energy which is calculated using the maximum shearing strain and the maximum shear stress is represented by the triangular area (AT). Soil particles friction, strain rate effects and the nonlinearity of the stress strain relationship in soils are described by the material damping ratio. The hysteretic damping is an appropriate technique to express soil damping behavior, viscous damping is another way to express energy dissipation. The main distinction between viscous damping and hysteresis damping is that viscous damping is frequency dependent.

2.4.2.3 Damping

When considering dynamic numerical modeling, damping is an important feature. The soil is

usually modeled by a finite domain limited by artificial boundaries capable of dissipating energy. This energy dissipation in the boundaries is referred to a radiation damping, which is not an inherent characteristic of the material. In addition to radiation damping, there exists material damping, which accounts for energy loss within the soil itself. This is largely due to microstructural mechanisms such as inter-particle sliding, friction, structure rearrangement, and pore fluid viscosity. The material damping component has been highlighted as one of the essential factors in the study of soil-foundation-structure interaction systems (Ambrosini, 2006; Wolf, 1985) since it relies on the soil's characteristics and not on the model's geometry and boundaries.

During dynamic numerical analyses, a variety of constitutive models have the capability to simulate energy dissipation. Some of these models require multiple parameters, which can only be obtained through advanced laboratory testing. Other straightforward elasto-plastic models necessitate an additional damping mechanism for the elastic part of the response, where no energy loss occurs. In such cases, the introduction of additional damping can be accomplished using viscous damping (also known as Rayleigh damping). A key consideration when utilizing simplified or complete Rayleigh damping is selecting an appropriate target damping ratio (Woodward and Griffiths, 1996) and identifying the frequency range where the response is frequency-independent (Kwok et al., 2007; Tsai et al., 2014).

Rayleigh damping

Rayleigh damping is employed in both linear and nonlinear elastic analyses. The damping matrix C is created by combining the stiffness K and mass M matrices in the following way:

$$C = \alpha[M] + \beta[K] \tag{5}$$

α is the mass-proportional and β is the stiffness-proportional damping constants. They are evaluated by the equations (6) if the damping ratios (ξi-ξj) associate with two specific frequencies (ωi-ωj) are known.

$$\alpha = \xi \frac{2\omega_i \omega_j}{\omega_i + \omega_j} \quad ; \quad \beta = \xi \frac{2}{\omega_i + \omega_j} \tag{6}$$

The critical damping ratio (ξi) can be calculated from the equation (7) at any angular frequency of the system (ωi), for a multi-degree of freedom system.

$$\alpha + \beta\omega_i^2 = 2\omega_i\xi_i \tag{7}$$

(Figure 2.22) displays three distinct curves: one specifies the overall damping, taking into consideration both the mass and stiffness, another curve shows only the part proportional to the stiffness (α=0), and the third curve represents the part proportional to the mass (β=0). The complete damping curve has a restricted frequency range, beyond which a greater damping effect can be observed. This range is bounded by a lower frequency f_0, representing the first mode of the soil column, calculated by the equation (8), and a large frequency f_1.

$$f_n = \frac{V_s}{4H} \tag{8}$$

Vs: Elastic shear wave velocity

H: Thickness of the soil column

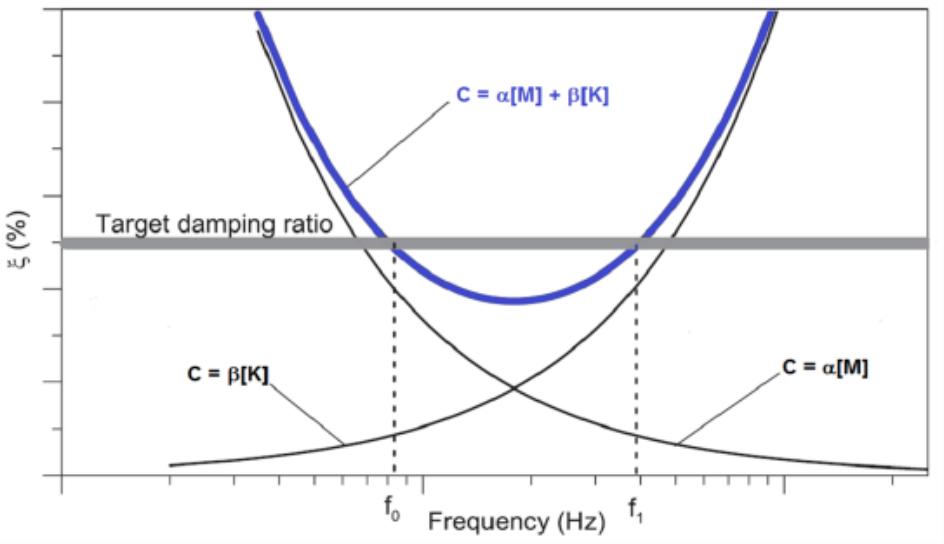

Figure 2.22: Variation of damping ratio with frequency (Lopez Jimenez, 2019)

When dealing with higher frequencies, one method to determine the largest frequency is the single control frequency approach, which asserts that f_1 equals f_n as noted by (Idriss et al., 1975; Suwal et al., 2014).

On the other hand, there exist multiple strategies within the two control frequencies approach to identify the largest frequency. The easiest way is to choose a higher frequency that matches the dominant frequency (f_p) of the input motion. (Kwok et al., 2007) propose a frequency equal to 5 times f_n. Other researchers recommend choosing $f_1=nf_n$. where n denotes the smallest, odd integer that gives an f_1 value greater than f_p as proposed by (Hudson et al., 1994; Rathje and Bray, 2001). According to (Park and Hashash, 2004) two dominant frequencies should cover the frequency range where the input motion content is significant.

Values in the range 1-5% are typically considered for target damping (Kumar et al., 2016; Mánica et al., 2014; Rangel-Núñez et al., 2008; Shahrour et al., 2012; Suwal et al., 2014).

It is also remarkable that the blue curve from (Figure 2.22) which represent the full damping combining the stiffness and the mass components reaches the minimum at:

$$\xi_{min} = (\alpha\beta)^{1/2} \tag{9}$$

$$\omega_{min} = (\alpha/\beta)^{1/2} \tag{10}$$

These equations, (9) and (10), represent the input parameters to specify the Rayleigh damping in numerical modeling.

The dissipation of energy in seismic analyses is better represented by the Rayleigh damping. This was proved in (Mánica et al., 2014) 3D numerical seismic study which analyzed the advantages and drawbacks of different types of damping (local, hysteretic and Rayleigh) in a typical stratigraphy of Mexico City using linear elastic constitutive model. Rayleigh damping was largely used in rigid inclusion and piles studies (Hatem, 2009; Lopez Jimenez, 2019; Shahrour et al., 2012; Van Nguyen et al., 2017).

2.4.2.4 Evolution of the dynamic parameters

The maximum shear modulus G_{max} controls the elastic behavior at very small strain levels ($\gamma \leq 10^{-3}$). In this situation, the dynamic shear modulus G_{sec} remains relatively constant and equal to the initial value G_{max}. However, at moderate and large strains, the cyclic soil response is characterized by stiffness and damping ratio. They are not constant with respect to the amplitude of shear strain. As is clear from (Figure 2.23), the greater the shear strain amplitude, the lower the stiffness and the greater the damping. These changes in stiffness and damping ratio are known as stiffness degradation and damping evolution, respectively.

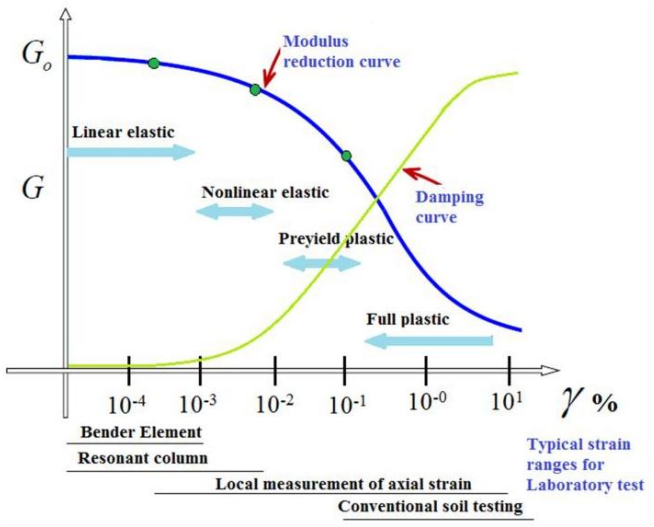

Figure 2.23:Dynamic parameters evolution with strain (Lopez Jimenez, 2019)

At very small strains, $\gamma < 10^{-3}$ %, soils exhibit linear elastic behavior. According to (Darendeli, 2001) the strain amplitude at which the shear modulus decreases to 98% of its original value is commonly referred to as the elastic deformation threshold. It is also called the nonlinearity threshold by (Ishihara, 1996; Vucetic and Dobry, 1991). Above the elastic threshold, soils behave in a nonlinear manner but still elastic. In other words, the stress-strain relationship is nonlinear, but the deformations are recoverable upon unloading. The cyclic (or plastic) deformation threshold is defined as the strain amplitude at which the deformations become irreversible. This threshold is also known as the degradation threshold by (Ishihara, 1996; Vucetic and Dobry, 1991). For this strain, the G/G_{max} ratio is around 0.6 to 0.8 (Darendeli, 2001). Volume changing in the soil can occur above this cyclic deformation threshold and they are subjected to shear. The nonlinearity of the stress-strain relationship leads to an increase in energy dissipation and in the material damping ratio, D, with the increase of the strain amplitude. The material damping ratio at low strains is denoted by D_{min}.

Studies and laboratory tests show that many parameters can influence the soil stiffness such as: void ratio, mean effective stress, cyclic strain amplitude, plasticity index, number of loading cycles and the over consolidation.

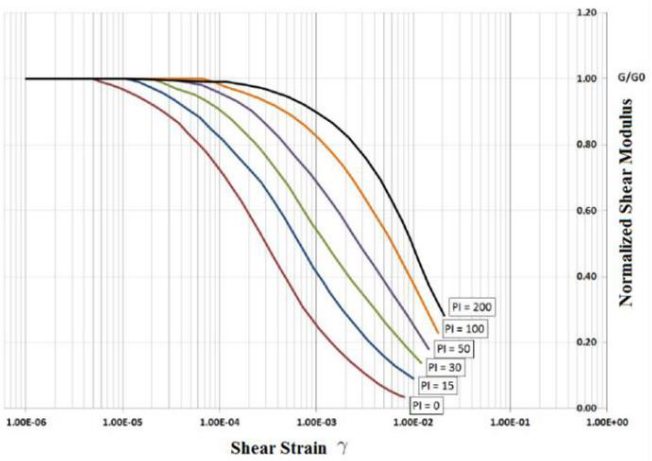

Figure 2.24:Influence of plasticity index on the G/Gmax - γ curve (Vucetic and Dobry, 1991)

(Vucetic and Dobry, 1991) developed a database from previous studies that present the G/G_{max} degradation curves. Various tests performed in several different laboratories as triaxial tests, resonant column tests, and direct shear tests constitute the database. G/G_{max} curves are constructed for six different plasticity indices (PI = 0, 15, 30, 50, 100, and 200). They showed that the plasticity index has a significant impact on the G/G_{max} degradation curves (Figure 2.24). The researchers found that there is no significant difference in G/G_{max} for a wide range of over consolidation ratios (OCR), which is consistent with the observation of (Kokusho et al., 1982).

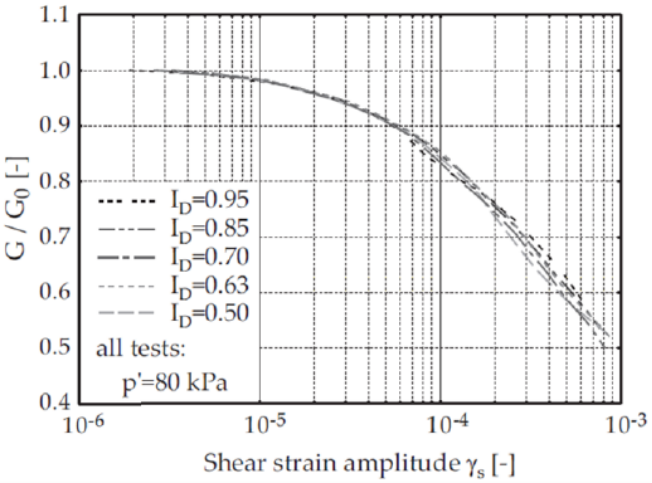

Figure 2.25: Influence of void ratio on the G/Gmax - γ curve (Benz, 2007)

According to (Benz, 2007), the void ratio has a significant influence on the degradation of normalized shear modulus. (Figure 2.25) illustrates the impact of void ratio on the degradation of normalized shear modulus. It is observed that for a given deformation, the G/G_{max} ratio

increases as the void ratio increases. Similarly, the deformation corresponding to a given G/G_{max} ratio increases as the void ratio increases.

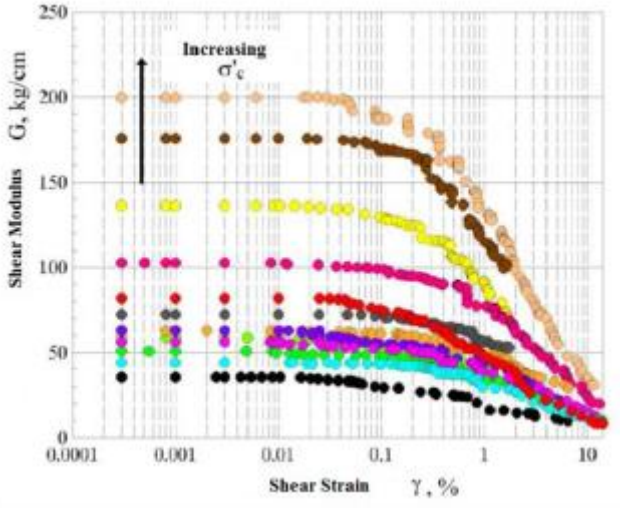

Figure 2.26: Influence of confining pressure on the G/Gmax - γ curve (Romo, 1995)

The confining pressure impact on the shear modulus evolution was studied by (Romo, 1995). As shown in (Figure 2.26), the shear modulus increases as the confining pressure increase.

(Table 2.1) summarizes the changes in soil properties with strain. The table shows that when the magnitude of shear strain is increased beyond the 10^{-1}% level, the repetition effect begins to appear.

Cyclic shear strain amplitude (%)	**Associated phenomena**	**Mechanical characteristics**	**Behavior**	**Effect of repetition**
Very Small **$< 10^{-3}$**	Vibration, wave propagation	Elastic	Practically linear	No (negligible)
Small **10^{-1} - 10^{-3}**	Cracks, differential settlements	Elasto-plastic	Non-linear	Yes (relevant)
Large **$>10^{-1}$**	Slide, compaction, liquefaction	Failure	Non-linear	Yes (relevant)

Table 2.1: Variation of soil properties with strain

2.4.2.5 Laboratory tests

To measure shear strain values, laboratory tests or in situ measurements make it possible. This section presents two laboratory tests that are used to determine the dynamic soil properties at small and large strain values.

Resonant column tests

Resonant column tests (Figure 2.27) are often used to determine the dynamic properties of soil at small strain. These properties have been characterized in strains ranging from 10^{-4}% to 5.10^{-1}% (Semblat and Pecker, 2009). In this test, a cylindrical soil sample is clamped at the bottom and dynamically excited at the top. An electric motor consisting of four drive coils surrounding four magnets attached to a drive plate creates a torsional force on top. Resonance frequency, shear wave velocity, and shear modulus are calculated using elastic theory based on the maximum amplitude of fundamental mode vibration. This non-destructive test can be repeated several times on the same specimen as long as no pore pressure occurs.

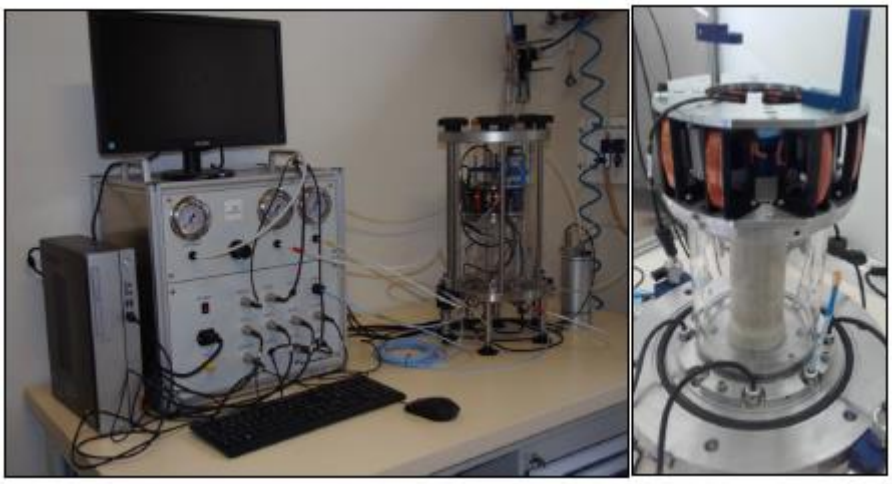

Figure 2.27: Resonant column of Antea Group laboratory (Lila, 2021)

Cyclic triaxial tests

Cyclic triaxial test is the most commonly used test for measuring cyclic soil properties at moderate to high strain levels. A cylindrical specimen is placed between upper and lower stress plates and enclosed by a thin rubber membrane (0.3 mm) in the triaxial test. Samples are loaded cyclically through saturation and consolidation phases. Load cycle can be controlled in stress (ASTM D3999-91, 2003) or strain (ASTM-D5311, 2011). Stresses and strains measured in cyclic triaxial tests are used to calculate shear modulus (G) and damping ratio (D) for moderate

and large strains (typically 10^{-2} to 10^{0} %). Small strain measurements are typically limited to 10^{-2}% due to uncertainty caused by the sample placement on the machine.

Figure 2.28: Cyclic triaxial test of Antea Group laboratory (Lila, 2021)

2.4.3 Seismic behavior of rigid inclusion

The behavior of rigid inclusions initially refers to that of piles. When subjected to a seismic event, the pile experiences two types of generated solicitations that overlap within the soil-pile-superstructure system: kinematic interaction and inertial interaction.

Kinematic interactions involve subjecting the pile to excitation resulting from ground motion induced by free-field propagation of seismic waves. Note that if there are multiple soil layers with different shear moduli, kinematic effects can be particularly pronounced at their interfaces. To evaluate pile deformations based on the free field soil deformation, several analytical methods have been proposed by various authors (Dobry and O' Rourke, 1983; Gazetas, 1984; Nikolaou et al., 2001). These multi-parameter analysis approaches have a very limited application domain where the analysis is performed in the frequency domain of unidirectional wave propagation.

The inertial interaction refers to the study of the response of the soil-pile system subjected to a dynamic load applied to the head of the pile induced by the motion of the superstructure caused by kinematic interaction. In most cases, the inertial interaction predominates over the kinematic interaction in the behavior of the soil-pile-superstructure system. Analytical models for the

study of inertial interaction often simulate the soil-pile interface by a series of springs (Winkler model) and dampers. These models have been progressively developed by various authors. (Novak and Aboul-Ella, 1978) proposed a model composed of a spring with a complex modulus function of frequency that considers only linear behavior. Then, the Matlock model was developed with a nonlinear spring and a linear damper independent of frequency. Various variants of springs and dampers have been introduced by (Boulanger et al., 1999; El Naggar and Novak, 1996) in their analytical models to improve model performance by approaching real behavior.

In addition to analytical approaches, numerous experimental studies (full-scale and reduced models) and numerical simulations (2D and 3D) have been conducted on the soil-pile-structure interaction. Physical models of inertial interaction were achieved through either impact (Bonab, 2003) or forced vibration of the pile head. Many tests have aimed to investigate both inertial and kinematic interactions simultaneously (Meymand, 1998), simulating an earthquake on a pile founded structure.

In addition to the coupled effect, (Chenaf, 2007) conducted a separate examination of the inertial and kinematic effects using centrifuged reduced-scale model tests. Numerous research studies have focused on numerical modeling of the dynamic interaction between soil-pile-structure under seismic conditions using the finite element method or the finite difference method in 2D and 3D. Although numerical models can be expensive due to long calculation times, their main advantage is that they enable the inclusion of behavior laws adapted to the soil and the consideration of different geometric configurations.

Regarding the seismic response of rigid inclusion, their behavior under kinematic effect is similar to that of piles. The distinction arises from their response to seismic loading, which is due to the inertial effect. Inertia forces created by the structure are transmitted to the piles through their heads that are embedded in the structure. The presence of granular load transfer mattress in the case of RI leads to indirect transfer of inertial forces towards the RI. As a result, the actual dynamic load applied to the heads of the RI is decreased due to energy dissipation in the transition zone between the structure and the rigid elements. This concept was implemented in the construction of the Rion-Antirion Bridge, located in a high-risk seismic zone (Pecker and Teyssandier, 1998).

An overview of prior research that has been carried out to study the response of rigid inclusions subjected to dynamic loading is presented in the following section.

2.5 Previous studies of the seismic behavior of rigid inclusions

2.5.1 Numerical modeling

Numerical simulations have been suggested to investigate the reinforcement of compressible soils. These simulations provide complementary results to the scaled or full-scale models, on which these simulations are validated. The simulations can be performed using finite difference method (FDM), finite element method (FEM), or discrete element methods (DEM), with certain models combining two methods. The thesis examines the numerical simulations using the FEM and the FDM.

The Finite Element Method (FEM) has been extensively utilized in geotechnical engineering. The finite element approach includes discretizing the physical domain to approximate the solution of a set of differential equations that regulate the equilibrium of a solid under boundary conditions described by forces and/or displacements. This approach substitutes the actual structure being investigated with a finite number of components that form a mesh and are connected by nodes. The behavior of each independent part is first addressed, and then these elements are integrated in a way that assures the balance of forces and compatibility with the actual deformations of the structure. The finite element technique is a useful tool for precisely analyzing continuous structures with complicated geometric features and loading circumstances. FEM is more detailed in section 2. Chapter 3.

The Finite Difference Method (FDM) is one of the oldest techniques that involves solving differential equations with boundary and initial conditions (Christian and Desai, 1977). In contrast to FEM, which defines stress, strain, and displacements everywhere and calculates a rigidity matrix, FDM uses algebraic expressions in terms of variations at discrete locations in space, reformulated at each step without the need for matrices (Billaux and Cundall, 1993). The FDM is described in section 2. chapter 4.

The numerical simulations require the use of explicit and implicit methods, specially to solve problems related to dynamic as well as static one.

IMPLICIT FORMULATION

The equation of dynamics is solved by discretizing the time interval. At time instant tn, the equation takes the form:

$$M\{\ddot{U}_n\} + C\{\dot{U}_n\} + K\{U_n\} = \{F_n\} \quad (11)$$

Where {Un}, $\{\dot{U}_n\}$, and $\{\ddot{U}_n\}$, are the displacement, velocity, and acceleration vectors, at time instant tn, respectively, and {Fn} is the force vector.

At each time step, a time integration procedure is used to calculate the displacements, velocities, and accelerations (Paultre, 2018). This equation is numerically solved using an integration method. In an implicit analysis, the components at a given time tn+1 are estimated from the components of the motion at the previous time step(s) as well as at time tn+1.

The equation of motion (11) at a time instant tn+1 is used to solve for the displacements at time tn+1 by iterating until equilibrium is achieved at each time step. A convergence criterion must be defined for this purpose. Implicit methods such as Newmark integration, and Bathe's methods are some examples of methods used for this purpose. Implicit methods are generally preferred as they are unconditionally stable (Paultre, 2018).

However, in the context of seismic analysis or wave propagation, the time step used must be able to capture the smallest period of excitation, in order to ensure adequate accuracy (Koltuniuk et al., 2013).

EXPLICIT FORMULATION

When using explicit time integration in an analysis the displacements at the time instant tn+1 are calculated by only considering the movements at the previous time(s) (Paultre, 2018). The equation of motion (11) at a time instant tn is employed to compute the motion components at time tn+1.

The explicit method is conditionally stable, meaning that a sufficiently small-time step must be used to ensure the stability of the analysis.

A comparison between explicit and implicit integration schemes is summarized in (Table 2.2).

Explicit method	Implicit method
The time step must be less than a certain critical time step to ensure the stability of the solution.	The stability of the solution is unconditional for the classical solution schemes.
Non-linear behavior laws are taken into account without any additional iterative algorithm.	An additional iterative procedure is necessary to take into account the non-linear behaviors.
No significant numerical damping is introduced for dynamic problems.	A time-dependent numerical damping is required when dealing with viscoplastic or dynamic cases.
No matrix is stored, and the memory (RAM) required is minimal.	A stiffness matrix must be stored, which requires a large memory capacity.
A calculation in large displacements does not require any additional procedure, thanks to the Lagrangian elements.	Additional calculations are often necessary to satisfy the conditions of a large displacement calculation.
Limited calculations per time increment	Numerous calculations per time increment

Table 2.2: Comparison between explicit and implicit resolution methods, according to (Itasca, 2022)

The finite difference method was used by (Han and Gabr, 2002) to conduct a numerical study, employing the concept of the elementary cell (Figure 2.29). Soil and load transfer platform were represented using the hyperbolic model of nonlinear elasticity proposed by (Duncan and Chang, 1970). According to the study both differential and total displacements are reduced at the inclusion level and the surface of the load transfer mattress. Moreover, the load transfer is increased, and the tension in the geosynthetic material rises with the thickness of the embankment reaching its maximum near the edge of the inclusion.

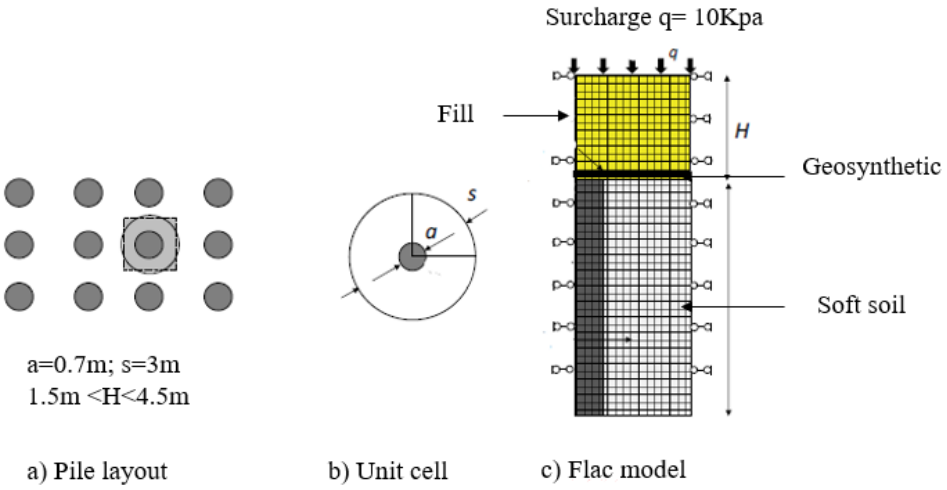

Figure 2.29: Axisymmetric numerical model configuration of (Han and Gabr, 2002) study

Another study, (Jennings and Naughton, 2012), conducted a comparative analysis of a numerical model based on Plaxis 2D, a finite element software, and on Flac, a finite difference software.

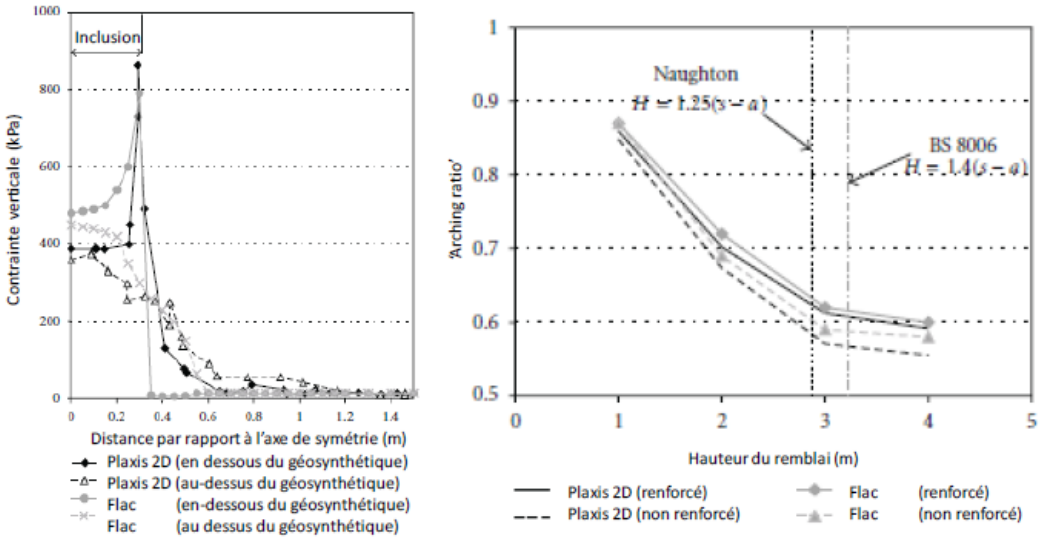

Figure 2.30: Results of (Jennings and Naughton, 2012) numerical model, on the vertical stress and arching ratio

Two constitutive laws were employed in the numerical model, the Hardening law for the mattress and the Mohr-Coulomb law for the compressible soil. The study finds that the results obtained from the two different numerical methods (Figure 2.30) are in good agreement. The numerical simulations reveal stress concentration in the proximity of the inclusion and the vertical stress at the inclusion edges.

(Zhang et al., 2022) analyzed the response of a single footing on soft soil reinforced with four rigid inclusions by employing three-dimensional finite difference modeling (FDM) (Figure 2.31). To simulate the system's behavior, the numerical model adopted two distinct constitutive laws: the modified Cam-Clay model (MCC) for the soft soil and the linear elastic-perfectly plastic material considering Mohr-Coulomb criteria for the mattress and the substratum.

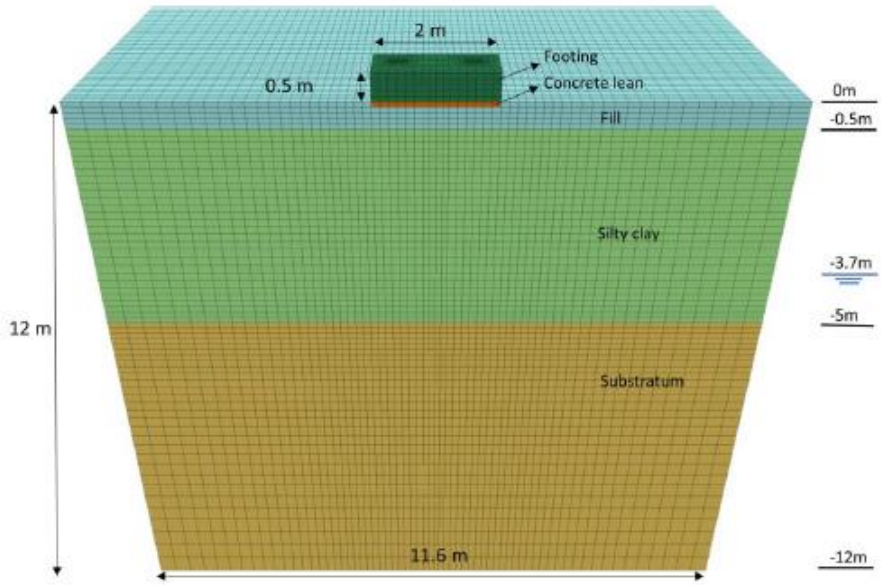

Figure 2.31:3D numerical model of (Zhang et al., 2022) study

A numerical parametric study was carried out to evaluate the impact of load transfer platform thickness and surface load eccentricity on the reinforcement performance. Results indicated that both the settlement efficiency and load efficiency decreased as the platform thickness increased under both centered and eccentric loading conditions. The inclusion reinforcement ceased to contribute to the load transfer mechanisms when the platform thickness became sufficiently thick compared to the footing size.

The behavior of the system was significantly influenced by the loading eccentricity, as it caused the footing to tilt and the inclusion efforts to increase. When dealing with eccentric loading conditions, the primary design factor became the variation in single inclusion load efficiency, rather than global load efficiency.

2.5.2 Experimental work

To study the behavior of rigid inclusions and load transfer mattress, full-scale tests were employed. The resulting data is then used to calibrate numerical models or verify analytical

calculations. (Girout, 2014) provided several examples of such tests.

2.5.2.1 Full scale tests

Full-scale tests have been conducted to study the reinforcement of compressible soils with rigid inclusions, (Abdullah and Edil, 2007; Liu et al., 2007). These tests provide an understanding of the load transfer to the inclusions and of the lateral and vertical displacements during the construction of the embankment and the settlement of the compressible soil. In (Liu et al., 2007) study a 5.6m high embankment reinforced by a network of inclusions approximately 1 meter of diameter (α = 8.7%). (Figure 2.32) shows the placement of the geosynthetic above the inclusions in the mattress.

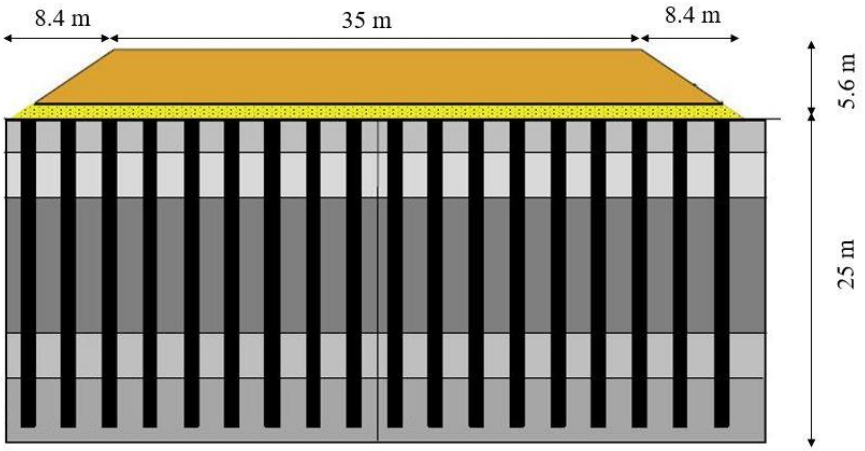

Figure 2.32: reinforced Backfill base with geosynthetic on rigid inclusion(Liu et al., 2007)

This study shows that the bearing capacity of the reinforced soil is tripled, the load transfer increases during the construction of the embankment, settlements are reduced, and lateral displacements on the slopes of the embankment are decreased.

The Chelles experimental site (Figure 2.33) was established during the national (ASIRI, 2012) project (Briançon and Simon, 2012; Nunez et al., 2013) to study the relative influence of the reinforcement at the base of the mattress. (Briançon and Simon, 2012) conducted a study based on this case, in which a 5 m high and 52 m long embankment was divided into four sections: 1R, 2R, 3R, and 4R, with section 1R representing the unreinforced case. Sections 2R, 3R, and 4R were reinforced with a network of eight inclusions (0.38 meters in diameter) distributed in

a square mesh pattern of 2m side length (α = 2.84%). Additionally, a compacted granular sand mattress was placed on sections 3R and 4R. For section 3R, the mattress was reinforced with a bidirectional geosynthetic sheet with a tension of Tε=5% = 37kN/m. And the mattress for section 4R, was reinforced with two geosynthetic sheets (with a stiffness of Tε=5% = 17kN/m).

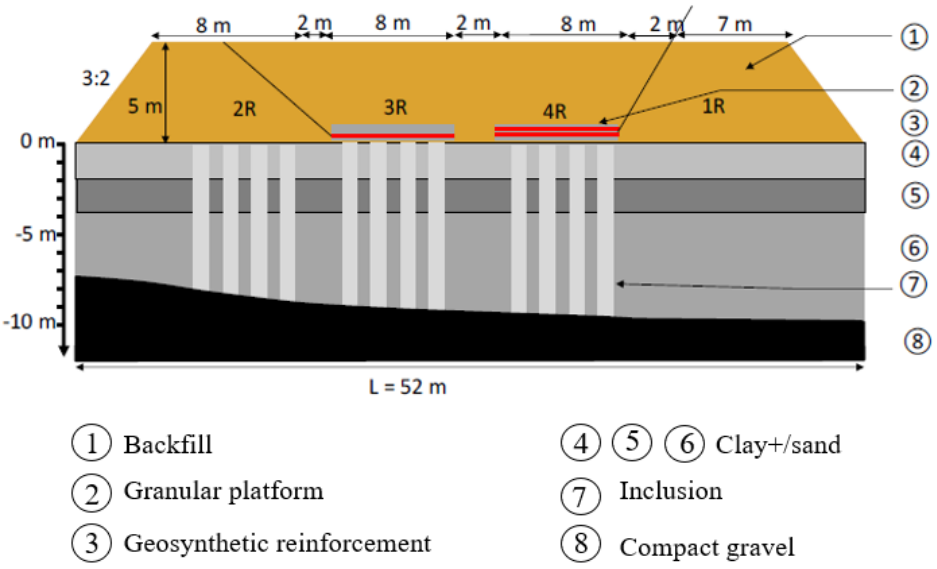

Figure 2.33: Instrumented site during the National Project (ASIRI, 2012)

This study's findings suggest that incorporating a granular mattress enhances the load transfer. Additionally, using inclusions to reinforce the compressible soil, coupled with one or more geosynthetics in the mattress, aids in reducing settlements. The geosynthetics experience their highest levels of stress along the inclusion edges. Moreover, with multi-layered reinforcement, the lower geosynthetic layer undergoes more deformation than the upper layer. Adding a second layer promotes uniform stress distribution across the mattress's top and minimizes differential settlements in the fill.

2.5.2.2 Scaled model (1xg)

Laboratory-scale models are frequently employed due to their familiarity and the ability to control boundary conditions. When modeling geotechnical structures at a reduced scale, it is essential to maintain analogous relationships between the prototype structure and the scaled model. The concept of the scaling factor, as introduced (Mandel, 1962), plays a crucial role. The scaling factor, expressed by equation (12) provides a measure of the proportion between the prototype scale $X^{(p)}$ and the model scale $X^{(m)}$.

$$N = \frac{X^{(p)}}{X^{(m)}} \quad (12)$$

(Jenck et al., 2005) conducted a study using a 2D model with plane deformation. The fill material was represented by Schneebeli rollers (Figure 2.34), while different compressible foams were used to model the compressible soil. A geosynthetic was placed within the mattress. The study's findings indicate that the critical height of the mattress is 2×s. The efficiency increases with a higher cover ratio. Surface settlements decrease when the mattress contains larger elements. For low mattress height's studies, the more compressible the materials the greater the differential surface settlements. The compressible soil must settle sufficiently relative to the secant stiffness of the geosynthetic for the membrane effect to occur.

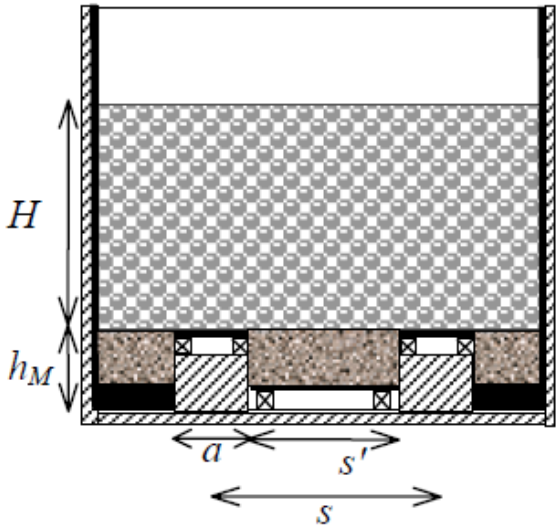

Figure 2.34:Model of (Jenck et al., 2005)

2.5.2.3 Centrifuge physical modeling

Physical modeling using centrifuges (Figure 2.35) has become popular in the field of geotechnical engineering around the world in recent years. This type of testing involves studying reduced-scale models to meet the needs of engineers and researchers. Compared to in situ testing, centrifuge tests can significantly reduce costs, with both types of testing providing complementary results. Centrifuged models allow a better understanding of soil structure interaction phenomena, especially in parametric studies. Furthermore, these models provide useful data for validating both analytical and numerical models.

A physical model is a scaled-down version of a full-sized structure, also called a "prototype".

A major advantage of centrifuge modeling is that the reduced model reproduces the same stresses as the prototype.

Figure 2.35: Modern centrifuge of the LCPC

2.5.2.4 Centrifugal reduced-scale models (N×g)

(Baudouin, 2010) focused on studying the reinforcement of compressible soils with a centrifuge model (N=27.8). Clay containers are reinforced with rigid inclusions (Figure 2.36). A granular load-distributing mattress is placed on top of it. On the prototype scale, the inclusions have a diameter of Ø = 0.50 m with a spacing of either 2.5 m or 2.0 m. Many tests were carried out during the experiment. The findings indicated a decrease in the differential settlement of the mattress as the thickness H increased. When H reached 1.5 m or exceeded it, the settlement was exceptionally minimal, measuring less than 2 cm. Additionally, the implementation of surcharges had a negligible influence on the settlements. The load transfer efficiency increased with both α and H, but the maximum efficiency of 65% was only achieved for "backfill."

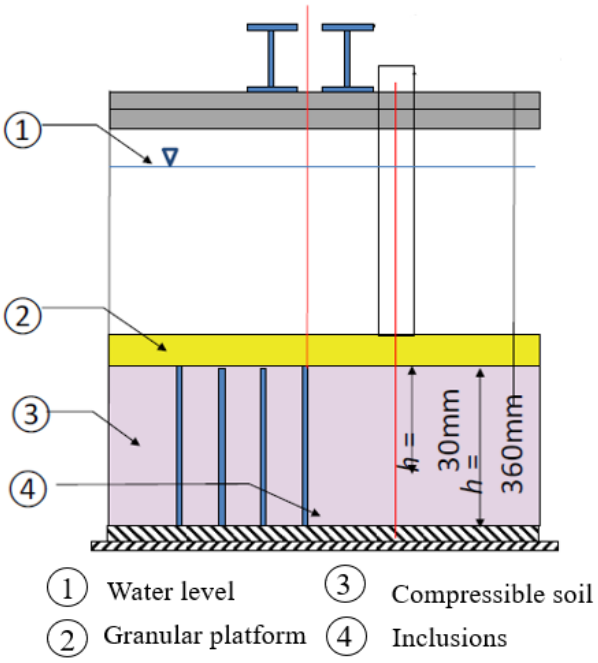

Figure 2.36:Compressible soi reinforced by rigid inclusion (Baudouin, 2010)

(Okyay et al., 2014) used a reduced-scale model (Figure 2.37) to simulate the settlement of a compressible soil around a network of rigid inclusions with a diameter (a = 25 mm) and spacing (s = 100 mm, 141 mm, or 200 mm) by displacing a plate.

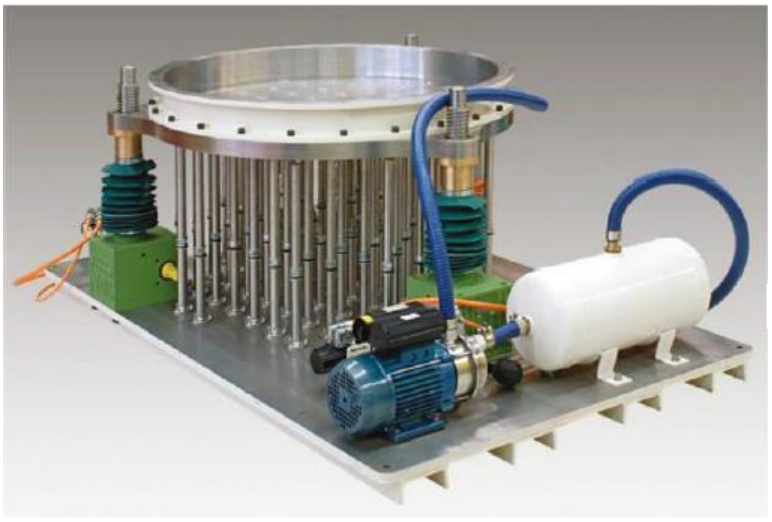

Figure 2.37: Model of (Okyay et al., 2014) study

A granular layer is placed in one or more rings of cumulative height H. Plugs (a = 50 mm) can be added to obtain higher cover ratios. A cylindrical tank with a flexible membrane at the bottom is used to apply homogeneous stress. This load can vary during the test. The researchers

concluded that load transfer increases with the increase of the cover ratio and the mattress thickness. Load transfer does not depend on the constant application of the overload. Surface settlements decrease as the thickness of the mattress increases. Despite not taking into account the reinforcement of the mattress, this model facilitated the execution of numerous tests.

2.6 Overview of constitutive models

The soil is composed of interconnected solid grains surrounded by air and water. When subjected to external loads, the soil exhibits a complex behavior due to the distinct mechanical characteristics of its components. Analyzing and understanding this behavior requires establishing relationships between stresses and strains for the involved materials. These relationships are mathematically expressed through constitutive models, which provide a framework for modeling soil behavior. Over the years, numerous constitutive models have been developed to capture the stress-strain response of soils. These models range from simple to complex, and their formulation is based on principles of solid mechanics based on experimental data or theoretical principles. The complexity and capabilities of these models vary, and the determination of model parameters is not uniform. In the following paragraph, some models are explained in detail.

2.6.1 Linear Elastic Model

The Linear Elastic model is utilized to characterize materials that exhibit small strains, where the stress is directly proportional to the strain. These materials regain their original shape once the applied loads are removed, and their behavior is independent of the rate of loading or straining.

Within the linear elastic range, the constitutive equations are expressed through Hooke's law. The fundamental relationship between stress and strain is fully described by two elastic constants, namely Poisson's ratio (v) and Young's modulus (E). In a homogeneous and isotropic material subjected to a three-dimensional state of stress and strain, the generalized Hooke's Law can be formulated using index notation.

$$\varepsilon_{ij} = \frac{1+v}{E}\sigma_{ij} - \frac{v}{E}\sigma_{kk}\delta_{ij} \tag{13}$$

Or

$$\sigma_{ij} = \frac{E}{1+v}\varepsilon_{ij} + \frac{vE}{(1+v)(1-2v)}\epsilon_{kk}\delta_{ij} \tag{14}$$

In geotechnical analysis, it is often useful to separate the overall state of stress and strain into mean and deviatoric responses.

$$\sigma_{ij} = \frac{1}{3}\sigma_{kk}\delta_{ij} + s_{ij} \qquad \varepsilon_{ij} = \frac{1}{3}\varepsilon_{kk}\delta_{ij} + e_{ij} \tag{15}$$

where s_{ij} is the deviator component of stress, e_{ij} is the distortion or shear deformation produced by the stress deviator s_{ij} and δ_{ij} is the Kronecker Delta function (Equations (16) and (17)), $\sigma_{kk} = \sigma_{xx} + \sigma_{yy} + \sigma_{zz} = 3\sigma_m$ and $\varepsilon_m = \frac{1}{3}\varepsilon_{kk}$ is the mean component.

To describe the relationship between stresses and strains, the generalized Hooke's Law, as presented in Equations (13) and (14), can be reformulated in terms of deviatoric and mean stresses and strains using Equations (15).

$$s_{ij} = 2G_{e_{ij}} \qquad \sigma_{kk} = 3K\varepsilon_{kk} \tag{16}$$

Where K us the bulk modulus and G is the shear modulus.

$$K = E/3(1-2v) \qquad G = E/2(1+v) \tag{17}$$

The linear elastic model is commonly employed in the analysis of concrete structures such as rigid inclusions, piles, transfer structures, and raft foundations. This model assumes a linear relationship between stress and strain, which is expected to remain valid under normal loads.

However, the literature has highlighted certain limitations of the linear elastic model, particularly when comparing theoretical calculations with experimental findings, especially when approaching failure (Lade, 2005). Lade's studies illustrate how the matrix used in elastic calculations may not always accurately represent the behavior of soils. According to the linear elastic theory, normal strains arise solely from normal stresses, and the same principle applies to shear stresses and strains. Nevertheless, practical experience demonstrates that when soil is subjected to shear stresses, it may undergo expansion, leading to an increase in normal (and

volumetric) strain. On the other hand, shear strain increments can occur due to changes in normal stress. As a result, non-linear elastic models have been developed to better approximate the real behavior of soils.

2.6.2 Plastic Model

Unlike elasticity, plasticity refers to the occurrence of irreversible deformations in a material under stress. The total deformation tensor comprises two components:

$$\varepsilon = \varepsilon^e + \varepsilon^p \tag{18}$$

Every model used to describe the behavior of a material must incorporate either a linear or non-linear elastic law, along with a plastic law that involves a yield surface, a flow rule, and a hardening rule.

The yield function is referred to as the plasticity criterion, which defines the limit between the elastic and irreversible deformations of the material. Once this limit is exceeded, the material's behavior becomes irreversible. The stress state and the hardening parameters have an impact on the yield surface, which is a mathematical function designated by the letter f, as illustrated in the equations below.

$$f(\sigma_{ij}, R) = 0 \tag{19}$$

$$\begin{cases} f < 0 \text{ Elastic domain} \\ f > 0 \text{ Impossible domain} \\ f = 0 \text{ The state of stress is on the boundary of the elastic domain} \end{cases}$$

The flow rule is an expression that represents how plastic deformation changes in response to variations in stress and strain. It illustrates the evolution of plastic deformation. Following (Hill, 1950) principle of maximum plastic work, Equation (20) is applicable at any point on the boundary.

$$\dot{\varepsilon^p} = \dot{\lambda}\frac{\partial f}{\partial \sigma} \tag{20}$$

The term $\lambda \geq 0$ is referred to as a plastic multiplier.

The deformation rate is normal to the yield surface, in this case, and this relationship is known as an associated law. Experience, however, does not validate this theory for soils. Therefore, a new concept is introduced, which involves a new plastic potential g represented by the flow rule. This flow rule corresponds to a non-associated law, given by the equation (21).

$$\dot{\varepsilon^p} = \dot{\lambda}\frac{\partial g}{\partial \sigma} \tag{21}$$

This approach takes into account the dilatancy of the material.

For some soil types, experiences have revealed that the yield surface can change when subjected to loading. This change is known as hardening when the surface expands or softening when it contracts.

2.6.2.1 Elastic perfectly Plastic Model with Mohr-Coulomb Failure Criteria

In this model, the yield surface is influenced by the stress state. It remains fixed in the stress space, acting as a failure criterion. Several failure criteria can be found in the literature, including Tresca, Von Mises, Mohr-Coulomb, and Drucker Prager. However, these criteria do not involve the material's hardening behavior and are not suitable for cyclic loadings. Plastic deformations are only possible at the peak level or when the final stress level is reached.
Specifically, the Mohr-Coulomb model combines Hooke's elastic law with Coulomb's failure criterion presented in equations (22) and (23) to describe this model.

$$\tau = \sigma_n \tan\phi + c \tag{22}$$

$$f = \sigma_1 - \sigma_3 + (\sigma_1 + \sigma_3)\sin\phi - 2c\cos\phi \tag{23}$$

The stress-strain relationship of the material consists of a linear elastic region with the Young's modulus E as the slope, followed by a perfectly plastic region at yield. The failure criterion in the (σ_n, τ) plane can be used to determine the friction angle and cohesion by analyzing the slope and y-intercept of the line, as described in equation (22). Additional parameters can be obtained through triaxial tests, as illustrated in (Figure 2.38).

Calculations using this model are efficient due to the constant stiffness. It is applicable to various soil types and is generally considered as an initial approximation of actual soil behavior. One key advantage of this model is its simplicity in formulation, requiring only five parameters:

ϕ, c, E, ν, and ψ, which can be easily determined through simple drained triaxial tests. A limitation of the Mohr-Coulomb model is its assumption of constant stiffness for the material.

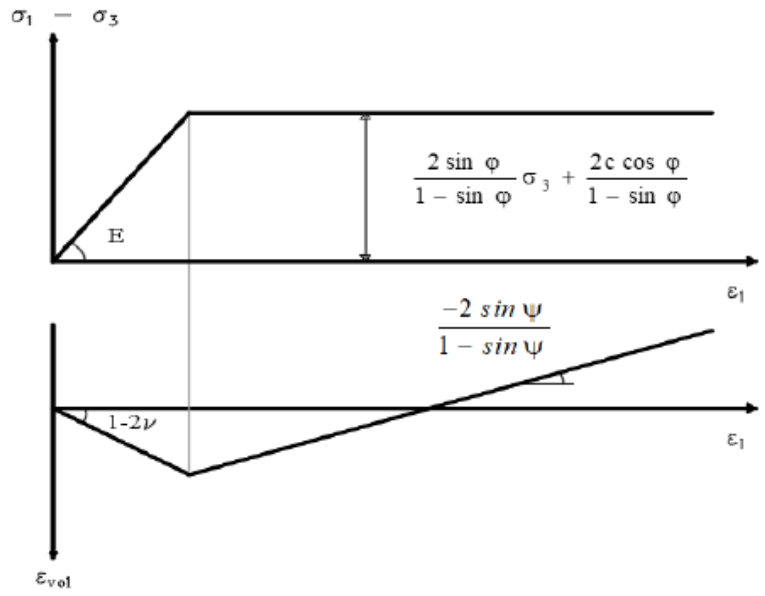

Figure 2.38: Mohr-Coulomb failure criterion based on triaxial test results

2.7 Conclusion

This chapter presents an overview of the research works which were done concerning the dynamic analysis of rigid inclusion systems. The reinforcement of soils with rigid inclusions offers advantages for construction in seismic zones. This reinforcement approach acts as a base isolation mechanism for the structure, under seismic loading. The transfer mattress serves as a zone for energy dissipation, facilitating the dissipation of energy between the structure and the rigid elements. Consequently, it reduces the soil motion transmission to the structure and limits the inertial forces transfer to the soil-inclusions system.

The chapter is divided into four sections:

The first part presents a description of the rigid inclusions system and its fields of applications. A comparison between the rigid inclusions and the pile systems is provided. The essential contrast between these two systems arises from the utilization of the load transfer mattress, and the absence of connectivity between the inclusion and the structure.

Section 2 provides an overview of the soil-structure interaction and the methods employed to address it. Various approaches, including numerical, analytical, and experimental methods, are presented for investigating the soil-structure interaction. Furthermore, previous studies examining the behavior of pile foundations and rigid inclusions under dynamic loading conditions are also discussed. Most of the simulations were carried out in two dimensions. The three-dimensional effect of inclusions is often overlooked and simplified (2D), the reason why it is important to take into account the 3D aspect of the motion of rigid inclusions.

Section 3 focuses on the seismic behavior of the soil and the rigid inclusion system. It begins by providing an overview of various types of dynamic loading. The section then examines the parameters that influence the soil response under dynamic loading, such as the stiffness degradation and increased damping with strain. The increase of the cover ratio and the mattress thickness cause an increase in the load transfer, and when considering elasto-plastic soil conditions, the plasticity of soil results in reduction in the energy transmitted to the superstructure which leads to a decrease in the internal forces transmitted to the rigid elements. In addition, several laboratory tests are presented.

Section 4 provides an overview of prior research investigating the seismic behavior of rigid inclusions, employing both numerical modeling and experimental approaches and a brief description of the constitutive models utilized in this study. In the following chapters, we present an in-depth study of the various aspects of the interaction between soil, mattress and rigid inclusion using a global finite element and finite difference approach. Emphasis will be placed on the kinematic interaction, the effect of the dimensions of the inclusions, the properties of the soil and the mattress, the presence of a foundation and the non-linearity of the system.

CHAPTER 3: LINEAR NUMERICAL ANALYSIS OF SEISMIC BEHAVIOR OF RIGID INCLUSION

3.1 Introduction

The literature review revealed that the use of rigid inclusions in seismic risk zones presents an interesting concept. In the context of seismic loading, this reinforcement system can be considered as an insulation system located at the base of the structure. The load transfer mattress acts as an energy dissipation zone that allows energy to be transmitted between the structure and the rigid reinforcement elements, thereby reducing the inertial effects of the superstructure.

This chapter focuses on the investigation the kinematic interaction within the soil-mattress-inclusions system. The analysis is carried out using a comprehensive approach in which the response of all elements of the system subjected to seismic loading is calculated. This is done using a three-dimensional linear modeling of the reinforcement system. This analysis becomes particularly useful when conducting a decoupled analysis of the system with superstructure, wherein the solicitation at the base of the structure is first determined (kinematic interaction), and then used to assess the response of the structure (inertial interaction).

The chapter consists of three main parts. The first part focuses on identifying the optimal modeling technique for rigid inclusions, while the second part presents a comprehensive analysis using a numerical model. This analysis deals with a soil system reinforced by a group of 5x5 rigid inclusions. The final part of this chapter is dedicated to the study of the impact of key parameters on the seismic response of the rigid inclusions. The results obtained from these calculations were compared in terms of displacements and internal forces within the inclusions.

3.2 Numerical modeling using Finite Element Method

The finite element approach allows determining the behavior of both the inclusions and the surrounding soil. Modeling the behavior of inclusions requires knowledge of their geometric and mechanical characteristics, as well as selecting a suitable soil behavior law which is considered the main characteristic of this method. The level of precision in considering this behavior will therefore determine the quality of the obtained solutions.

3.2.1 Finite Element Method

The finite element method permits, by discretizing the spatial domain of the real medium, the computation of an approximate solution for the set of differential equations governing the equilibrium problem of a medium subjected to boundary conditions specified in terms of forces and/or displacements. It involves replacing the physical structure under study with a finite number of elements, which constitute a mesh. These elements are interconnected through a set of points known as nodes. Initially, the behavior of each independent part is considered, and then these parts are assembled in a manner that ensures force equilibrium and compatibility of the actual displacements within the structure.

The finite element method is a highly efficient technique as it allows for the precise examination of continuous structures characterized by intricate geometric properties and complex loading conditions.
Inclusions behavior can be modeled with the finite element method through three different approaches: a two-dimensional representation (using plane stress or plane strain), an axisymmetric approach (accounting for a rotational symmetry), or a three-dimensional approach.

The three-dimensional approach is considered the most realistic option as it takes into account the unique phenomena that occur at the soil-inclusion interface, such as sliding and detachment. It also allows the incorporating of soil nonlinearity in all its aspects. To execute the 3D technique, substantial resources are needed to create a detailed mesh around the inclusions.

3.2.2 Three-dimensional Finite Element Software (Code Aster)

Code ASTER is an open-source software for numerical simulation in structural mechanics, primarily developed by the "mechanical and acoustic analysis" department of EDF's R&D service.

The numerical analyses were conducted using the Code Aster. This software involves an unconventional application of the finite element method. It solves static/quasi-static or dynamic problems through the dynamic equilibrium equation in both the frequency and time domains. Primarily, it is a solver based on the theory of continuum mechanics, employing the finite element method to address various mechanical, thermal, acoustic, seismic, and other types of problems.

Code aster aims to perform structural calculations for phenomena such as thermal, mechanical, thermomechanical, or thermo-hydro-mechanical coupling, including both linear and nonlinear behaviors. The nonlinearities incorporate material behaviors (such as plasticity, viscoplasticity, damage, hydration and drying of concrete, etc.), large deformations or rotations, and contact with friction.

Common industrial studies require the utilization of meshing and graphical visualization tools, which are not included within the code itself. However, several tools can be employed for these operations through integrated interface procedures within the code. In the case of this thesis, 'Salome Meca' is being utilized.

3.2.3 Meshing and time discretization

In dynamic analysis, mesh configuration should ensure accurate wave transmission within the domain. The size of mesh elements must be sufficiently small to allow for the proper transmission of waves without numerical distortion. This size depends on the frequencies involved and the wave propagation velocity. A commonly applied empirical rule in the Finite Element Method (FEM) suggests that the presence of at least 10 points per wavelength is typically satisfactory when employing linear elastic finite elements. (Watanabe et al., 2017) discussed and validated this rule and indicated that the mesh employed in propagation problems must meet the following criterion:

$$\Delta x_{FEM} = \frac{V_s}{10 \times f_{max}} \tag{24}$$

Where Δx_{FEM} and f_{max} represent the maximum dimension of an element and the highest frequency to be transmitted, respectively, and Vs indicates the shear wave propagation velocity.

3.2.4 Boundary Condition

Conventional numerical methods require modelling within a limited domain. In static cases,

artificial boundaries are introduced at a certain distance from the region of interest. Conversely, in dynamic cases, these boundaries cause wave reflections and impede energy dissipation. By using a larger domain, this effect can be reduced as most of the energy is dissipated within the domain. It should be noted that using a larger model will result in a longer computation time. One way to overcome this challenge is to use absorbing boundaries. When dynamically modelling a structure, it is important to position the boundaries at a sufficient distance from the structure to minimize wave reflection. When the damping factor is high, this required distance is relatively small (Seed et al., 1975). Conversely, when the damping factor is low, a much greater distance is required, resulting in an excessively large and impractical model.

The solution is to configure these boundaries to effectively simulate free field motion by absorbing waves from the structure. However, for the absorbing boundaries to be efficient, they should be placed at a certain distance from the structure and the foundation.

Code Aster uses specialised elements, known as paraxial elements (Code Aster, 2017), which are used to satisfy the Sommerfeld condition. They are used to apply the dynamic excitation and to eliminate diffracted plane waves and prevent their reflection back into the domain.

3.3 Rigid inclusion modeling

In three-dimensional numerical analyses, researchers have employed various strategies to model piles and rigid inclusions, (Banerjee et al., 2014; Giannakos et al., 2012; Goh and Zhang, 2017; Kourkoulis et al., 2012a; Van Nguyen et al., 2017), including volumetric element, beam element, hybrid method and pile void method.

3.3.1 Volumetric element

This approach implies utilizing solid elements or zones that are configured to replicate the geometric properties of the inclusions (Figure 3.1). These zones are similar to the ones used for modeling the soil but possess distinct material characteristics (Hazzar et al., 2017; Van Nguyen et al., 2017). The main advantage of this technique is that it takes into account the physical cross-sectional area of the rigid inclusion. However, extracting internal forces can be challenging due to the need for additional post-processing techniques and data manipulation.

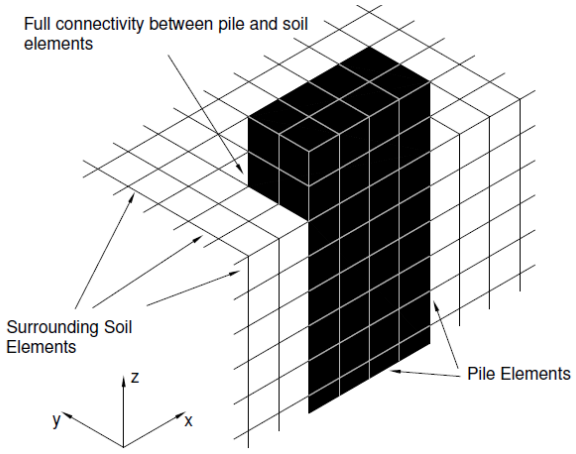

Figure 3.1: Isometric view of solid element model (Wotherspoon, 2006)

3.3.2 Beam element

This approach involves employing structural elements within the software, specifically the beam element (Sadek and Shahrour, 2004). This element type is a two-noded finite element with six degrees of freedom per node, with three translational and three rotational components.

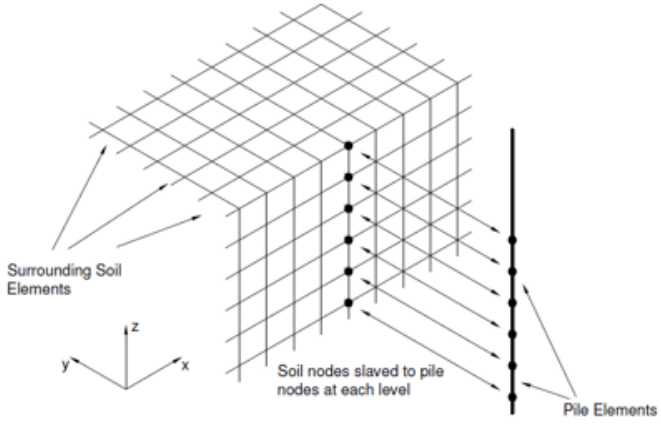

Figure 3.2: Isometric view of beam element modelling (Wotherspoon, 2006)

This technique, (Figure 3.2), consists of representing the inclusions by beam elements, which are rigidly connected to the soil. Loads are transferred between the inclusions and the soil through the nodes connected at different depths. This method allows to reduce time calculation. Another advantage of this method is that the internal forces can be easily determined despite its drawback of not considering the physical cross-sectional area of the rigid element.

3.3.3 Hybrid method

This technique involves representing the vertical reinforcements by incorporating solid elements with beam elements positioned along their central axis with reduced flexural rigidity (Banerjee et al., 2014; Lopez Jimenez, 2019). Generally, the flexural rigidity of the beam element (EI) is set at a value 10^{-6} times that of the flexural rigidity of the inclusion. The internal forces in the rigid elements are determined by multiplying the calculated forces in the beam elements by the scaling factor of 10^{6}. This method simplifies the assessment of internal forces in the vertical reinforcements while considering the physical cross-section of the rigid element. Additionally, it allows for the detection of sliding and detachment of the rigid elements from the surrounding soil using interface elements.

3.3.4 Pile void method

The pile void method consists of modelling the vertical reinforcements as void elements with the introduction of beam elements in their central axis. For each depth, connection conditions are defined between the inclusion nodes and the nodes of the void's boundary, as shown in (Figure 3.3). The use of this method makes it easy to determine the internal forces in the vertical reinforcements, taking into account the physical cross section of the rigid elements (Giannakos et al., 2012; Wotherspoon, 2006). This method is extensively utilized and highly recommended, when considering the volumetric shape of rigid inclusions, over the hybrid method while working with code Aster.

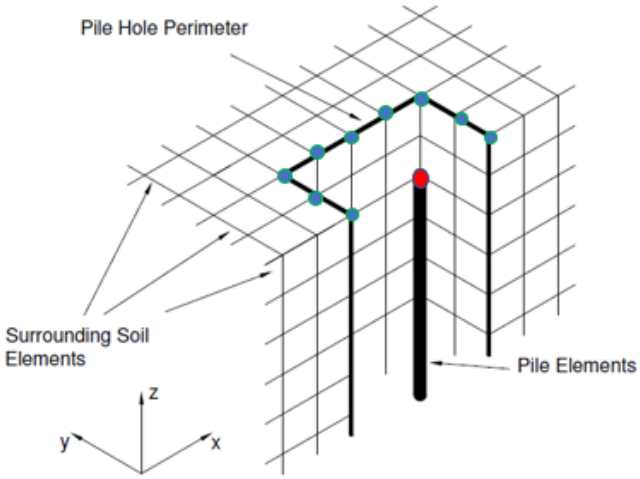

Figure 3.3: Isometric view of the pile void model (Wotherspoon, 2006)

3.4 One rigid inclusion Numerical Model

To examine the influence of various modeling techniques for rigid inclusions on the system responses and determine the optimal approach for integrating the rigid inclusion into the reference model, a dedicated analysis of a single rigid inclusion is conducted. This analysis employs the Finite Element Method (FEM) with code Aster. The geometry is provided by the "Salome-Meca" software. In this analysis, beam elements and pile void approaches (Figure 3.4) are utilized to simulate the behavior of a single rigid inclusion subjected to dynamic loading.

3.4.1 Model geometry and characteristics

This case study focuses on a simple model measuring 3 x 3 x 15 m^3 containing one rectangular rigid inclusion of dimensions 0.4 m x 0.4m and a length 9.5m placed in the center of the model. The implementation of a rectangular shape was recommended to simplify the mesh generation of the model when using code Aster. It is a floating inclusion situated within a soil layer that possesses uniform mechanical properties at different depths. A load transfer mattress, with dimensions of 1 x 1 x 0.5 m^3, is directly placed on the rigid inclusion without being anchored. The soil and the mattress are modelled with 8-node hexahedral elements and the inclusion is modelled with both the beam element method and the pile void method. Soil, mattress, and rigid inclusion properties are provided in (Table 3.1). The choice of these properties was based on a comprehensive review of relevant literature sources (Guide AFPS/CFMS, 2013), (Eurocode EC8, 1998).

The soil has an Elastic modulus (Es) of 97 MPa, a Poisson's ratio (υ) of 0.35 and a density (ρ) of 1610 kg/m^3. The fundamental frequency of the soil is 2.5 Hz, and the mechanical behavior of the soil, mattress, and rigid inclusion is simulated using a linear elastic constitutive model. The rigid inclusion is defined using concrete material. No interface is considered between the inclusion and the compressible soil. Table 2.1 summarizes material parameters used in this study.

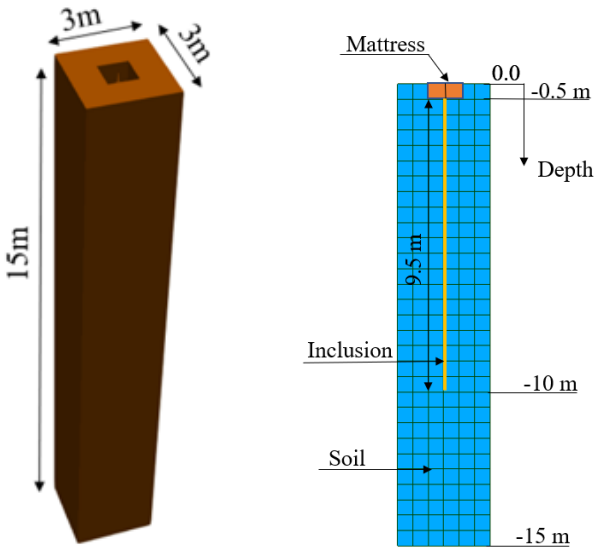

Figure 3.4: Basic geometry of the numerical model, a) Pile Void method, b) Beam element method

Parameters	Rigid inclusion	LTP	Soft soil
Young Modulus E (MPa)	40000	200	95
Volumetric weight (kg/m³)	2500	1800	1610
Poisson's ratio	0.2	0.3	0.35

Table 3.1: Material properties considered for the numerical model

3.4.2 Dynamic input motion

The study is performed using the earthquake record "Friuli, Italy-01" that occurred in Italy, Tolmezzo, with maximum acceleration of 0.25g m/s² and a magnitude of 6.5. Figure 3.5 provide detailed information regarding this specific recording. The loading is applied in the form of imposed velocity at the base of the model in the Y direction. Additionally, Rayleigh damping is applied to the soft soil, with a damping ratio of 5%. In order to minimize wave reflections at the model boundaries during dynamic calculations, it is necessary to apply suitable boundary conditions. To achieve this, the paraxial elements, available in code Aster are used because of their capability not just for imposing dynamic excitations but also for absorbing the outgoing diffracted waves.

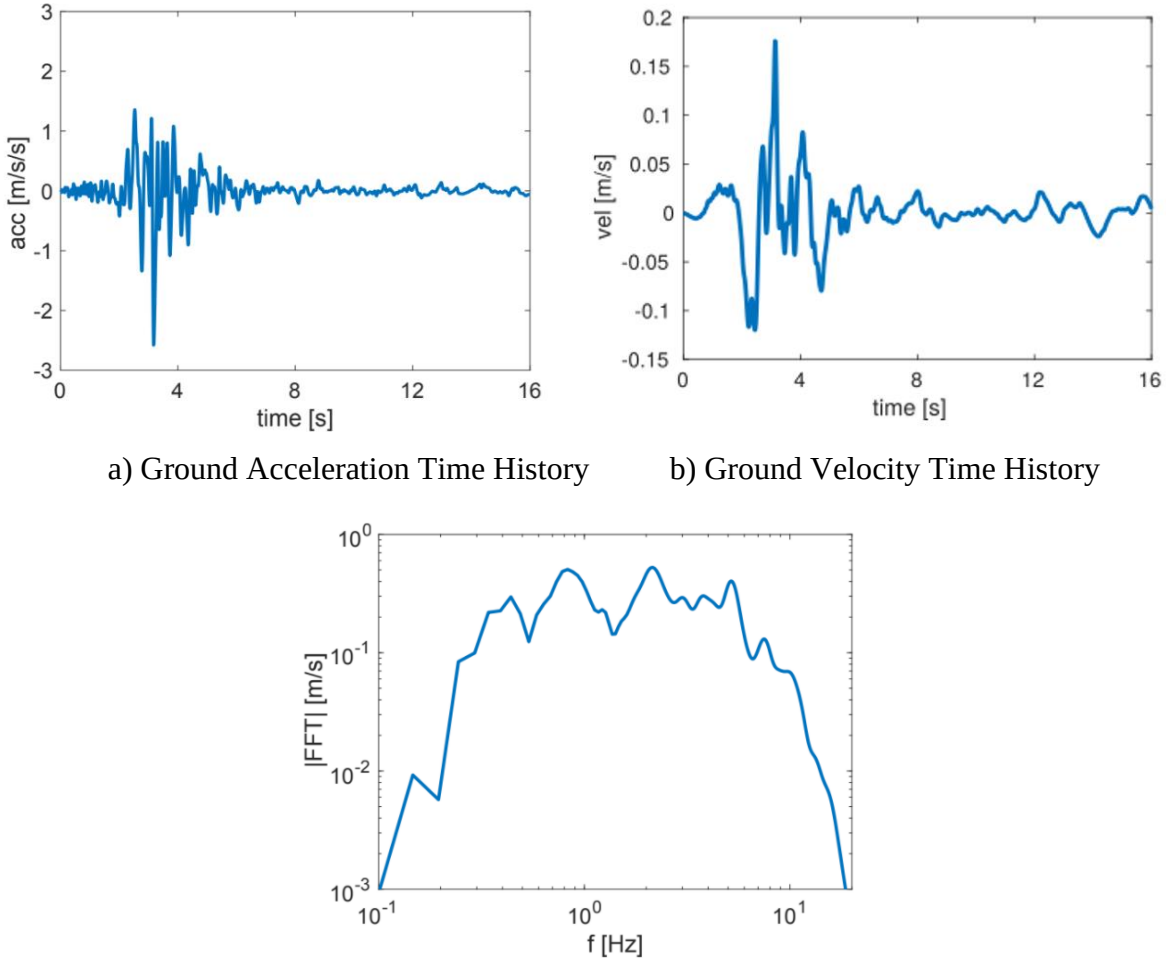

a) Ground Acceleration Time History b) Ground Velocity Time History

c) Fourier Amplitude Spectrum

Figure 3.5: Dynamic input motion: a) Ground Acceleration time history, b) Ground Velocity time history, and c) Fourier Amplitude Spectrum

3.5 Results and discussion

3.5.1 Reference case

In this section, we examine the effect of the inclusion modeling technique on the seismic response of the soil-inclusion-mattress system. (Figure 3.6) provides a comparative analysis of the internal forces generated by employing both the beam element (BE) method and the pile void (PV) method for modeling the inclusion. The bending moment of the inclusion in both modeling methods (Figure 3.6-a) exhibits a relatively consistent behavior within a depth range of 2.5 to 7.5 meters, with slight deviations observed near the upper and lower parts of the inclusion. The results reveal an increase of 40% in the bending moment at a depth of 1m and 9m when adopting the pile void method for modeling the rigid inclusion, compared to the beam element approach. Similarly, the shear forces (Figure 3.6-b) display a 15% increase in the moment at 1m depth when employing the pile void method. However, this tendency is not the

same beyond 7.5m, where the pile void method shows a decrease of 35% at 9m depth compared to the beam element method.

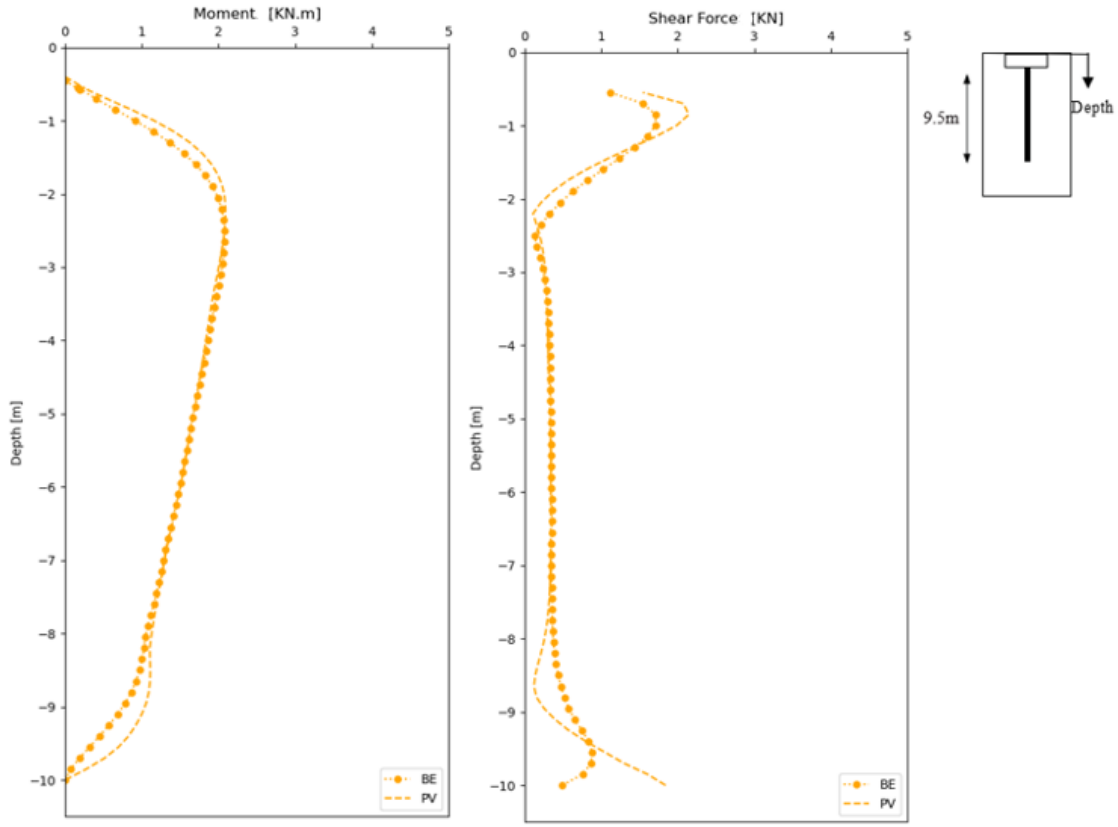

a) Maximum bending moment b) Maximum shear force

Figure 3.6: Efforts in the inclusion with different modelling techniques

3.5.2 Parametric study

This section presents a study to examine the impact of inclusion dimensions, and soil rigidity on the response of the rigid inclusion employing different modelling techniques.

3.5.2.1 Influence of the RI dimensions

In order to analyze how inclusion dimensions, impact the variations between the results obtained from different inclusion modeling techniques, calculations were performed on the reference example of single rigid inclusion, considering three different dimensions (0.4 x 0.4 m², 0.6 x 0.6 m², and 0.9 x 0.9 m²). (Figure 3.7) illustrates the maximum bending moments and shear forces for different inclusion dimensions modeled using both the beam element and pile void methods. The findings indicate that increasing the dimensions of the inclusion amplifies the disparity in results between the two methods used for modeling the inclusion (Figure 3.7-

a).

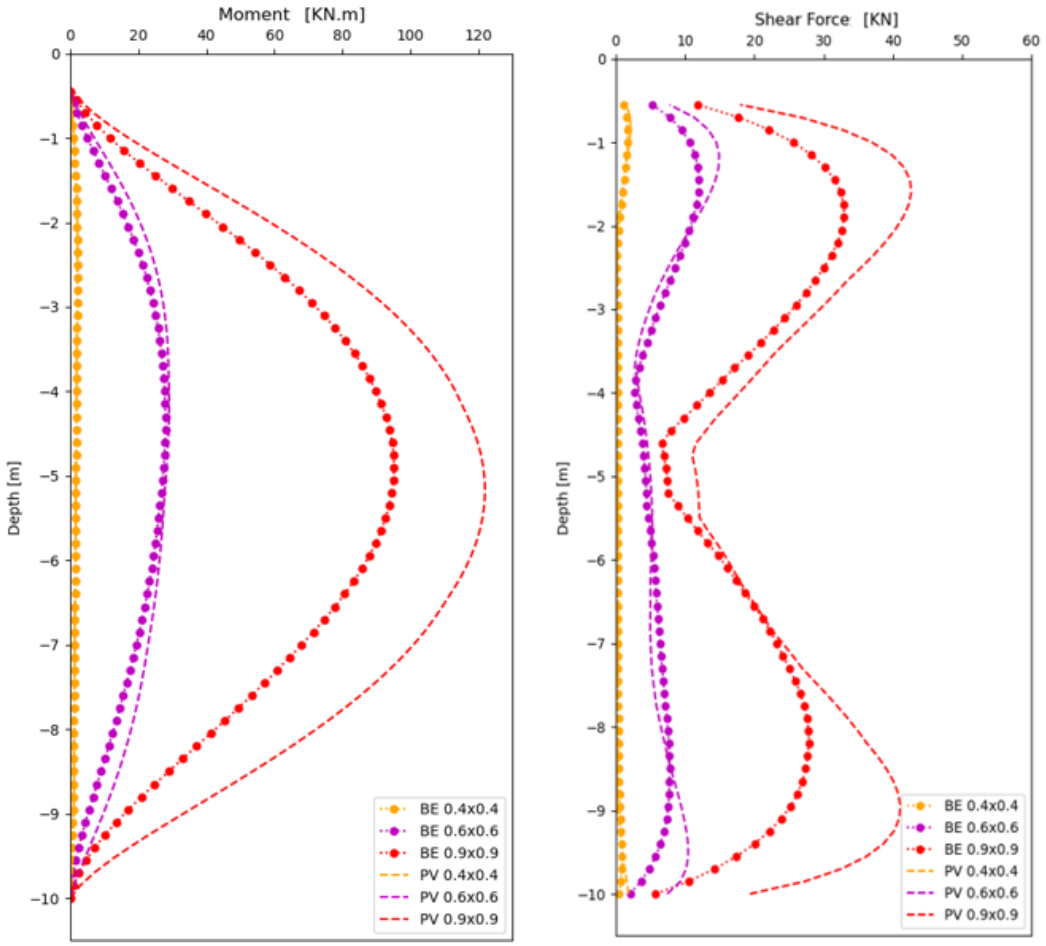

a) Bending moment b) Shear force

Figure 3.7: Efforts in the inclusion with different modelling techniques for different inclusion dimension

For the 0.4 x 0.4 m² dimensions, the results show no significant differences except for slight variations observed at the top and bottom sections of the inclusion. This constant behavior is also observed for the 0.6 x 0.6 m² dimensions. Within the depth range of 4 to 6 meters, both the beam element method and pile void method demonstrate a relatively stable behavior in terms of the bending moment of the inclusion. However, as the depth approaches the upper and lower parts of the inclusion, slight deviations become noticeable. Specifically, at a depth of 2 meters, where the beam element method exhibits a bending moment of 16.7 kN.m, whereas the pile void method indicates a moment of 21 kN.m.

However, as the dimension of the inclusion increases reaching 0.9 x 0.9 m², the disparity becomes more pronounced, resulting in a 27% difference at a depth of 5m, which corresponds to the maximum moment. At this depth, the pile void method produces a higher moment of

121.5 kN.m, compared to the 95.5 kN.m obtained with the beam element method.
Concerning the shear forces (Figure 3.7-b), the results demonstrate that as the dimensions of the inclusion increase, the disparity between the results obtained from both methods also increases.

We can conclude that for small rigid inclusion dimensions, the difference between the results calculated by the two modelling techniques remains insignificant. And as the inclusion dimensions become significantly larger, the "beam element" method tends to oversimplify the behaviour of the inclusion. This oversimplification can lead to differences in the calculated moments compared to the pile void method. As dimensions increase, the assumptions and simplifications made in the beam element method may become less accurate in capturing the true behaviour and interaction of the inclusion with the surrounding system. Consequently, the beam element method may underestimate the true moments, whereas the more comprehensive pile void method, which takes into account the volume and interaction of the inclusion, provides more accurate and reliable results.

3.5.2.2 Influence of soil rigidity

(Figure 3.8) highlights the impact of soil rigidity on the responses obtained using different inclusion modeling techniques. The results indicate that there is no noticeable distinction between the beam element and pile void methods at depths between 2 and 8 meters for both the 30MPa and 95MPa moduli and between 3 and 7 meters for a modulus of 150 MPa. As we move closer to the head and the base of the inclusion, a small distinction becomes apparent between the results obtained from the two modeling techniques.

At a depth of 1m, the moments obtained by the beam element method are 3.6 kN.m, 1.6 kN.m, and 1.1 kN.m for soil modulus values of 30MPa, 95MPa, and 150 MPa, respectively (Figure 3.8-a). These moments increase to the following values: 4.2 kN.m, 1.8 kN.m, and 1.3 kN.m for the pile void method. However, this variation remains negligible, indicating that the soil rigidity does not significantly influence the choice of the inclusion modeling method.

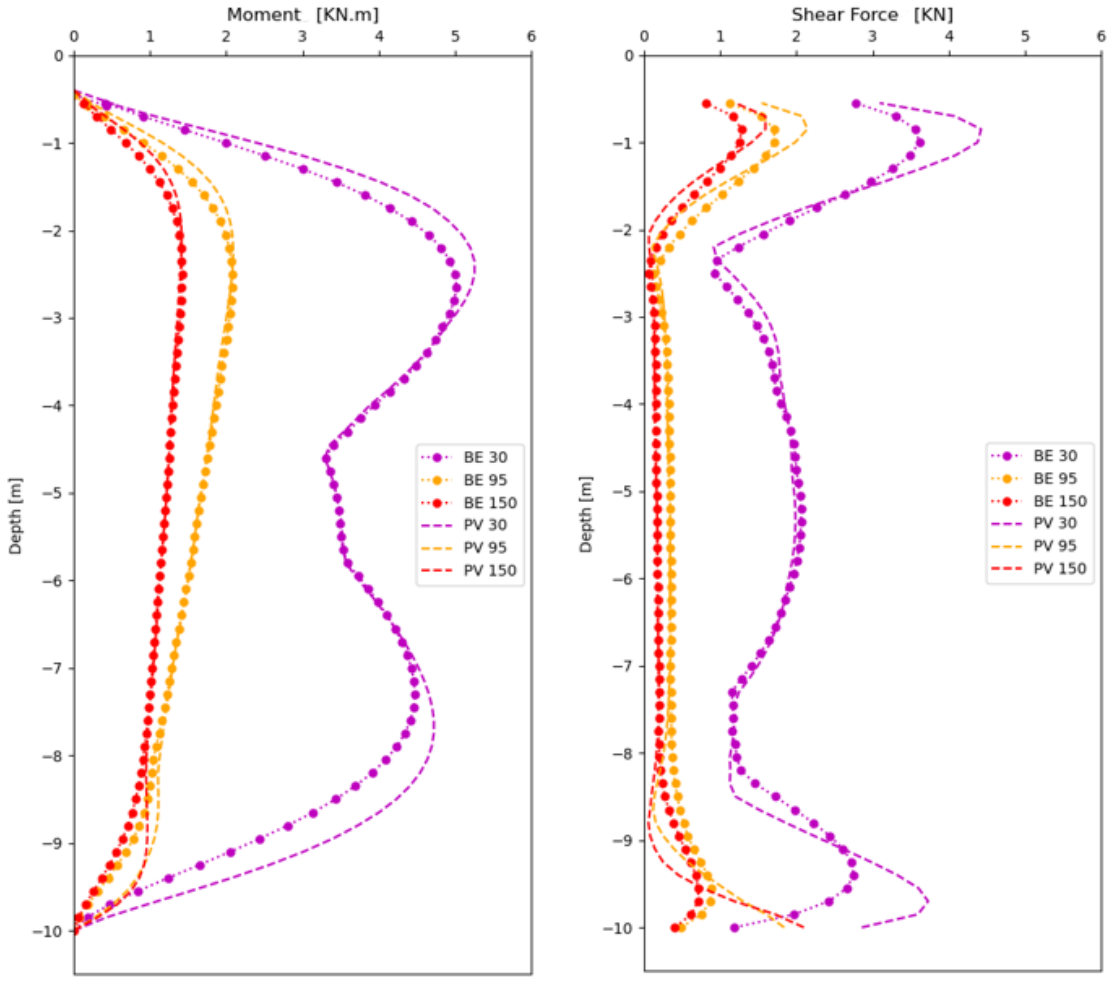

a) Bending moment b) Shear force

Figure 3.8: Efforts in the inclusion with different modelling techniques for different soil rigidity

The results obtained for the shear forces (Figure 3.8-b) exhibit a similar pattern of variation as the moments.

The primary objective of this study is to determine the optimal approach for modeling the inclusion in the reference model. To ensure the direct applicability of the chosen method, the parameters used in this study are aligned with those used in the reference model. The results of this study indicate that the beam element method is suitable for the reference model. The utilization of this technique offers many advantages including simplified meshing, reduced calculation time, and simple determination of the internal forces.

3.6 Presentation of the reference model of a group of rigid inclusions

3.6.1 Introduction

The present work aims to evaluate the kinematic interaction of a soil-mattress-inclusion system under seismic waves. In order to understand the seismic behavior of the system, a three-dimensional finite element method (FEM) is employed using (code Aster). The geometry of the domain is provided by 'Salome-Meca'. The model consists of 3D 8-node hexahedral elements representing the soil and the mattress, and beam elements representing the inclusions.
The particular choice of beam elements to represent the rigid inclusions is based on the previous analysis (Section 3.3.2) which showed no significant difference between the two modelling methods for small inclusion dimensions. Furthermore, the beam element facilitates the calculation of internal forces in the inclusions.

3.6.2 Geometry of the reference model

This study presents a full FEM 3D model comprising 25 floating rigid inclusions. The dimensions of the soil volume considered in this study are 35 x 35 x 15 m³. The model focuses on a group of 5 x 5 rigid inclusions of 40 cm diameter with a length of L=9.5 m each, resulting in a length-to-diameter ratio of 23.75, embedded in a 15m soft soil with uniform mechanical properties. (Figure 3.9) illustrates the discretization of the model. The numerical model comprises 147000 hexahedral zones that represent the soil mass.

The dimensions of the discretized model and the element size were chosen in accordance with the large wavelength principle (Kuhlemeyer and Lysmer, 1973). The maximum size of the elements composing the model was set to 1m, allowing for the application of frequencies between 0 and 15 Hz without any disruptions caused by the zone dimensions (Section 3.2.3).

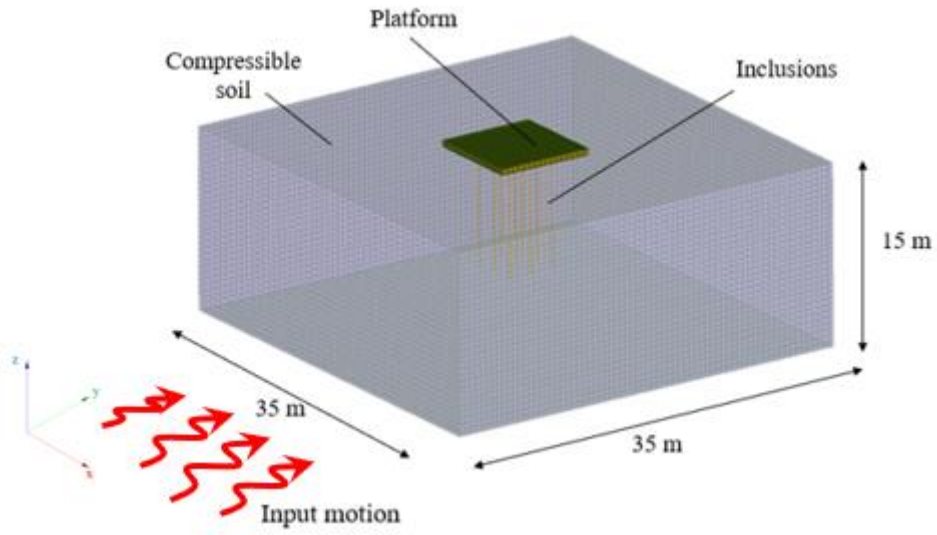

Figure 3.9: Basic geometry of the numerical model

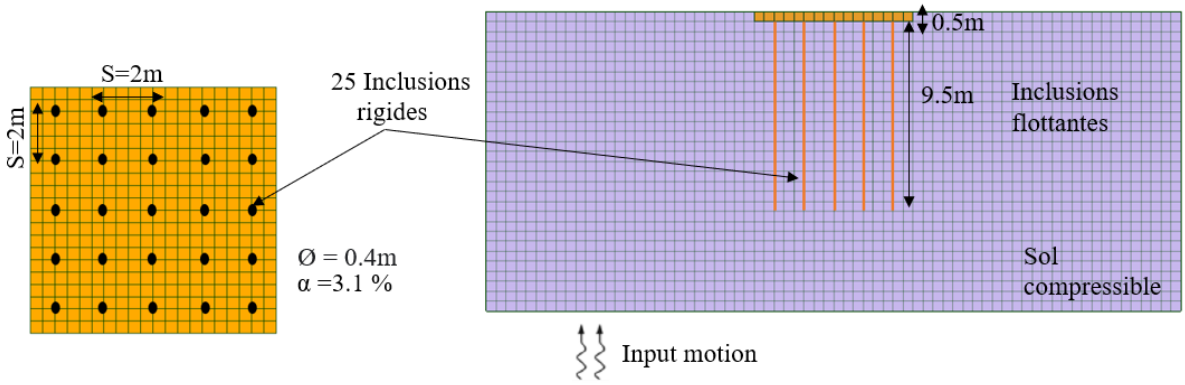

Figure 3.10: Plan view of the mattress and cross-section of the model

The inclusion elements were arranged in a 5 × 5 rectangular grids, with a separation distance of S=2 m in both directions, (S/D = 5) with a cover ratio of 3.4% (Figure 3.10). The cover ratio represents the ratio between the surface area of a rigid element to its reinforced area.

A load transfer platform, measuring 0.50 m in height, was installed above the rigid inclusions without any anchoring. This specific height value falls within the range commonly employed in similar studies investigating rigid inclusion systems subjected to dynamic loading. Previous studies such as (Hatem, 2009; Lopez Jimenez, 2019; Messioud et al., 2016; Okyay et al., 2012) have utilized a thickness of 0.6m for the platform.

Soil, mattress, and inclusions parameters can be found in (Table 3.1). The shear wave velocity for the soft soil is around 150 m/s. The model does not incorporate the presence of a water table.

In terms of the material properties of the rigid inclusion, the young's modulus was selected as 40 GPa, a value commonly found within the typical range for concrete in deep foundation applications. The behavior of soil, mattress, and rigid inclusions is considered as linear elastic.

In order to incorporate the damping effects in the soil, a Rayleigh damping approach was implemented with a damping factor of 5%. This value falls within the typical range of 1% to 5% commonly used to account for damping effects (Hatem, 2009; Lopez Jimenez, 2019). More details of Rayleigh damping can be referenced in (section 2.4.2.3 of chapter 2).

3.6.3 Rigid inclusions and boundary conditions

To accurately represent the semi-infinite nature of the soil deposits, artificial boundaries were implemented. In the static analysis phase, the side boundaries were fixed horizontally, while the bottom boundary was fixed in all directions. However, for the dynamic analysis, these initial boundary conditions were substituted with paraxial boundaries at the model's base to apply the velocity input, and at the sides to prevent wave reflections.

3.6.4 Dynamic input motion

The dynamic analyses in this study were conducted using the seismic records of the Friuli earthquake. The original earthquake record is presented in (Figure 3.5).

In order to compute the fundamental frequency of the soil, the shear wave velocity-based equation $fn = (2n - 1) Vs/4H$ can be utilized. In this equation, Vs denotes the velocity of shear waves (m/s), H represents the overall depth of the layer (m), and n indicates the mode number (Kramer, 1996). In situations with minimal damping, the resonant frequency closely approximates the natural frequency. In the context of the analyzed soil profile, the fundamental frequency is derived based on the elastic response observed in the free field, resulting in a calculated value of 2.5 Hz.

3.7 Rigid vertical element response

3.7.1 Analysis procedure

The analysis procedure begins with the generation of an initial stress state. Next, the vertical reinforcements are installed, and the model is brought to equilibrium under the influence of the vertical elements weight. The final step of the static analysis involves activating the earth platform. For the dynamic analysis, absorbing boundaries are introduced, and the dynamic

calculations are performed by applying shear waves using velocity at the base of the model.

3.7.2 Accelerations

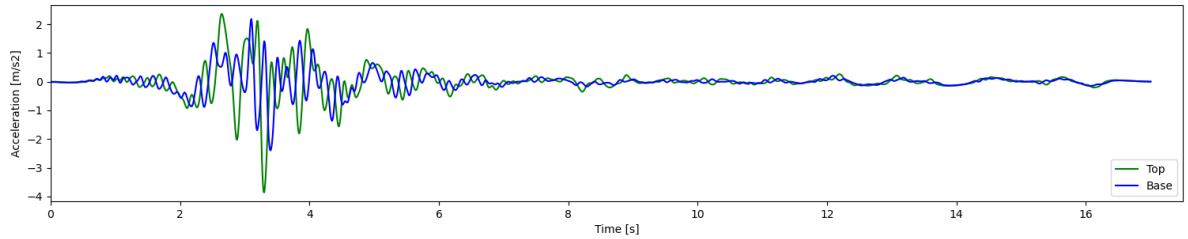

Figure 3.11: Surface and base acceleration

(Figure 3.11) presents a comparison of the acceleration profiles obtained at the top and the base of the model. The maximum absolute acceleration value recorded at the surface of the model reaches 3.8 m/s², indicating a 1.5 times amplification compared to the input motion at the base. The acceleration measurements at the surface are out of phase with the ones at the base. This difference is caused by the way rigid inclusion groups move, affecting the motion at the surface (kinematic interaction).

3.7.3 Shear forces and bending moments

(Figure 3.12) illustrates the internal forces induced in the central rigid inclusion. The graphs display the envelope of the bending moments and shear forces. It is observed that the bending moment exhibits a typical profile with a maximum value of 7.5 kN.m at 3m Depth. While the shear forces reach, their maximum value of 5 kN at the top of the inclusion. These results represent the baseline case and serve as a point of reference for comparing the outcomes of the parametric study.

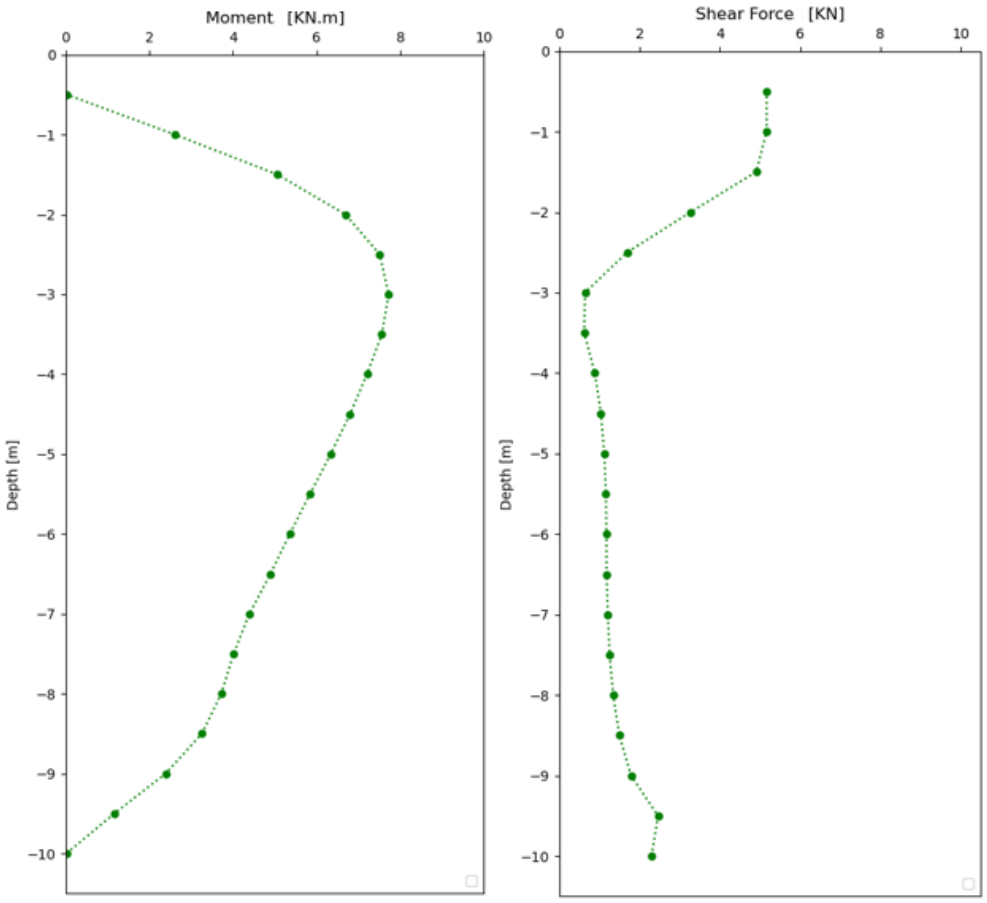

a) Bending moment b) Shear force

Figure 3.12: Internal forces distribution within the central rigid inclusion

3.7.4 Horizontal displacements

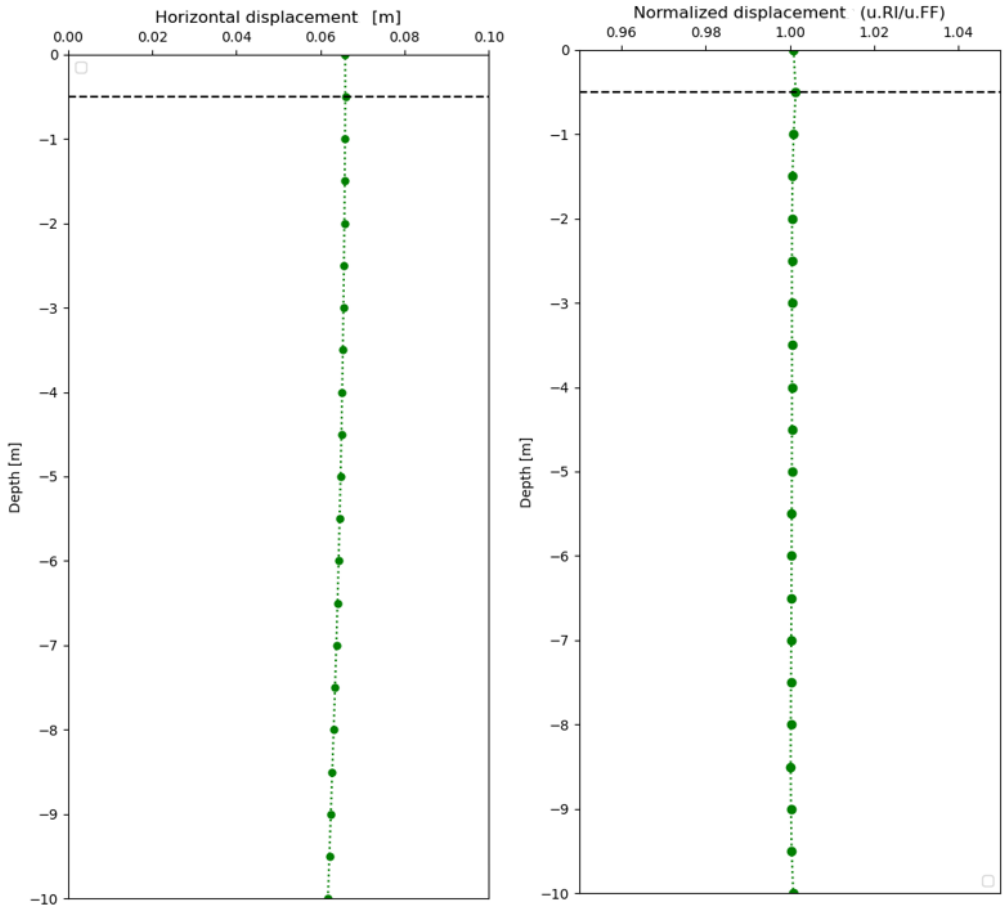

a) Horizontal displacement b) Normalized displacement

Figure 3.13: Maximum and normalized horizontal displacement

(Figure 3.13-a) showcases the variation in displacements within the central rigid inclusion as a function of depth. The displacements within the inclusions exhibit a linear relationship, with the highest value observed at the top (0.067 m) and gradually decreasing towards the base.
The displacement values are normalized relative to those of the free field and are presented in (Figure 3.13-b). The variation in displacements within the inclusion remains extremely small.

3.8 Parametric study

In this section, a detailed analysis is carried out to assess the impact of various parameters on the kinematic interaction between soil, mattress, and inclusions. The parameters investigated include the inclusions diameter, depth, and position. Furthermore, the influence of soil and mattress mechanical properties especially its rigidity is also investigated. The section provides an overview of the shear forces, and bending moments experienced along the rigid elements.

The values presented correspond to the maximum values recorded during the dynamic analysis at the central rigid inclusion. The curves initiate at a depth of 0.5m, indicating the top of the inclusion, and it ends at a depth of 10m, indicating the base of the inclusion. These parametric analyses offer valuable comprehension of the behavior and performance of the rigid inclusions.

3.8.1 Influence of the diameter of the rigid inclusion

The diameter of the rigid inclusions is recognized as an important parameter that influences their response and plays a crucial role in the design of reinforcement systems.

(Figure 3.14) illustrate the influence of the inclusion diameters on the internal forces along the inclusion. In (Figure 3.14-a) the bending moment envelope is presented for different diameters of rigid inclusions, ranging from 0.3m to 0.6m. The depicted values follow an approximately parabolic relationship, with zero values at both the head and the base of the inclusion. The bending moment reaches its maximum of 7.5 kN.m for the reference case with a diameter (Φ) of 0.4m at a depth of 4m. The findings indicate that as the diameter increases, the moment also increases, reaching approximately four times the magnitude of the reference case when the diameter is 0.6m, reaching a value of 32 kN.m. However, the bending moments decrease by a factor of two as the inclusion diameter decreases from 0.4 to 0.3 reaching 3.5 kN.m.

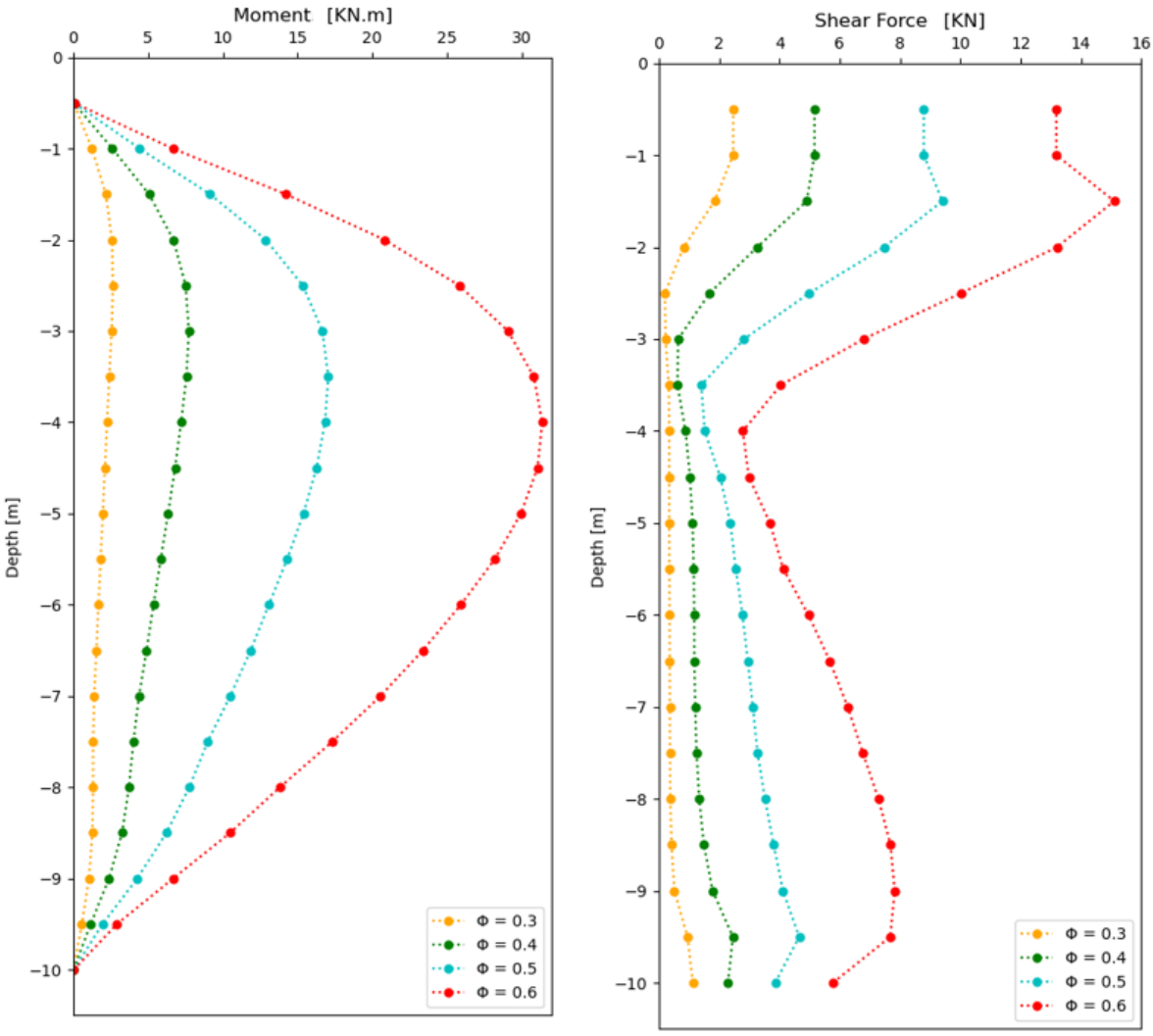

a) Bending moment b) Shear force

Figure 3.14: Influence of the inclusions diameter on the efforts along the central rigid elements

Regarding the shear forces (Figure 3.14-b), it is observed that increasing the diameter results in a significant augmentation of these forces. The maximum shear forces are observed at a depth of 1.5 m for all the examined diameters. Notably, for a diameter of 0.6m, the shear force reaches a substantial magnitude of 15.5 KN, which is three times greater than the reference case that has a value of 5 KN. However, for a diameter of 0.3m, the shear forces decrease, reaching a magnitude that is two times smaller (2.4KN) than the reference model.

(Figure 3.15) illustrates the variation of the horizontal displacements of the central rigid inclusion normalized to the free field for various diameters as a function of depth. The first 0.5m correspond to the displacement in the mattress. The obtained results indicate that the displacement of the inclusion head increases when the diameter of the rigid inclusions increases.

The displacement at the head and base of the inclusion with a diameter of 0.6m is slightly larger compared to the reference case, but this variation remains negligible.

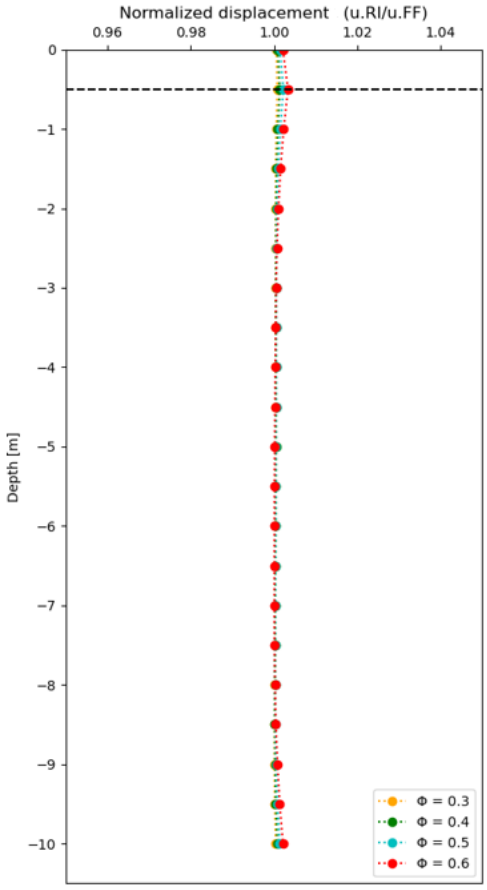

Figure 3.15: Influence of the inclusions diameter on the normalized horizontal displacement

3.8.2 Influence of the rigidity of the soil

The analysis was performed for three different soil rigidity (Es = 30, 95, 150 MPa), while the other parameters remained identical to the reference case study. The results of this analysis are shown in (Figure 3.16). It is worth noting that the soil rigidity has a significant impact on the system response. Increasing the elastic modulus from 30 MPa to 150 MPa reduces the maximum bending moment from 15 kN.m to 6 kN.m respectively which means a reduction of 60% from the reference case at 3m depth. This is due to the stiffer soil surrounded the inclusions which provides lateral support. Similarly, the shear forces at the same depth have decreased from 3kN to 0.4kN, indicating a reduction of 87% compared to the results of the reference case. The maximum shear forces are observed at 1m depth.

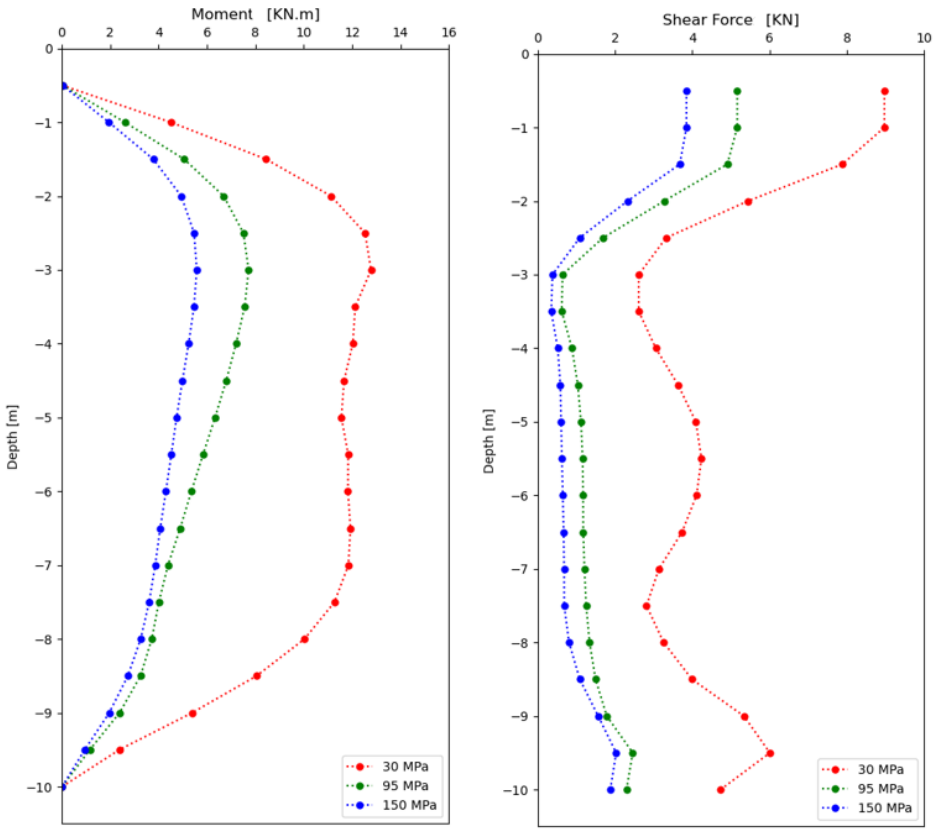

a) Bending moment b) Shear force

Figure 3.16: Influence of the soil property on the bending moment along the rigid vertical elements.

3.8.3 Influence of the length of the rigid inclusion

(Figure 3.17) illustrates the variations in bending moment and shear forces for three distinct lengths of floating rigid inclusions: 4.5m, 9.5m, and 14m. It is evident from the analysis that, irrespective of the inclusion length whether 9.5m or 14m, the bending moment reaches its peak magnitude of 8 kN.m at a depth of 3m. However, for the 4.5m length inclusion, the maximum bending moment is reached at a slightly shallower depth of 2.5m, measuring 7.5 kN.m.

Initially, the shear forces exhibit their highest values at the head of the inclusion. Subsequently, they progressively decrease and reach a minimum value of 0.5 kN at a depth of 3m for all inclusion lengths. Following this minimum, the shear forces rise again, nearly approaching the values observed in the upper portion of the graph for the 4.5m length inclusion. However, this behavior is not observed in the case of other inclusion lengths, suggesting that a sufficient length is crucial for the inclusion to effectively perform its intended role.

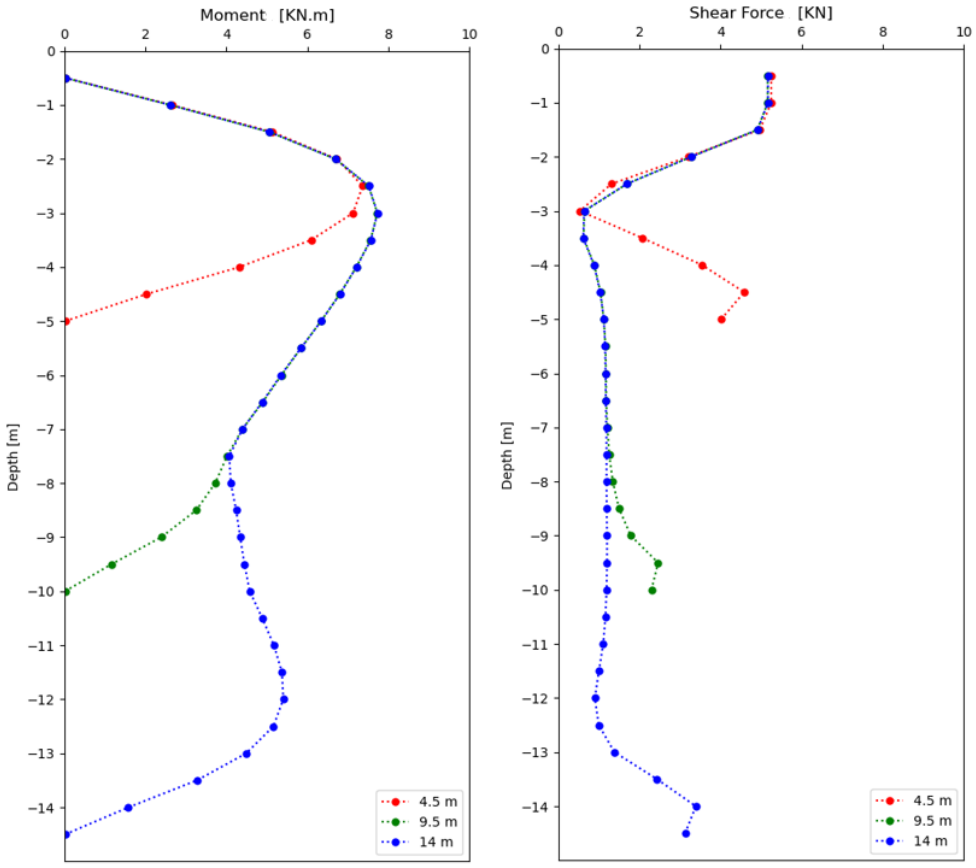

a) Bending moment b) Shear force

Figure 3.17: Influence of the inclusion length in the efforts along the rigid central element

3.8.4 Influence of the characteristics of the mattress

The role of the load transfer mattress is to homogenize settlement and ensure proper load transmission to the heads of the inclusions. The rigidity of the load transfer mattress is a crucial parameter in the construction of reinforcement systems, as it influences the behavior of the reinforcement system. The impact of this parameter is examined by varying the elastic modulus of the mattress across three different values: 100 MPa, 200 MPa, and 300 MPa (Figure 3.18). The other parameters remain the same as those in the reference study. It is observed that increasing the deformation modulus of the mattress has a moderate effect on the response of the system specially in the first three meters of the inclusions. An increase from 100 to 300 MPa leads to approximately 11% increase in the bending moment at 2m depth. However, its influence on the shear force at the head of the inclusions is moderate with small impact. The increase of the mattress rigidity from 200 to 300MPa results in an increase of 8% compared to the reference model whereas a reduction of 17% is observed for a modulus of 100 MPa.

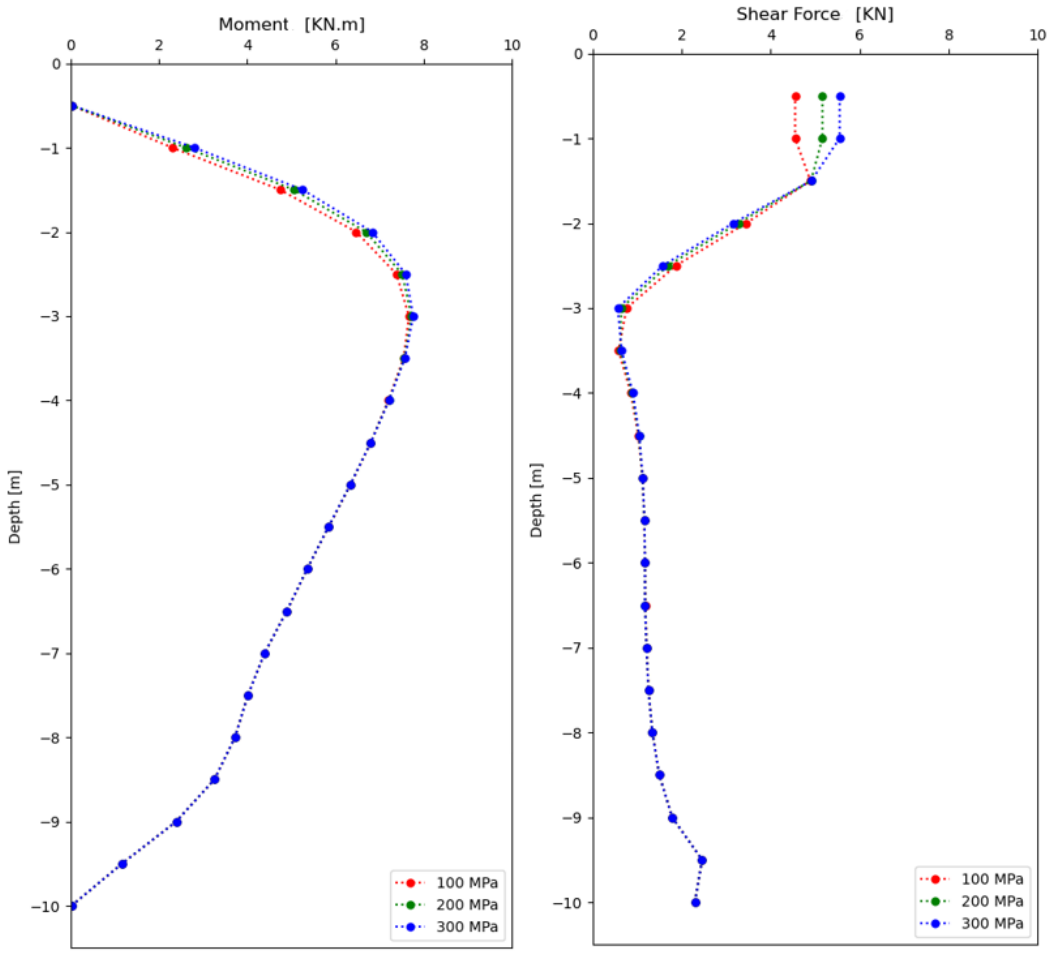

a) Bending moment b) Shear force

Figure 3.18: Influence of the mattress rigidity on the efforts along the rigid element

3.8.5 Influence of the position of the rigid inclusion

The distribution of seismic efforts is not uniform among the different inclusions, as it depends on the position of each element within the group. In order to analyze this aspect, we compared the internal forces at different positions of the inclusions as it shown in (Figure 3.19).

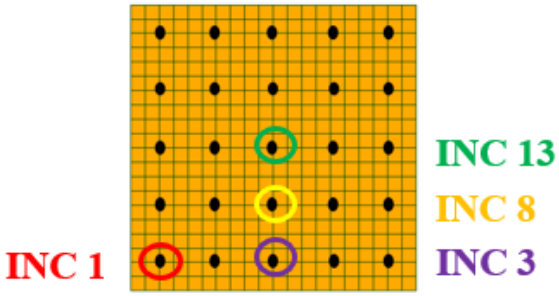

Figure 3.19: Positional Analysis of Rigid Inclusions in the System

(Figure 3.20) depicts the impact of the inclusion position on the bending moments and shear forces. It can be observed that the position of the inclusion has a slight influence on the forces within the rigid inclusion: the maximum bending moment for the edge inclusion (INC 1) is 6% higher than that obtained for the central inclusion (INC 13), attributed to the phenomenon known as the "shadow effect." As for the maximum shear force, a very slight variation is noted. It can be concluded that the least stressed inclusion is located at the center, while the dynamic forces increase from the center towards the edge of the group. This is due to a stronger kinematic effect for the latter.

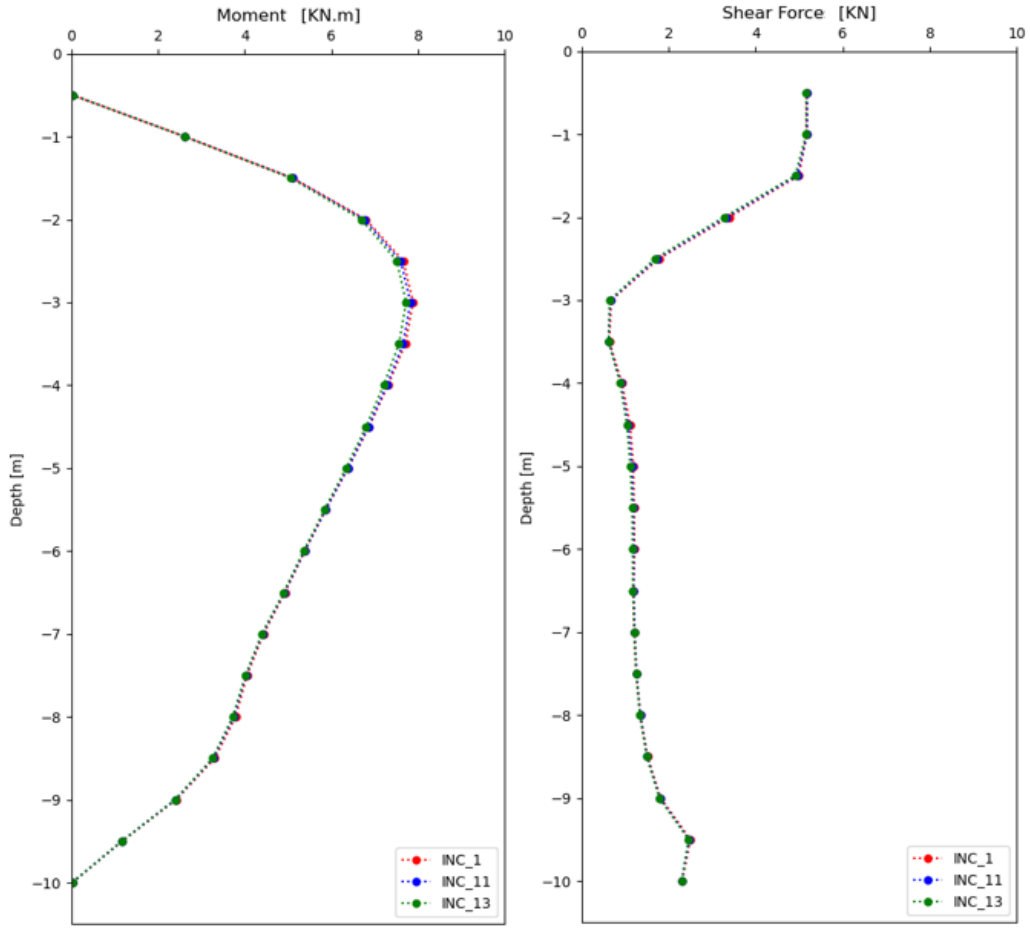

a) Bending moment b) Shear force

Figure 3.20: Influence of Rigid Inclusion Positions on the Seismic Response of the rigid element

3.9 Conclusion

The present chapter presents a comprehensive analysis using three-dimensional finite element method to examine the kinematic interaction of the soil-mattress-inclusions system. This chapter comprises two sections. The first section dedicated to exploring the most suitable method for modeling the rigid inclusions. While the second one consists of studying the influence of certain parameters on their response.

A preliminary analysis was performed to examine the behavior of a single rigid inclusion using two different modeling techniques. The first technique, referred to as the pile void method, involved modeling the inclusion by introducing void element for the vertical reinforcement and incorporating a central beam element. Connection conditions were established between the inclusion nodes and the boundary nodes of the void element. Conversely, the second method exclusively utilized beam element to represent the inclusion within the soil.
The results obtained show that considering a beam element for the rigid inclusion gives similar results to the pile void method for small dimensions.

The second part of the study involves a parametric investigation conducted on a three-dimensional dynamic study involving a group of 25 rigid inclusions. The parameters investigated included the inclusions diameter, depth, and position. As well as soil and mattress mechanical properties especially their stiffness. The calculations were performed using linear elasticity, and the rigid inclusions were represented by beam elements. The obtained results are subsequently presented and compared in terms of shear forces and bending moments.

The findings indicate that the rigid inclusions closely follow the motion of the soil, with only slight deviations observed near the head area where the load transfer mattress has a subtle influence on the deformation of the inclusions.

The findings suggest that larger diameters of the rigid inclusions lead to increased displacements of the inclusion head. Furthermore, there is a corresponding increase in internal forces with larger inclusion diameters.
Increasing the rigidity of the soil brings about a reduction in the internal forces acting on the rigid inclusions. This outcome can be attributed to the presence of stiffer soil surrounding the

inclusions, providing lateral support. However, the influence of mattress rigidity on the system behavior is moderate, particularly in the first three meters of the inclusions. A higher level of mattress rigidity causes an increase in the bending moments and shear forces experienced at the head of the inclusions.

The results obtained from varying the inclusion length highlight the importance of having an adequate length for the inclusion to perform its intended role effectively.

The distribution of seismic effort is not uniform among the different inclusions, as it depends on the position of each element within the group. The results show that the least stressed inclusion is located at the center, while the dynamic forces increase from the center towards the edge of the group.

In this chapter, the soft soil was assumed to exhibit linear elastic behavior. However, when subjected to dynamic loadings, significant deformations occur that cannot be accurately captured by an elastic soil model. To accurately represent the soil surrounding the inclusions, a non-linear model was utilized in the next chapter, along with an examination of the influence of the presence of a raft structure.

CHAPTER 4: NON-LINEAR NUMERICAL MODELING OF SEISMIC BEHAVIOR OF RIGID INCLUSION

4.1 Introduction

It is well known that the soils exhibit nonlinear behavior even at low strain level and this important issue should be integrated in the soil structure interaction problems. The response of soil to dynamic loadings is significantly influenced by its non-linear behavior, which enables the consideration of large deformations beyond the capabilities of an elastic soil model. To accurately capture the behavior of the soil surrounding the inclusions, it is crucial to utilize a non-linear model that accurately represents the soil's mechanical characteristics. This enables a more realistic representation of the system's response, accounting for the soil's true behavior under dynamic conditions.

This chapter aims to investigate the influence of soil non linearity on the seismic behavior of the rigid inclusion-soil system. The analysis is conducted using the linear elastic-perfectly plastic constitutive model, which incorporates the Mohr-Coulomb failure criterion, in order to address the nonlinearity and potential shear failure in the soil elements and the mattress. The Mohr-Coulomb model is widely utilized in simulating the dynamic response of soft soil deposits under varying load conditions, (Hatem, 2009; Hokmabadi and Fatahi, 2016; Lopez Jimenez, 2019). This model provides a satisfactory representation of the soil's behavior, accounting for its nonlinear characteristics.
The reason of using such simulations is due to the fact that the more sophisticated constitutive models which aim to precisely reproduce the soil nonlinearity are often complex and rarely used in modeling.

Due to the complexity and time-consuming nature of using Code Aster to model non-linear soil behavior, especially when dealing with a large-scale model, it was necessary to find a more efficient solution to meet the thesis timeline. As a result, the finite difference explicit code Flac3D (Fast Lagrangian Analysis of Continua) was adopted as an alternative computational tool for this chapter, facilitating the research process and enabling the exploration of a wider range of scenarios with a reasonable run time. This program was successfully used to investigate both linear and non-linear dynamic soil-structure complex problems (Alsaleh, 2007; Mezeh et al., 2018; Shahrour et al., 2012)

This chapter is divided into three sections. The first section discusses the numerical method employed in the analysis. The second section provides an overview of the elastic-perfectly plastic model with the Mohr-Coulomb failure criteria and introduces a model of soil reinforced with a grid of 3x3 rigid inclusions. The final section of this chapter concentrates on studying the effects of introducing nonlinearities into the mattress, the soil, and their combination. Additionally, it includes a parametric study and examines the influence of the presence of a raft foundation on the seismic response of the group.

4.2 Numerical modeling using Finite Difference Method

The focus of this chapter is on the time history analysis of the seismic response of a group of rigid inclusions embedded in the soil taking into account the non-linearity of the soil. This investigation necessitates the utilization of specialized methodologies that consider the interaction between various elements of the system, the non-linear behavior of the soil, the seismic loading, and the three-dimensional nature of the problem. To achieve this, the numerical modeling is conducted using FLAC3D (Fast Lagrangian Analysis of Continua in 3 Dimensions) software, developed by Itasca Consulting Group Inc. The explicit finite difference method is employed for Lagrangian analysis, allowing dynamic modeling.

4.2.1 Three-dimensional Finite Difference Software (Flac3D)

The numerical analyses in this chapter were conducted using the FLAC3D software, which employs a non-conventional implementation of the explicit finite difference method known as the Lagrangian approach (Billaux and Cundall, 1993). This approach solves static/quasi-static or dynamic problems by means of the dynamic equilibrium equation. Recognizing that a portion of the system's accumulated strain energy transforms into kinetic energy, which subsequently propagates and dissipates within the surrounding material, the explicit solution scheme accounts for this phenomenon through the inclusion of dynamic equilibrium equations. As a result, imbalances originating in a specific area propagate throughout the entire mass. The incremental resolution mode guarantees the stability of the numerical scheme by ensuring compliance with stress and deformation paths at each time step. The explicit solution scheme utilized in the FLAC code is a key distinguishing factor, which avoids the assembly of elemental matrices, resulting in a significant reduction in memory usage, specifically Random Access Memory (RAM). In fact, only the variables at the end of each time step are stored, and not the stiffness matrix, as is the case with the finite element method.

4.2.2 Explicit Finite Difference Method (FDM)

The finite difference method is a simple numerical method (older in comparison to the finite element method) employed to solve differential equations. In this approach, each derivative is substituted by an algebraic expression written in terms of the variables involved in the system of equations at discrete locations in space. The derivatives are approximated using finite differences, assuming a linear change over finite intervals of time and distance, hence the name of the method.

The primary computational procedures are depicted in (Figure 4.1). At each time increment, the strain rates are derived from the nodal velocities, which represent the temporal derivative of displacement. Subsequently, the stresses are assessed by applying a constitutive model. Following that, utilizing the stresses and forces, the dynamic equations of motion are employed to compute the updated nodal velocities. This concludes one time increment, and the process is repeated by incorporating the revised velocities. Using the explicit approach, the new values of the variables are computed based on the known values that remain constant during the variable calculations. When calculating stresses from velocities, the velocity values are unchanged for the duration of the operation, even though the newly determined stresses have an effect on them. To ensure calculation stability, the time step must be very small, smaller than the time required for information to propagate between elements. Hence, there exists a critical time step at which the calculation time step must remain smaller. If this condition is satisfied, the behavior of materials, whether linear or nonlinear, is captured during the loading process. The explicit solution of the problem offers the advantage of incorporating nonlinear constitutive laws without additional iterations and with minimal computer memory requirements.

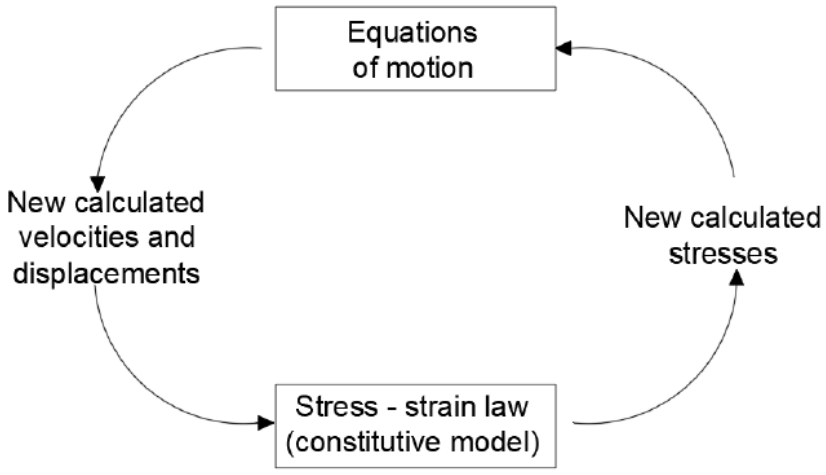

Figure 4.1: General calculation sequence in FLAC3D (Billaux and Cundall, 1993)

4.2.3 Lagrangian Analysis

In the Lagrangian analysis method, the spatial positions of the mesh nodes correspond to individual particles within the medium and are defined relative to an initial configuration. When dealing with substantial deformations, the node coordinates are updated at each time increment, resulting in a deformation of the mesh that reflects the modeled medium. This differs from the Eulerian formulation, where the material undergoes displacement and deformation with respect to a fixed mesh.

4.2.4 Damping

Flac3D employs two types of damping mechanisms: Rayleigh damping and local damping. Rayleigh damping is utilized in the analysis of linear and nonlinear elastic continuous medium and is largely detailed in Section 2.4.2.3 of Chapter 2.

When dealing with the elastic behavior of a material, the use of damping is necessary to dissipate a certain proportion of energy. Typically, damping values ranging from 2% to 10% are commonly applied in the context of geotechnical materials. However, it is worth noting that in plasticity, a portion of energy is naturally dissipated as the material undergoes plastic deformation. As a result, a damping coefficient is required to prevent unrealistic resonance in the system during wave propagation. The selection of the appropriate damping coefficient is more critical in linear analysis compared to nonlinear analysis as the primary source of energy dissipation arises from soil plasticity. In our study, which incorporates soil nonlinearities, Rayleigh damping was applied to the soil.

The local damping is a software feature used to prevent extensive computation time when Rayleigh damping is employed. It is simpler compared to Rayleigh damping since it eliminates the need to specify a particular frequency. This feature proves advantageous in our modeling approach, especially when considering the presence of structural elements like rigid inclusions and shallow foundations, which experience high seismic wave propagation velocities. Employing Rayleigh damping in such cases would require an unreasonably small-time step. Furthermore, it is worth noting that damping effects in rigid elements generally have a minimal influence on the seismic responses of reinforced soil structures.

4.2.5 Boundary conditions

Given the considerable depth of the soil at the site, the incorporation of artificial boundaries becomes essential (Lopez Jimenez, 2019; OKYAY, 2015). If no boundary conditions are applied, waves are reflected at the lateral and lower ends of the block, which is not realistic

since the soil is considered "infinite." This phenomenon is known as the box effect, where waves can be perceived as confined within a box, continuously bouncing back and mixing with waves generated by dynamic loading. It is crucial to establish boundary conditions that absorb these waves and prevent their reflection. In this regard, Flac3D offers two solutions (Figure 4.2).

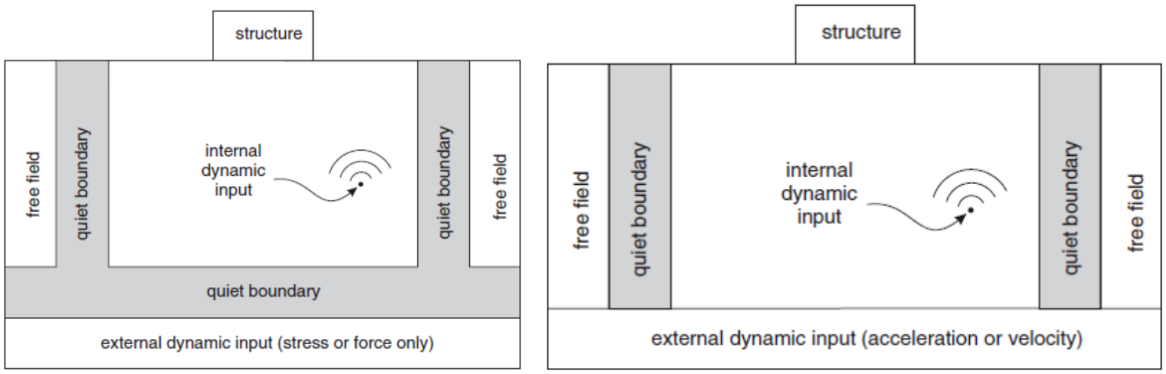

a) Flexible base b) Rigid base

Figure 4.2: Types of dynamic loading and boundary conditions available in FLAC3D.

In the computational analyses performed in this study, the static analysis phase required the horizontal fixation of the side boundaries and the complete immobilization of the bottom section. However, for the dynamic analysis, a different set of boundary conditions was adopted. Specifically, the base of the model was assumed to be rigid to facilitate the imposition of velocity inputs, while free-field boundary conditions were implemented on the lateral boundaries to effectively avoid wave reflections (Lysmer and Kuhlemeyer, 1969).

4.2.5.1 Quiet Boundaries

The implementation of fixed or elastic boundary conditions during dynamic analysis leads to the reflection of outward propagating waves within the model, resulting in inadequate energy dissipation. To address this issue, one possible solution is to utilize larger models. However, this approach requires significant computational demands, as the material damping must absorb the energy from waves reflected at distant boundaries. An alternative and more effective option is the adoption of "quiet" boundaries, developed by (Lysmer and Kuhlemeyer, 1969) and integrated into Flac3D. These specialized boundaries ensure complete absorption when the incident angle of body waves exceeds 30°. At the model boundaries, independent dashpots are employed in both the normal and shear directions, producing viscous normal and shear tractions represented by equations (25) and (26).

$$t_n = -\rho V_p \nu_n \quad (25)$$

$$t_s = -\rho V_s \nu_s \quad (26)$$

With ρ represents the mass density, while V_p and V_s correspond to the velocities of the p-wave and s-wave, respectively. Similarly, ν_n and ν_s denote the normal and shear components of velocity at the boundaries. In the numerical analysis, the tensions at the boundaries are computed and incorporated at each time increment using a methodology analogous to the application of boundary loads. The utilization of these viscous boundaries occurs within the time domain.

Using quiet boundaries in dynamic analyses is discouraged when the input motion is applied at the top or bottom of the model, as it can lead to wave energy leakage through the sides. Considering the specific conditions of this study, where the dynamic load is applied at the bottom of the model, it becomes imperative to adopt a free-field boundary condition.

4.2.5.2 Free Field Boundaries

The accurate numerical analysis of the soil-foundation-structure system under seismic loading necessitates the consideration of boundary conditions that reproduce the free-field ground motion. Flac3D addresses this requirement by employing free-field boundaries along the vertical sides of the model. Following the static equilibrium, these free-field boundaries are implemented for dynamic analysis. These boundaries represent the semi-infinite nature of the ground through interconnected plane grids, which are connected to the main grid via viscous dashpots to create a quiet boundary. This arrangement prevents the distortion of upward-propagating plane waves. The unbalanced forces from the secondary grid are then applied to the main grid boundary, with their normal direction aligned with the x-axis, as described by the following equations.

$$F_x = -\rho V_p \left(v_x^m - v_x^{ff}\right) A + F_x^{ff} \quad (27)$$

$$F_y = -\rho V_s \left(v_y^m - v_y^{ff}\right) A + F_y^{ff} \quad (28)$$

$$F_z = -\rho V_s \left(v_z^m - v_z^{ff}\right) A + F_z^{ff} \quad (29)$$

where ρ represents the mass density, V_p and V_s denote the velocities of the p-wave and s-wave, respectively. A corresponds to the area of influence of the free field gridpoint. v_x^m, v_y^m, and v_z^m

indicate the x, y, and z velocities of the gridpoint in the main grid at the side boundary, while v_x^{ff}, v_y^{ff}, and v_z^{ff} represent the x, y, and z velocities of the gridpoint in the side free field. F_x^{ff}, F_y^{ff}, and F_z^{ff} signify the free-field gridpoint force with contributions from the σ_{xx}^{ff}, σ_{yy}^{ff},, and σ_{zz}^{ff}, stresses of the free-field zones surrounding the gridpoint, respectively. Similar expressions can be derived for the other sides.

4.3 Presentation of the reference model

4.3.1 Introduction

In order to proceed with the calculations conducted in the third chapter and obtain results within a reasonable timeframe, a downscaled model was employed using Flac3D.

4.3.2 Geometry of the reference model

This study introduces a 3D model consisting of a soil volume with dimensions of 22 x 22 x 15 m³, which incorporates a group of 3x3 rigid inclusions, with a length of L=9.5 m. This group is positioned within a soil layer characterized by uniform mechanical properties at various depths. The rigid inclusions, with a diameter of 40 cm, are considered as floating inclusions. They are spaced at intervals of S=2 m (S/D=5, where D represents the diameter of the inclusion). The load distribution mattress, measuring 0.50 m in height and 6 x 6 m² in surface, is directly placed on the inclusions, without any anchorage. Detailed information regarding the soil and inclusions properties can be found in (Table 4.1).

The soil investigated is categorized as Class D according to EC8 standards. In this study, the soil exhibits a Young's modulus (E_s) of 100 MPa, a Poisson's ratio (ν_s) of 0.3, and a mass density (ρ_s) of 1600 kg/m³. On the other hand, the mattress possesses the following characteristics:
a Young's modulus (E_m) of 200 MPa, a Poisson's ratio (ν_m) of 0.3, and a mass density (ρ_m) of 1800 kg/m³. The fundamental frequency of the soil layer is determined to be 2.5 Hz. In terms of the material properties of the rigid inclusions, the young's modulus was selected as 40 GPa, a value commonly found within the typical range for concrete or reinforced concrete in deep foundation applications. The behavior of the rigid inclusions is assumed to be linear elastic, while the behavior of the mattress and the soil varies depending on the specific case analyzed, as discussed in section 4.3.3.

Parameters	Rigid inclusion	LTP	Soft soil
Young Modulus E (MPa)	40000	200	100
Volumetric weight (kg/m³)	2500	1800	1600
Poisson's ratio	0.2	0.3	0.3
Cohesion (kPa)	-	0	8
Friction angle (°)	-	38	25
Dilation (°)	-	0	0

Table 4.1: Material properties considered for the numerical model

A Rayleigh-type damping model is adopted for the soft soil, while a "local damping" is employed for the structural elements. The damping ratio is set at 5% for the soil and 2% for the structural elements. The calculations are performed using the Friuli recording (Figure 4.5). The mesh selected for the analysis is depicted in (Figure 4.3), composed of a total of 32000 hexahedral zones.

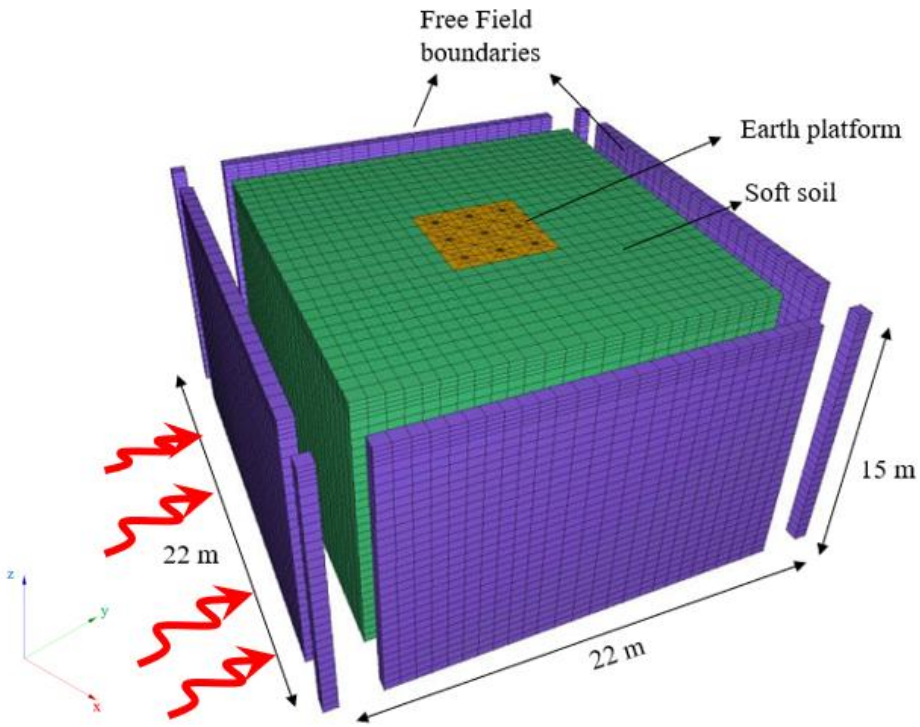

Figure 4.3: Geometry of the numerical model

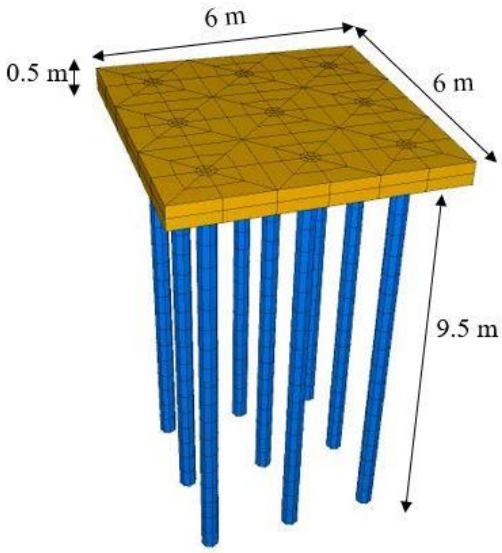

Figure 4.4: Geometry of the mattress and rigid inclusions

The vertical reinforcements in this study were simulated using a hybrid method, as outlined in Section 3.3 of Chapter 3. This method combines solid elements with the incorporation of beam elements along their central axis. By incorporating the physical cross section of the inclusions, this technique enables a more accurate representation of their behavior. The hybrid method, as described by (Banerjee et al., 2014; Kourkoulis et al., 2012b), allows for direct calculation of inclusion forces from the beam elements.

To accurately represent the infinite nature of the soil deposits, boundary conditions were incorporated. During the static analysis phase, the horizontal movement of the side boundaries was constrained, while the bottom part was fixed in all directions. However, these initial boundary conditions were modified for the dynamic analysis. In the dynamic analysis, a rigid base was assumed to apply the earthquake, while free-field boundary conditions were implemented on the sides to prevent wave reflections.

The loading is imposed as a velocity at the base of the soil mass in the Y direction, utilizing the Friuli earthquake record from Italy. Only the first 5 seconds of the accelerogram were used for the calculation. The dynamic input motion is provided in (Figure 4.5), more detailed information can be found in section 4.2 of chapter 3.

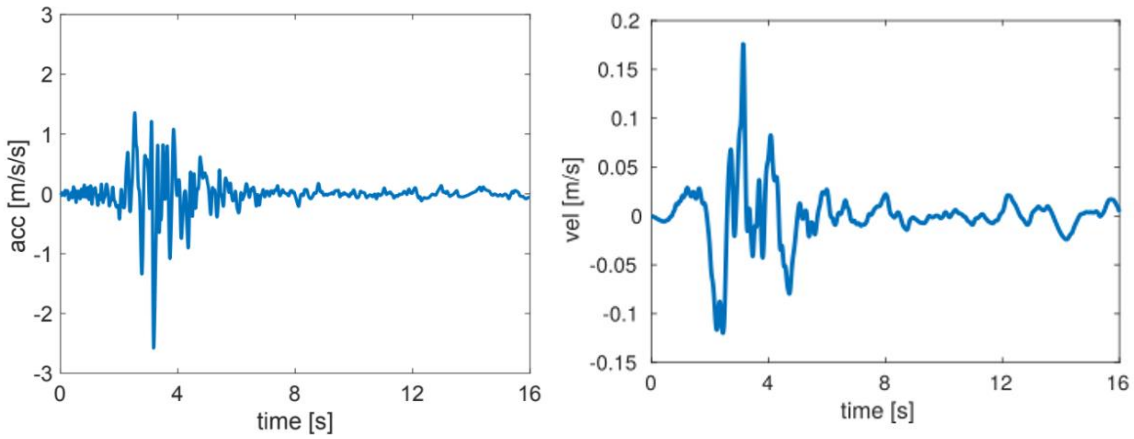

a) Acceleration b) Velocity

Figure 4.5: Time history record: a) Accelerations, b) Velocity

4.3.3 Analyzed Cases

In this part of the study, various case scenarios were analyzed, considering different combinations of constitutive models for the mattress and soil, along with the presence or absence of the raft foundation. The table below summarizes the studied cases and their corresponding configurations.

Case	Mattress Constitutive Model	Soil Constitutive Model	Raft Foundation
1	Linear Elastic	Linear Elastic	No
2	Mohr Coulomb	Linear Elastic	No
3	Mohr Coulomb	Mohr Coulomb	No
4	Mohr Coulomb	Mohr Coulomb	Yes

Table 4.2: Examined Cases

The study follows a systematic approach, gradually increasing the complexity of the model by starting with a linear elastic model for the entire system, then incorporates Mohr Coulomb in the mattress, then in both soil and mattress, and finally considering the same conditions as before but with the addition of a shallow foundation.

The first case represents a baseline scenario where both the mattress and soil are modeled using a linear elastic constitutive model. This case serves as a reference to compare against the other cases and provides insight into the behavior of the system under simplified linear conditions.

In the second case the mattress is modeled using a Mohr Coulomb constitutive model, while the soil retains the linear elastic behavior. This case aims to explore the influence of the constitutive model in the mattress on the overall response of the system.

Moving forward, the third case considers a scenario where both the mattress and soil are modeled using the Mohr Coulomb constitutive model. This allows for the investigation of the combined effect of non-linear behavior in both components.

The fourth case introduces the presence of raft foundations, with dimensions of 7.5 x 7.5 x 0.5 m^3 (Figure 4.6). The Mohr-Coulomb constitutive model is employed to simulate both the mattress and soil, while the linear elastic model is used to simulate the inclusions and the raft foundation. Additionally, a 100 kPa load is applied on the top surface of the raft.

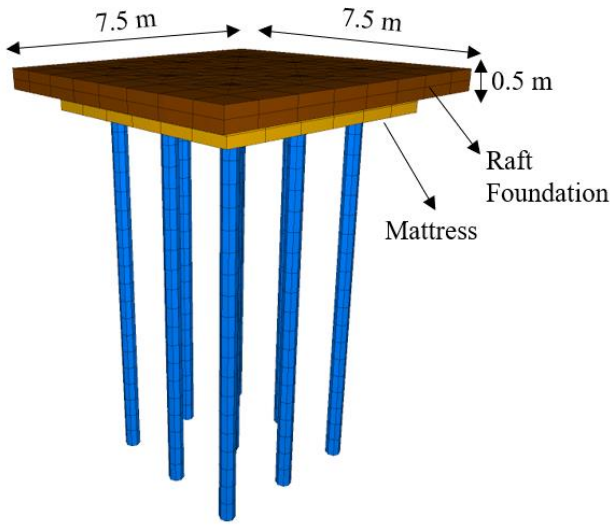

Figure 4.6: Raft foundation dimensions

The incorporation of the raft foundation adds complexity to the system and examines the combined effects of non-linear behavior and the presence of a raft foundation. Detailed information regarding raft properties can be found in (Table 4.3).

Parameters	Rigid inclusion
Young Modulus E (MPa)	40000
Volumetric weight (kg/m³)	2500
Poisson's ratio	0.2

Table 4.3: Material properties of the raft

The main objective of this study is to explore the influence of varying in constitutive models applied to the mattress and the soil, aiming to gain valuable insights into their behaviors and responses. By investigating different models, such as linear elastic, Mohr-Coulomb failure criteria, we seek to understand how these models impact the system's response. Through comprehensive analyses and simulations, we can observe the differences in deformation results and overall responses under different constitutive models.

The analysis procedure for each case study began by generating an initial stress state. Displacements were fixed at the bottom boundary of the model, while horizontal displacements were fixed at the lateral boundaries. The model was then brought to equilibrium by considering the self-weight of the soil. Following this, the vertical reinforcements were incorporated, and the model was brought to equilibrium considering the weight of these elements. The subsequent phase involved activating the earth platform in the static analysis. For the dynamic analysis, free field boundaries were implemented, and the calculations were conducted by introducing the velocity input of the earthquake at the base of the model.

4.3.4 Results and discussions for the different case studies

The comparison between the results highlights the impact of utilizing different constitutive models on the displacements, shear forces and moments experienced within the system as well as the impact of the presence of the raft foundation.

(Figure 4.7) depict the variations in velocity at the surface of the model. A significant amplification of motion is observed at the mattress surface when compared to the loading applied at the base of the model "Friuli". The velocity reaches its maximum 0.21 m/s for all cases, in comparison to the maximum velocity of the loading at the base of the model, which is equal to 0.17 m/s. At a specific time of 3.37 seconds, the velocity in cases 1 and 2 reaches a value of 0.175 m/s, surpassing the velocity of cases 3 and 4, which is 0.134 m/s. This observed variation can be attributed to the development of soil plasticity in cases 3 and 4.

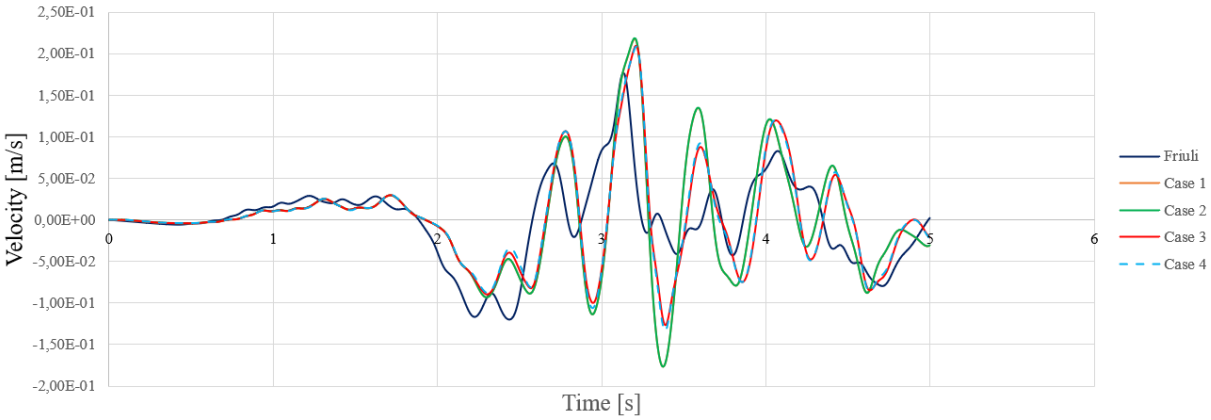

Figure 4.7: Variation of Surface Velocity

4.3.4.1 Comparison of Internal Forces along the rigid elements

(Figure 4.8) shows the curves of the envelop of moments along the central inclusions considering different case studies with different mattress and soil behavior (elastic or elasto-plastic). The moments graph begins at a depth of -0.5m, aligning with the location of the rigid inclusion's head. In all the cases, the bending moments at the heads of these inclusions are approximately null. This implies that the incorporation of an earth platform within the rigid inclusion system helps minimize shear forces and bending moments experienced by the head elements. This becomes particularly advantageous for structures situated in areas exposed to high seismic activity. The platform serves to restrict the transfer of movement to the structure, thereby reducing inertial forces.

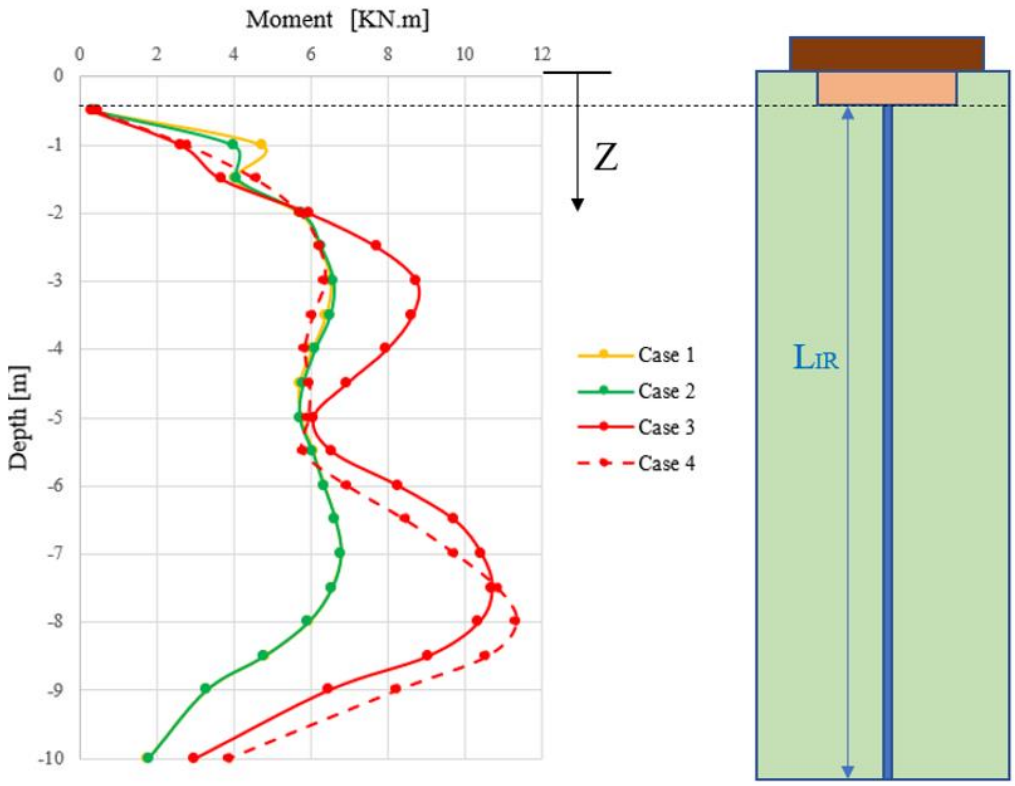

Figure 4.8: Maximum bending moment in the central rigid inclusions for different case studies

In all the cases, the moments increase with depth. The bending moments in case 1 and 2 are similar and reach a maximum of 6.3 kN.m at 3m and 7 m depth. The values are more significant in case 3 where an increase of 40% were obtained at 3m depth and 55% at 7m depth.

The implementation of the raft in case 4 results in a reduction of the moment within the first few meters, specifically a 40% reduction at a depth of 3 meters compared to case 3. However, it also results in an increase in the moment, reaching a maximum of 11.6 KN.m at an 8m depth.

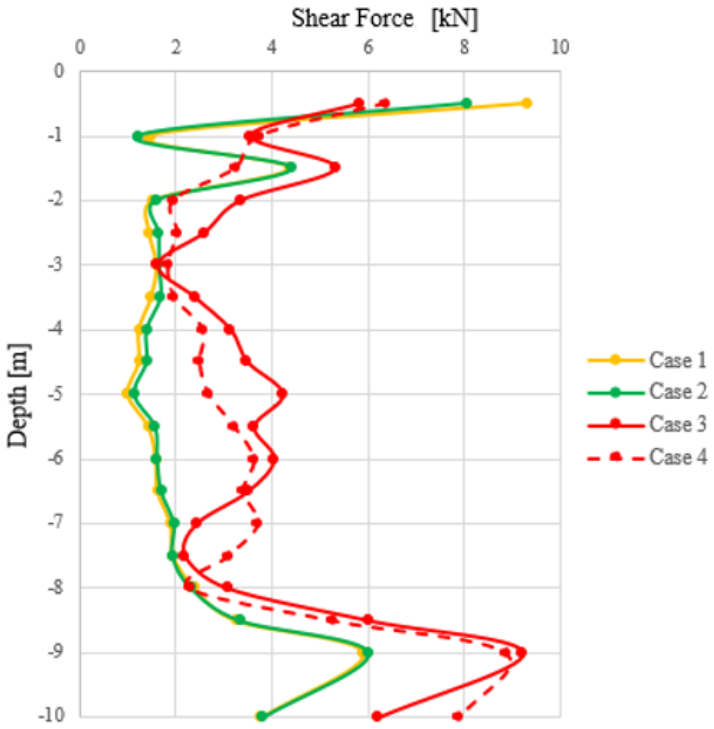

Figure 4.9: Shear Force in the central rigid inclusions for different case studies

The shear forces experienced by the central rigid inclusion exhibit higher magnitudes in the elasto-plastic calculations compared to the elastic calculations. The differences in values indicate an increase of approximately 193% between case 1 and case 3 at 1 m depth, and 53% at a depth of 9 meters. Notably, in case 3, where the elasto-plastic approach is employed to model the soil behavior, the shear forces are significantly greater, providing a more accurate representation of the soil's actual behavior, considering its plastic deformation. These values obtained from the elasto-plastic analysis are more reliable than those derived from the linear elastic case. The implementation of the raft foundation, specifically case 4, resulted in a decrease of 67% in shear forces at a 2m depth when compared to case 3.

4.3.4.2 Comparison of Horizontal Displacements along the rigid elements

(Figure 4.10) presents a comparison between the envelop of the horizontal displacements at the central rigid inclusion of the group for the different case studies, as well as the displacements observed in the free field conditions with linear elastic (FF_LE) and with Mohr Coulomb (FF_MC). The displacements within the first 0.5 m depth correspond to the mattress, while the displacements below 0.5 m correspond to that of the rigid inclusion. The horizontal displacements observed for the central rigid inclusion in cases 1 and 2, considering a linear

elastic constitutive model for the soil, is nearly identical and reaches a value of 0.025 m at the top of the model. However, when incorporating the elastic perfectly plastic behavior with Mohr coulomb failure criteria, this value is reduced to approximately 0.022 m, representing a reduction of 13% at the top of the model. This variation can be attributed to both soil energy dissipation and the interaction between the soil and rigid element.

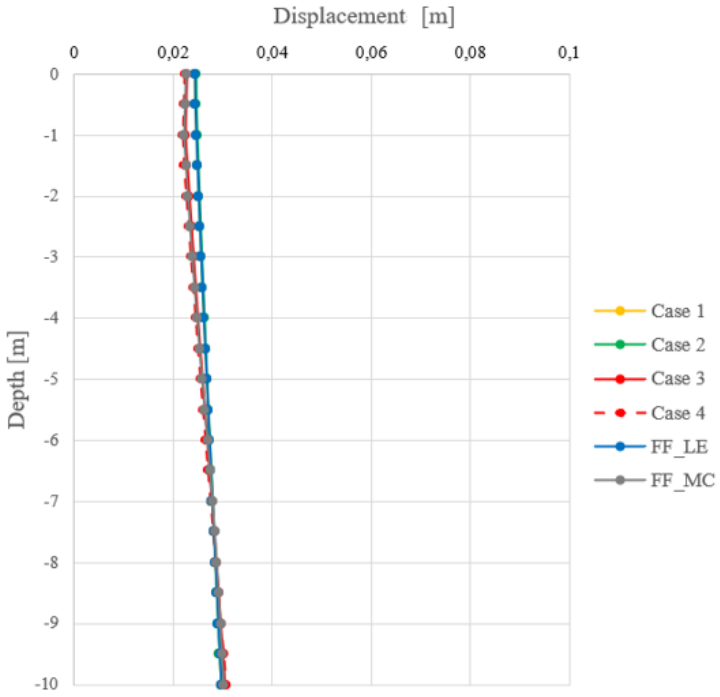

Figure 4.10:Horizontal displacements for different case studies

It can be observed that the inclusion follows the soil movement. In cases 3 and 4, the behavior is similar except for the upper part of the inclusion, where the plasticity of the soil and the presence of the raft have resulted in a reduction in the deformation of the inclusion compared to cases 1 and 2. However, these variations are considered negligible. This aligns with the outcomes reported in the pile literature (Lopez Jimenez, 2019; Sadek, 2003), where it is generally observed that the pile tends to track soil movements, except for situations where there is a notable inertial effect, particularly near the pile head.

These case studies highlight the importance of choosing the appropriate constitutive model taking into account the nonlinearities for evaluating internal forces within the inclusions. While linear elasticity can be sufficient in certain situations, the utilization of linear elastic perfectly

plastic with Mohr-Coulomb failure criteria allows for a better consideration of the material behaviors and provide more accurate predictions in more complex scenarios.

These studies indicate that when modeling the mattress alone, using the Mohr-Coulomb, it results in similar variations to those obtained with the linear model. However, it is important to highlight the importance of considering nonlinearity in the entire system including the soil, rather than solely focusing on the mattress.

4.4 Parametric study

4.4.1 Influence of the cover ratio

The cover ratio plays a significant role when it comes to the design and dimensioning of reinforcement systems. It is a crucial parameter affecting the stability of the soil-inclusions-mattress-structure system. Increasing the cover ratio, which results in an increase in the inclusions radius, can enhance the bearing capacity of the vertical element, considering both the friction and tip effects. Understanding its influence on the seismic response is essential, so in order to investigate the impact of the cover ratio, we conducted numerical simulations on the (case 4) study using two other different cover ratio values apart from the reference value (α =2%, 3%, and 5%) which correspond to inclusion diameters of (0.3m, 0.4m, and 0.5m) respectively. This investigation aims to provide a comprehensive understanding of how the cover ratio impact the response of the system. The obtained results are presented in Figures below.

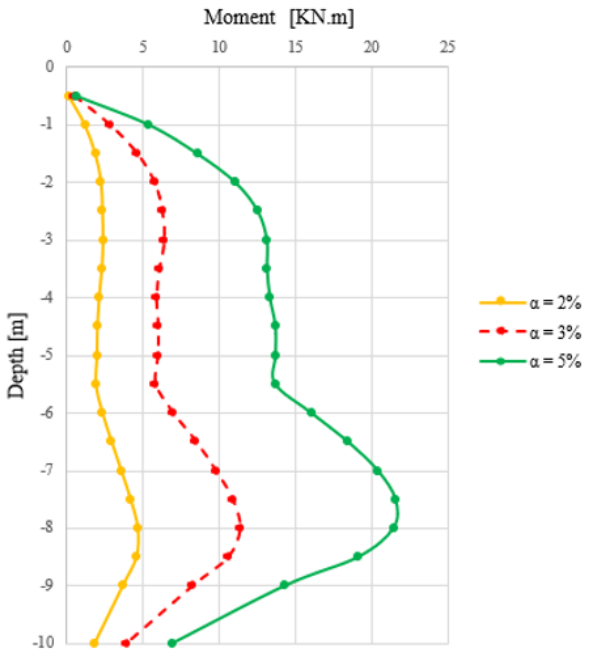

Figure 4.11: Bending moment along the central rigid element for different cover ratio values

Figure 4.11 and Figure 4.12 show that the bending moments and shear forces resulting from the kinematic interaction within the inclusions increase with increasing the cover ratio. A higher cover ratio provides better confinement to the inclusion and increase its contact with the soil. The maximum bending moment is observed at 8m depth and has values of 4.6 kN.m, 11 kN.m and 21.5 kN.m for the cover ratios α =2%, 3%, and 5% respectively. This implies a decrease of 58% for α = 2% and an increase of 95% for α = 5% compared to the reference case (11 kN.m). The fact that the moment resulting from kinematic interaction is primarily linked to inertia, and therefore strongly dependent on the diameter, may partially account for the observed outcomes. Therefore, our subsequent analysis will involve the introduction of a dimensionless parameter to mitigate the influence of diameter and illustrate the effects of nonlinearities.

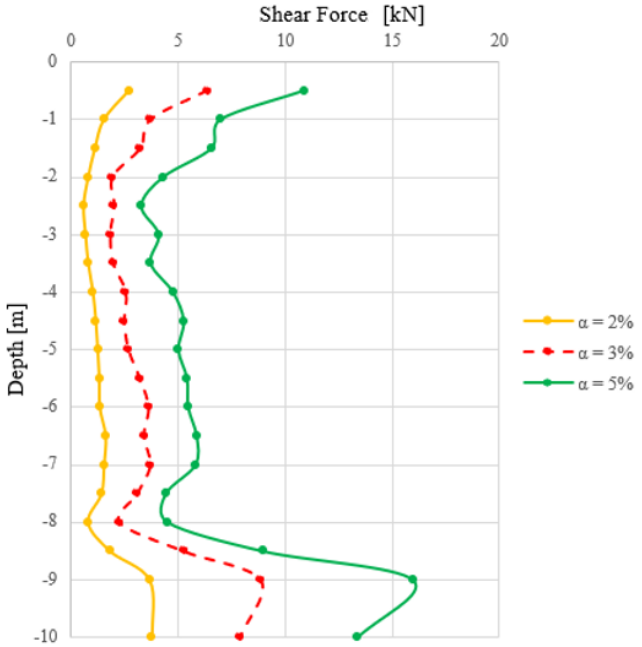

Figure 4.12: Shear force along the central rigid element for different cover ratio values

At a depth of 9m, the shear force values corresponding to the cover ratios α = 2%, 3%, and 5% are 3.6 kN, 8.8 kN, and 16 kN, respectively. A comparison of these shear forces with the reference case (α = 3%) reveals significant variations. For α = 2%, the shear force is approximately 59.1% lower than the reference case, indicating a considerable decrease. On the other hand, for α = 5%, the shear force is approximately 81.8% higher than the reference case, indicating a substantial increase. This rise in the internal forces can be attributed to the improvement in the contact area and the confinement between the inclusions and surrounding

material, leading to higher load transfer capacities and resulting in an increased shear forces and bending moments.

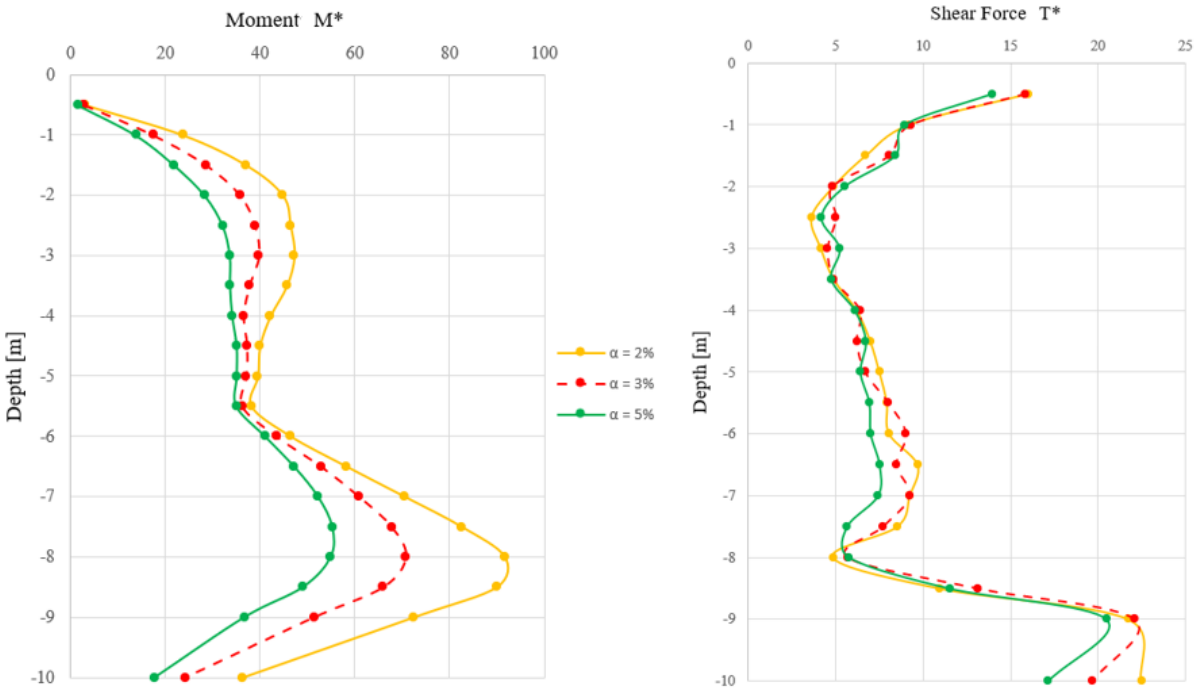

a) Normalized bending moment M* b) Normalized shear force T*

Figure 4.13: Influence of the cover ratio on the response of rigid inclusion: a) Normalized bending moment, b) Normalized shear force. [M= M/ ρD⁴ag], [T*=T/ ρD³ag]*

To enhance the comprehension of this phenomenon and to distinguish among the effects of inertia, non-linearity, and potentially group effects, the results were presented in a dimensionless format. In this context, it has been established in the literature that the group effect becomes negligible when the spacing is equal to or greater than five times the diameter so to examine the non-linearity effect, the moment is normalized by ρD⁴ag, M*=M/(ρD⁴ag) and the shear force by ρD³ag, T*= T/(ρD³ag) (Shahrour et al., 2001; Xu and Fatahi, 2018) where ρ, D and ag are the volumic weigth, the diameter of the inclusion and the peak ground acceleration (PGA) of the applied earthquake. (Figure 4.13-a) illustrates that as 'α' increases, the kinematic interaction correspondingly rises, leading to a reduction in the moment M*. This observation signifies an augmented level of non-linearity and increased energy dissipation at the interface between the soil and the inclusion. The same analysis approach is applicable to the shear force results presented in (Figure 4.13-b).

4.4.2 Influence of the load over the raft

The analysis was extended to include an additional loading case with an overload of 200 kPa. This study was conducted using “Case 4” with an elasto-plastic calculation approach. The resulting envelop bending moments and shear forces along the central vertical rigid element are illustrated in Figure 4.14 and Figure 4.15, respectively.

As anticipated, the moments exhibit a clear correlation with the magnitude of the applied overload. Notably, starting from a depth of 3.5m, the moments progressively increase with the augmentation of the overload. In particular, there is a significant rise of approximately 25% in the bending moments at 5.5m depth, increasing from 5.8 kN.m to 7.3 kN.m.

However, it is interesting to observe that the maximum bending moment experienced only a marginal increment from 11.3 kN.m to 11.6 kN.m at a depth of 8m. This phenomenon suggests that certain depths and locations in the inclusions system may exhibit a more restrained response to the applied overload, potentially influenced by factors such as load distribution.

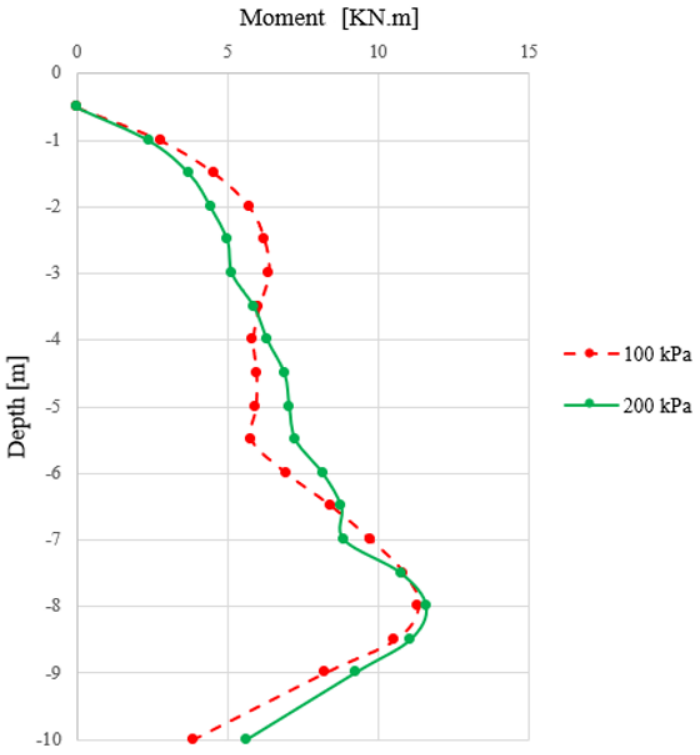

Figure 4.14: Bending moment along the central rigid element for different overload values

The comparison of shear forces, depicted in (Figure 4.15), provides important insights into the behavior of the foundation system under different loading conditions. Notably, the analysis

reveals that the maximum shear force values occur at two critical locations: the head and the toe of the rigid inclusion.

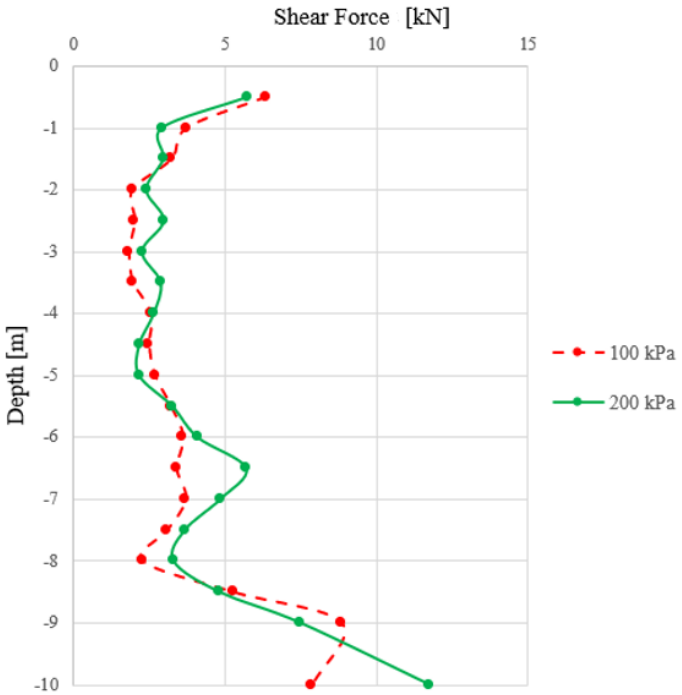

Figure 4.15: Shear force along the central rigid element for different overload values

For the 100 kPa overload, the maximum shear forces are observed to be 6.3 kN at the head and 7.8 kN at the toe of the rigid inclusion. Similarly, for the 200 kPa overload, the maximum shear forces are approximately 5.7 kN at the head and 11.8 kN at the toe.

Interestingly, for the sections between the head and the toe of the rigid inclusion, the shear forces remain relatively consistent for the 100 kPa overload. However, for the 200 kPa overload, there is an evident increase in the shear forces at the toe amounting to approximately 51% of the magnitude observed in the 100 kPa overload case.

4.4.3 Influence of the position of rigid inclusions

This section is dedicated to understanding how the rigid inclusions positions within the group influences various aspects. The comparative analysis encompasses different inclusion locations, namely, at the Corner, in Between, and at the Center, as visually represented in (Figure 4.16). Examining the effects of inclusion placement is crucial in understanding their impact on the behavior of the system.

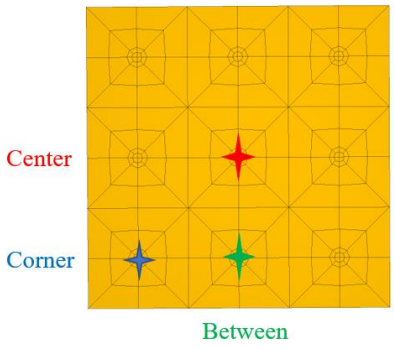

Figure 4.16: Rigid inclusion position

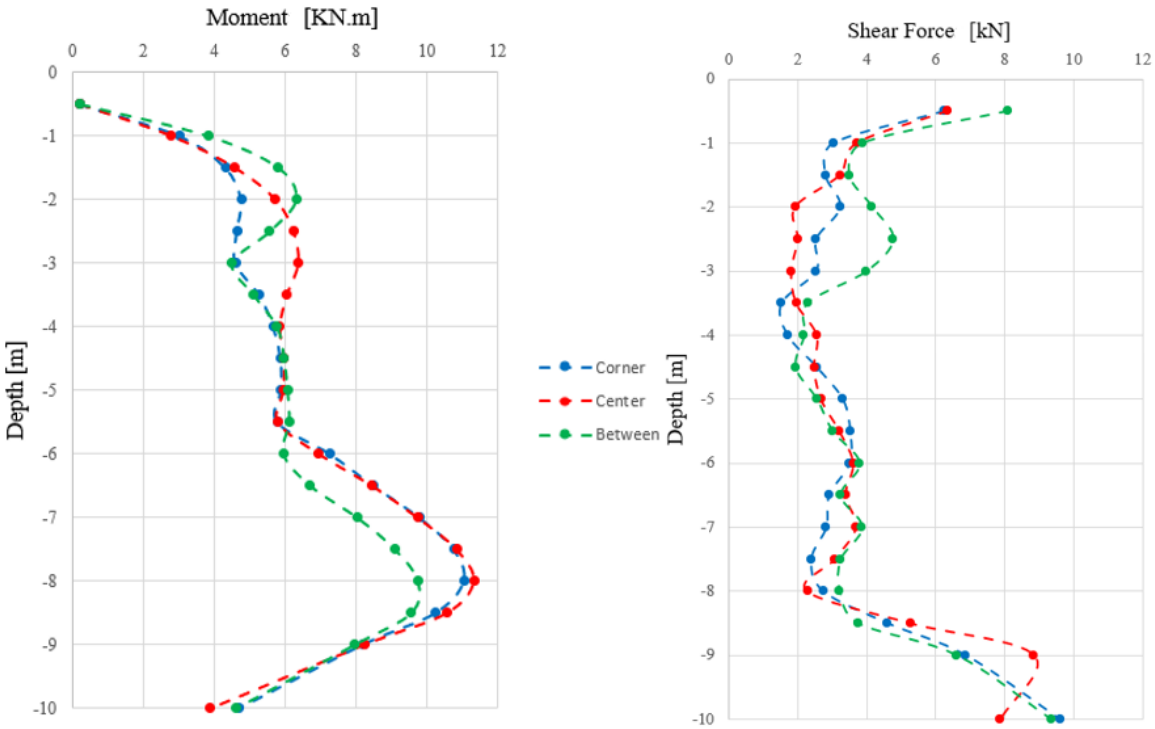

a) Bending moment b) Shear force

Figure 4.17: Influence of the position of rigid inclusions in the efforts: a) Bending moment b) Shear force

(Figure 4.17) illustrates the influence of inclusion position on internal forces. Small variations in the distribution of these forces are observed. This study is conducted on the 'Case 4' study. The moments induced in the corner inclusion exhibit nearly identical values to those in the central inclusion, with only a slight variation between the 1.5m and 4m of the inclusion. Where, at approximately 3 meters, the central inclusion experiences an increase of approximately 40% compared to the corner inclusion. The 'Between' inclusion exhibits a moment envelope that, remains consistently lower than the values observed in the other positions starting at 3 meters. It reaches a maximum of 10 kN·m, representing an 11.5% reduction compared to the maximum moments recorded in the other positions. This behavior may be attributed to the arrangement of inclusions and their spacing, which is five times the diameter, causing the inclusion to behave as if it were isolated.

The results obtained for the shear forces reveal a similar variation to that of the bending moment. A more significant variation in shear force occurs at a depth of 2.5 meters, with an increase of approximately 25% and 135% for the 'corner' and 'between' inclusions respectively compared to the central inclusion values.

4.4.4 Influence of Load Amplitude

This study is conducted based on analyses performed using the Friuli recording for two more different values of load acceleration amplitude (agmax =0.1g, and 0.4g) with g=10m/s².
(Figure 4.18) depicts the acceleration recorded at the model's surface for various loadings. It is noticeable that the larger the load amplitude, the greater the acceleration recorded at the surface. The maximum accelerations are reached at t = 3.3s for all the load amplitudes 0.1g, 0.25g, and 0.4g, with corresponding values of 1.6 m/s², 3.5 m/s², and 5 m/s², respectively.

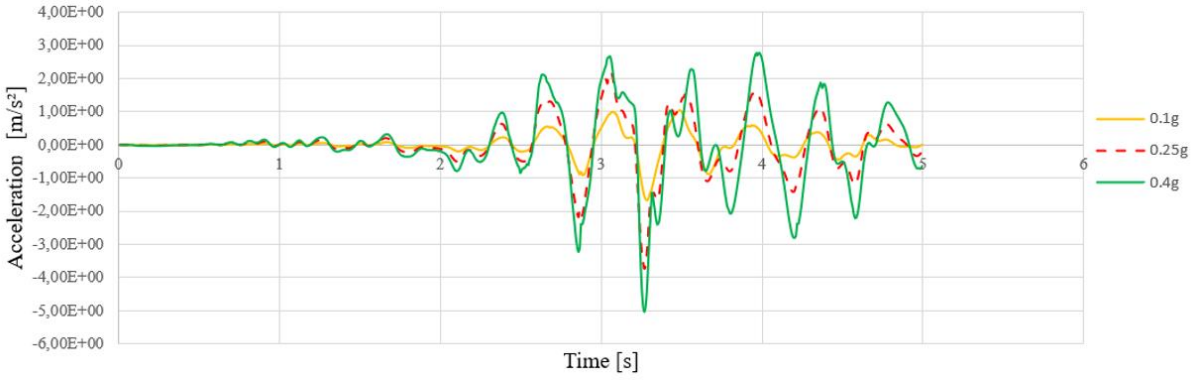

Figure 4.18: Acceleration at the Top of the Model for Various Loading Amplitudes

To investigate and gain deeper insights into the impact of the loading amplitude, the acceleration results are represented in a normalized format relative to the maximum acceleration recorded at the model's base for various amplitudes (Figure 4.19). A phase shift becomes noticeable from the peak values at t=3.3s and continues until the end of the calculation. It is noteworthy that, for the larger 0.4g amplitude, the normalized accelerations are found to be lower compared to those obtained for the other amplitudes. This can be attributed to more pronounced soil plasticity.

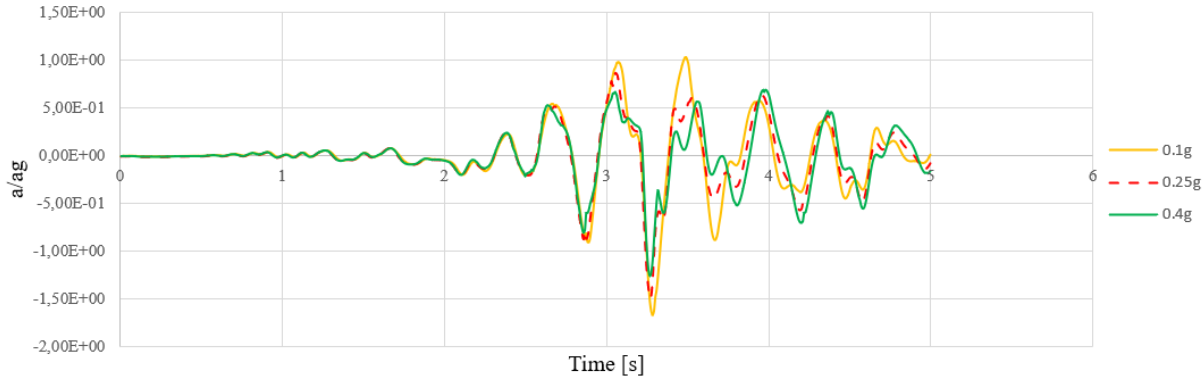

Figure 4.19: Normalized Acceleration at the Top of the Model Relative to the Maximum Ground Acceleration for Different Loadings

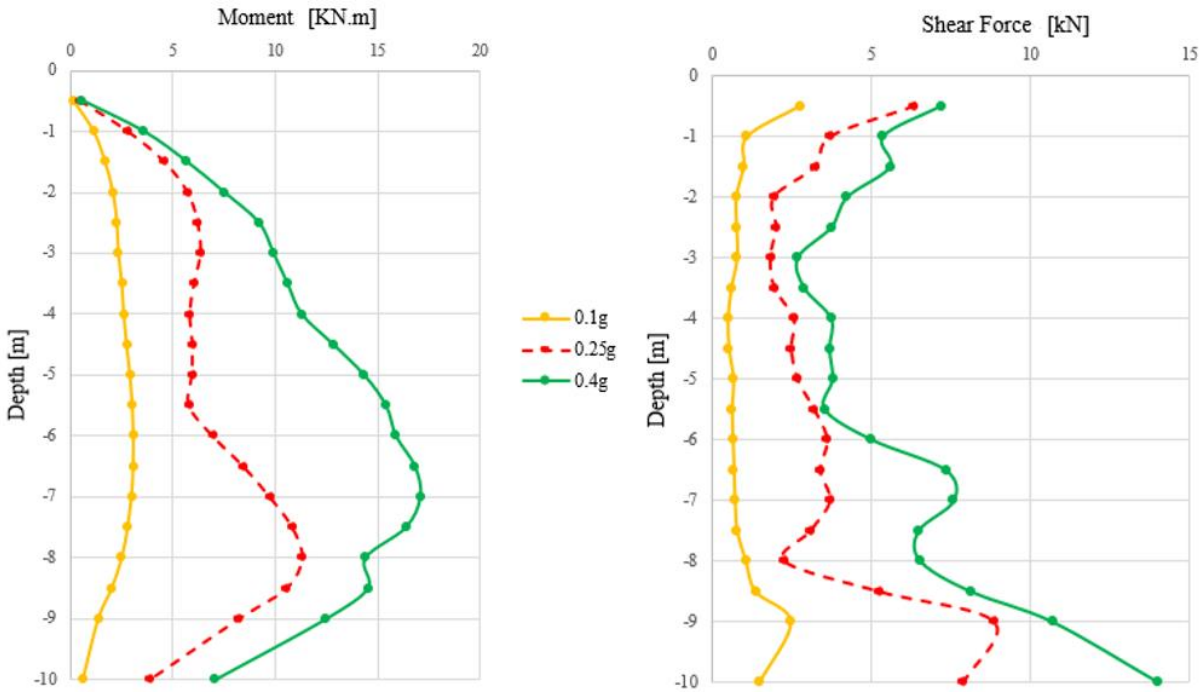

a) Bending moment

b) Shear force

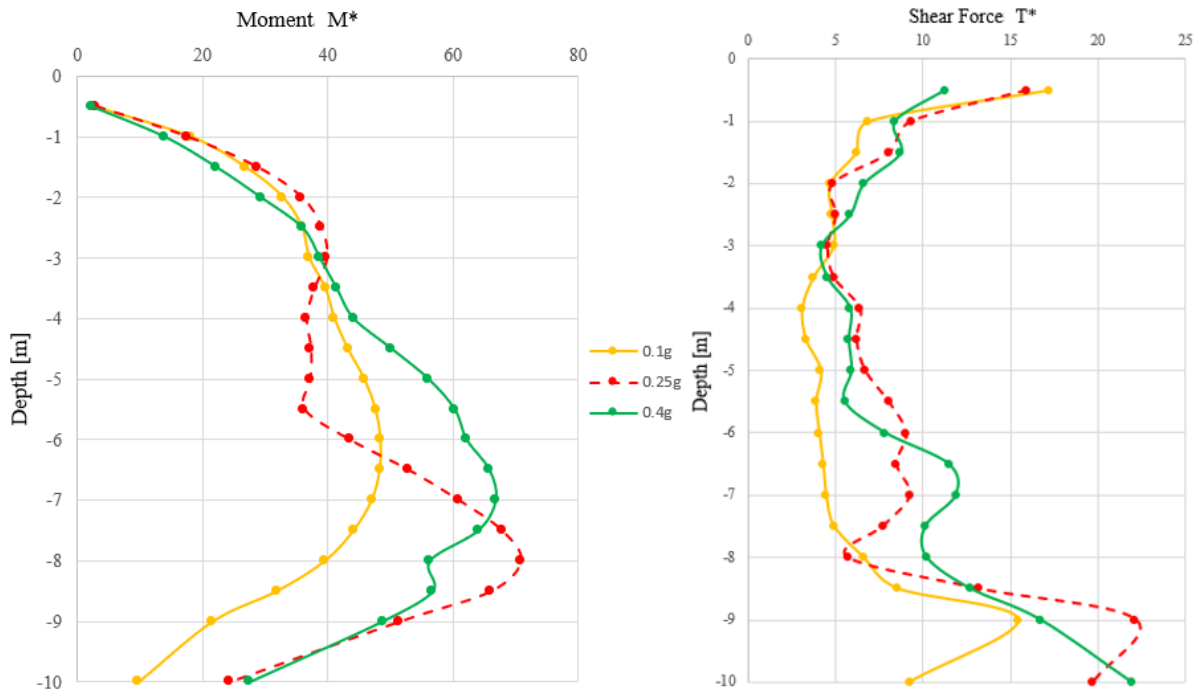

c) Normalized bending moments d) Normalized shear forces

Figure 4.20: Influence of the loading amplitude on the response of the inclusions

(Figure 4.20-a) shows the seismic induced internal forces along the inclusions for different values of input accelerations (0.1g, 0.25g and 0.4g). It is notable that an increase in the loading amplitude from 0.25g to 0.4g correlates with a 75% rise in moments at a depth of 7 meters when compared to the reference model of 0.25g. On the other hand, a decrease in the loading amplitude from 0.25g to 0.1g results in a 69% reduction in moments at a depth of 7 meters.
While (Figure 4.20-b) represents the shear forces along the inclusion. Results shows that an increase in the loading amplitude from 0.25g to 0.4g results in an increase of 105% at 7 meters depth. While a decrease in the loading amplitude from the reference case 0.25g to 0.1g causes an 81% reduction in shear forces at the same depth.

To enhance our comprehension of the influence of the load amplitude and to clarify the effect of non-linearity, (Figure 4.20-c-d) show the dimensionless profile of internal forces M* and V* using the same normalization technique outlined in (section 4.4.1). It is notable that by normalizing moments [$M^*=M/\rho D^4 ag$] and shear forces [$T^*=T/\rho D^3 ag$], the curves converge towards the reference curve of 0.25g. Furthermore, the maximum moment within the inclusion under a load amplitude of 0.4g exhibits a reduction of approximately 5.5% compared to the peak achieved in the reference case.

The non-linearity effect and the interaction between the soil and the inclusion can be the reason of this variations. The increase in loading amplitude is responsible for the rise in plasticity, which in turn increases damping within the soil. Normally, this should result in a reduction of forces. However, the frequency can also be considered as a third factor that comes into play, it can be either the system's own frequency or the frequency of the applied load. Usually, the frequency drops when the system degrades causing a shift in frequency, which, in turn, leads to changes in the system's modes. Moreover, when the dynamic load frequency closely aligns with the system's frequency, the response amplification is more pronounced.

To gain a deeper understanding of the frequency's effect and to observe the vibration modes, (Figure 4.21) depicts the moment variation for each loading amplitude at different instances corresponding to the maximum moments reached. The maximum moments were reached at t = 3.15s for the 0.1g and 0.4g cases and at t=2.5s for the 0.4g case. It can be noticeable that the moments curve shape of the 0.1g case refers to the first mode while for the other cases, it rather refers to a combination between the first and second mode which highlights a modification of the frequency response of system with the increase of non-linearity level.

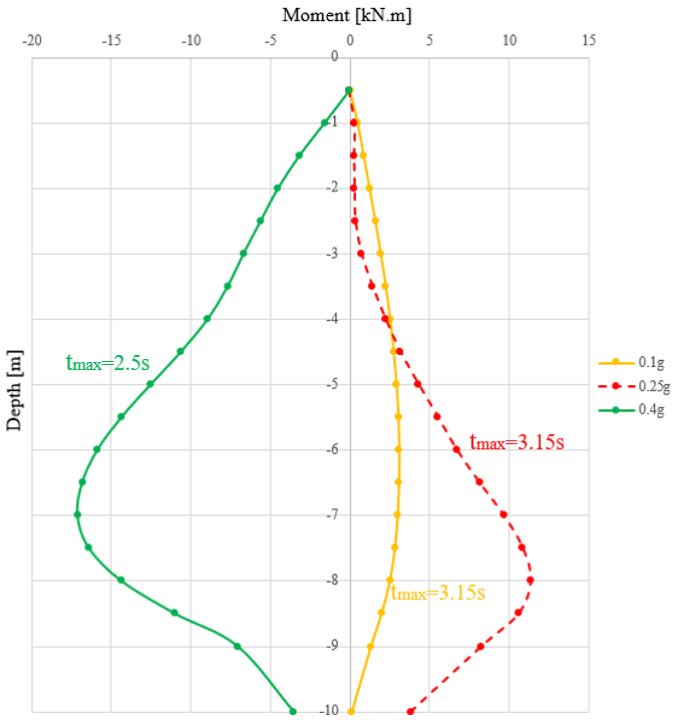

Figure 4.21: Bending Moment along the Central Rigid Element for the Instant in which the Moment Envelope is Maximal

4.5 Conclusion

In conclusion, this chapter has conducted a non linear detailed three-dimensional analysis of the soil-mattress-inclusions system using Finite Difference method. The study used a step-by-step approach to gradually improve the model's complexity. Starting with a simple linear elastic model for the entire system, then introducing the Mohr Coulomb model in the mattress, in the soil and both in the soil and mattress. Furthermore, the investigation was extended to include the analysis of a system including a shallow raft foundation.

The results of the numerical simulations show that the motion experienced at the surface of the mattress is notably changed by the soil behaviors, and foundation. For the analyzed cases, the velocity recorded at the ground surface are greater compared to the ones of the input motion. The results also show that the nonlinearities in the system influence its seismic induced response of the soil-inclusion system. The analyzed cases show that when the elasto-plastic approach is employed to model the soil behavior, the moments and shear forces are significantly greater, providing a more accurate representation of the soil's actual behavior, considering its plastic behavior. These values obtained from the elasto-plastic analysis are more reliable than those derived from the linear elastic case. The implementation of the raft foundation resulted in a decrease in shear forces and moments. The analysis of results emphasizes that introducing the soil non-linearity in seismic analysis will not necessarily lead to a decrease of the resulting internal forces, the response of the system is also dependent on the soil condition at the interface of soil-inclusion.

The study highlights the influence of the cover ratio on the outcomes. Results show that the internal forces resulting from the kinematic interaction within the inclusions increase with increasing the cover ratio. A higher cover ratio provides better confinement to the inclusion and increase its contact with the soil. The moment resulting from kinematic interaction is primarily linked to inertia, and therefore strongly dependent on the diameter, and may partially account for the observed outcomes.

The normalized results reveal that increasing the diameter of the inclusion leads to a reduction in internal forces. This reduction is primarily attributed to the enhanced kinematic interaction, resulting in greater energy dissipation, particularly at the interface between the inclusion and the soil. This establishes the presence of non-linearity.

The study shows that the position of the rigid inclusion has an influence on the response of the system and the load distribution is affected by their positions. Adding to that the increase of the overload over the raft produces greater internal forces along the rigid element.

When studying the influence of the load amplitude, a notable reduction is observed in the normalized bending moment and shear forces along the vertical rigid inclusion. However, a reduction by approximately 5.5% has occurred when comparing the maximum bending moment of the load amplitudes of 0.25g and 0.4g. The results indicate that an increase in loading amplitude results in increased plasticity, subsequently causing a reduction in dynamic amplification through energy dissipation. In order to correctly analyze these results, three effects must be taking into account: the nonlinearity, the plasticity of the soil and the interaction between the rigid element and the soil as well as the frequency whether the frequency of the entire system or the frequency of the loading.

GENERAL CONCLUSIONS

The objective of this study was to investigate the behavior of soil reinforced with rigid inclusions under dynamic loading conditions using 3D numerical modeling approaches. Apart from the literature review, the research is divided into two main chapters. The first chapter has focused on analyzing the system and its kinematic interaction under seismic loading, while the second chapter has examined the influence of nonlinearities in the model, as well as the presence of the raft foundation, on the response of the system. Three-dimensional modeling approaches incorporating both finite element and finite difference methods were employed for this research. The study examined the impacts of various parameters on the system response, including soil characteristics, mattress properties, dimensions, and placement of the inclusions, as well as the influence of the raft and the applied load.

The concept of rigid inclusions and their various applications was presented, through the literature review. In order to investigate the kinematic and inertial interactions, different methodologies were discussed, such as numerical, analytical, and experimental techniques. Additionally, previous research studies comparing and analyzing the response of pile foundations and rigid inclusions under dynamic loading conditions were also explored.

Based on the literature review, it can be concluded that the utilization of rigid inclusions for soil reinforcement provides several benefits for construction in seismic zones. This reinforcement approach acts as a base isolation mechanism for the structure, under seismic loading. The transfer mattress serves as a zone for energy dissipation, facilitating the dissipation of energy between the structure and the rigid elements. Consequently, it reduces the transmission of soil motion to the structure and limits the transfer of inertial forces to the soil-inclusions system.

In this thesis, a preliminary analysis was conducted to investigate the influence of the rigid inclusion modelling techniques on the response of a single rigid inclusion model. The first technique, known as the pile void method, represents the inclusion by beam element placed at the center of a void element. The second technique, referred to as the beam element method, exclusively utilizes beam elements to model the inclusion.

The obtained results indicate that utilizing a beam element to model the rigid inclusion produces similar outcomes as the pile void method, particularly for smaller dimensions. This observation simplifies the meshing process in the comprehensive 3D model, which includes a parametric investigation conducted on a group of 25 rigid inclusions modelled by beam elements. The parameters investigated included the inclusions diameter, length, and position. As well as soil and mattress mechanical properties especially their stiffness. The calculations were performed using linear elastic constitutive model.

The findings indicated that the rigid inclusions closely follow the motion of the soil, with only slight deviations observed near the head area where the load transfer mattress has a subtle influence on the deformation of the inclusions. The results suggested that larger diameters of the rigid inclusions lead to increase displacements of the inclusion head and increase internal forces in the inclusion.

Increasing the rigidity of the soil brings about a reduction in the internal forces acting on the rigid inclusions. This outcome could be attributed to the presence of stiffer soil surrounding the inclusions, providing lateral support. However, the influence of mattress rigidity on the system behavior was moderate, particularly in the first three meters of the inclusions. A higher level of mattress rigidity causes an increase in the bending moments and shear forces experienced at the head of the inclusions.

The results obtained by varying the length of the inclusions highlight the significance of having an appropriate length for the inclusion to effectively fulfill its intended purpose. Regarding their positions, the findings demonstrated that the inclusion with the least amount of stress is situated at the center, while the dynamic forces progressively increase from the center towards the edge of the group.

The second phase of the study was dedicated to examining the impacts of nonlinear behavior of the system using the linear elastic perfectly plastic constitutive model with Mohr Coulomb failure criteria to represent the behavior of the soil and the mattress, along with the presence of the raft foundation. The study followed a step-by-step approach, beginning with a linear elastic model for the entire system, then incorporating the Mohr Coulomb in the mattress, then in both soil and mattress, and finally considering the same conditions as before but with the addition of

a shallow foundation. The present work was conducted using the finite difference method for a group of 9 rigid inclusions.

The results show that the nonlinear behavior of the system influence its outcomes. The analyzed cases showed that when the linear elastic perfectly plastic with Mohr-Coulomb failure criteria model is employed, the moments and shear forces were significantly greater, providing a more accurate representation of the soil's actual behavior, considering its plastic deformation. These values obtained from the nonlinear analysis were more reliable than those derived from the linear analysis. The implementation of the raft foundation resulted in a decrease in shear forces and moments.

These case studies have highlighted the importance of considering the nonlinear behavior of the system by employing a suitable constitutive model to evaluate internal forces within the inclusions, allowing for a better consideration of the material behaviors and providing more accurate predictions in more complex scenarios. These studies have indicated that when modeling the mattress alone, using nonlinear behavior, it resulted in similar variations to those obtained with the linear model. However, it is important to highlight the importance of considering the nonlinear behavior of the entire system including the soil, rather than solely focusing on the mattress.

The influence of the cover ratio on the response of the system was also studied. The normalized results reveal that increasing the cover ratio leads to a reduction in the internal forces. This reduction is primarily attributed to the enhanced kinematic interaction, resulting in greater energy dissipation, particularly at the interface between the inclusion and the soil. This establishes the presence of non-linearity. The increase of the overload applied to the raft has also resulted in higher internal forces along the rigid element.

The final parametric study concerning the influence of the load amplitude, show a notable reduction in the normalized bending moment and shear forces along the vertical rigid inclusion. However, a reduction by approximately 5.5% has occurred when comparing the maximum bending moment of the load amplitudes of 0.25g and 0.4g. The results indicate that an increase in loading amplitude results in increased plasticity, subsequently causing a reduction in dynamic amplification through energy dissipation. In order to correctly analyze these results, three effects must be taking into account: the nonlinearity, the plasticity of the soil and the

interaction between the rigid element and the soil as well as the frequency whether the frequency of the entire system or the frequency of the loading.

SUGGESTIONS FOR FURTHER RESEARCH WORKS

The current study has been conducted under specific loading conditions, investigating the seismic response of rigid inclusions. To enhance our comprehension, future exploration of this issue with diverse load records would be valuable. This would enable us to delve deeper into the influence of the loading's frequency content on the inclusion's behavior. Furthermore, extending the scope of this research to include more sophisticated constitutive models could provide more comprehensive insights, contingent upon the availability of experimental data, and the validation through centrifuge testing and vibration table experiments.

As this study exclusively focused on a single soil type, there lies a necessity to broaden our understanding. Including various soil configuration setups is imperative for a comprehensive understanding of the inclusion's behavior. Alongside this, considering interfaces between different components of the system holds equal importance.

Beyond examining the soil, other important aspects remain to be investigated. For instance, incorporating a superstructure into the system could reveal new insights. Additionally, the study of inertial interactions within the system holds potential for enriching our understanding and would also be beneficial areas for future research.

REFERENCES:

Abdullah, C.H., Edil, T.B., 2007. Behaviour of geogrid-reinforced load transfer platforms for embankment on rammed aggregate piers. Geosynth. Int. 14, 141–153. https://doi.org/10.1680/gein.2007.14.3.141

Alsaleh, H., 2007. Modélisation non-linéaire en trois dimensions de l'interaction sol-micropieux-pont sous chargements sismiques. Université des Sciences et Technologies de Lille, France.

Ambrosini, R.D., 2006. Material damping vs. radiation damping in soil–structure interaction analysis. Comput. Geotech. 33, 86–92. https://doi.org/10.1016/j.compgeo.2006.03.001

ASIRI, 2012. Recommandations pour la conception, le dimensionnement, l'exécution et le contrôle de l'amélioration des sols de fondations par inclusions rigides.

ASTM D3999-91, 2003. Standard Test Methods for the Determination of the Modulus and Damping Properties of Soils Using the Cyclic Triaxial Apparatus. West Con-Shohocken PA Annu. Book ASTM Stand. ASTM Int.

ASTM-D5311, 2011. Standard Test Method for Load Controlled Cyclic Triaxial Strength of Soil. West Con-Shohocken PA Annu. Book ASTM Stand. ASTM Int.

Aubry, D., 1986. Une approche intégrée de l'interaction sismique sol-structure, journées communes fondations, propriété des sols et impératifs sismiques, cfms-afps. Rev. Fr. Géotechnique 81–100.

Balfour, B., 2013. Vibro Concrete Columns. Available at: http://www.balfourbeatty.com/media/28611/vcp-bbge-web.pdf.

Banerjee, S., Goh, S.-H., Lee, F.-H., 2014. Earthquake-induced bending moment in fixed-head piles in soft clay. Géotechnique 64, 431–446.

Barani, S., De Ferrari, R., Ferretti, G., 2013. Influence of Soil Modeling Uncertainties on Site Response. Earthq. Spectra 29, 705–732. https://doi.org/10.1193/1.4000159

Barton, Y.O., Pande, G.N., 1982. Laterally loaded piles in sand: centrifuge tests and finite element analyses. Presented at the Numerical Models in Geomechanics, pp. 749–758.

Baudouin, G., 2010. Sols renforcés par inclusions rigides : modélisation physique en centrifugeuse de remblais et de dallage (These de doctorat). Nantes.

Benz, T., 2007. Small-Strain Stiffness of Soils and its Numerical Consequences (PHD Thesis). Univesity of Stuttgart.

Berthelot, P., Pezot, B., Liausu, Ph., 2003. Amélioration des sols naturels ou anthropiques par colonnes semi- rigides : Le procédé CMC. Presented at the Eds. Proc. of the 13th European Conf. on Soil Mechanics and geotechnical Engineering (XIII ECSMGE), Praga, pp. 25–29.

Billaux, D., Cundall, P., 1993. Simulation des géomatériaux par la méthode des éléments Lagrangiens. Rev. Fr. Géotechnique 9–21. https://doi.org/10.1051/geotech/1993063009

Bonab, M.H.A., 2003. Modélisation physique et numérique d'un pieu isolé dans du sable soumis à un impact latéral en tête (These de doctorat). Université de Caen.

Boulanger, R.W., Curras, C.J., Kutter, B.L., Wilson, D.W., Abghari, A., 1999. Seismic Soil-Pile-Structure Interaction Experiments and Analyses. J. Geotech. Geoenvironmental Eng. 125, 750–759. https://doi.org/10.1061/(ASCE)1090-0241(1999)125:9(750)

Briançon, L., 2002. Renforcement des sols par inclusions rigides - Etat de l'art. REX, Paris, p. 185.

Briançon, L., Kastner, R., Simon, B., Dias, D., 2004. Etat des connaissances-Amélioration des sols par inclusions rigides. Proc Int Symp Ground Improv. 15–44.

Briançon, L., Simon, B., 2012. Performance of Pile-Supported Embankment over Soft Soil: Full-Scale Experiment. J. Geotech. Geoenvironmental Eng. 138, 551–561. https://doi.org/10.1061/(ASCE)GT.1943-5606.0000561

Cai, Y.X., Gould, P.L., Desai, C.S., 2000. Nonlinear analysis of 3D seismic interaction of soil–pile–structure systems and application. Eng. Struct. 22, 191–199. https://doi.org/10.1016/S0141-0296(98)00108-4

chang, G.S., Kutter, B.L., 1998. Centrifugal Modeling of Soil-Pile-Structure Interaction. Presented at the 25th Symposium on Engineering Geology and Geotechnical Engineering.

Chenaf, N., 2007. Interaction inertielle et interaction cinématique sol - pieu (These de doctorat). Nantes.

Christian, J.T., Desai, C.S., 1977. Numerical methods in geotechnical engineering. N. Y. McGraw-Hill.
Chu, D., Truman, K.Z., 2004. Effects of pile foundation configurations in seismic soil-pile-structure interaction. Presented at the 13th World Conference on Earthquake Engineering, Vancouver, B.C., Canada.
Chung, Y., 2000. Etude Numérique de L'interaction Sol-Pieu-Structure Sous Chargement Sismique. (These de doctorat). Université des Sciences et Technologie de lille.
Clough, R.W., Penzien, J., 1975. Dynamics Of Structures. Second Edi. McGraw-Hill.
Collin, J.G., 2004. Column supported embankment design considerations. Presented at the LABUZ J. F., BENTLER J.G. Eds. Proc. of the 52nd Annual Geotechnical Engineering Conf., University of Minnesota, Minneapolis, pp. 51–78.
Combault, J., Pecker, A., 2000. Rion-Antirion Bridge, Greece – Concept, Design, and Construction. Struct. Eng. Int. 22–27.
Dano, C., Hicher, P.-Y., Tailliez, S., 2004. Engineering Properties of Grouted Sands. J. Geotech. Geoenvironmental Eng. 130, 328–338. https://doi.org/10.1061/(ASCE)1090-0241(2004)130:3(328)
Darendeli, M., 2001. Development of a new family of normalized modulus reduction and material damping curves. (PHD Thesis). The University of Texas at Austin.
Deb, K., 2010. A mathematical model to study the soil arching effect in stone column-supported embankment resting on soft foundation soil. Appl. Math. Model. 34, 3871–3883. https://doi.org/10.1016/j.apm.2010.03.026
Dobry, R., O' Rourke, M.J., 1983. Discussion on `Seismic response of end-bearing piles' by Flores-Berrones, R., Whitman, R. V. J. Geotech. Eng. Div. 109 778.
Dobry, R., Pecker, A., Mavroeidis, G., Zeghal, M., Gohl, B., Yang, D., 2003. Damping/global energy balance in FE model of bridge foundation lateral response. Soil Dyn. Earthq. Eng. 23, 483–495. https://doi.org/10.1016/S0267-7261(03)00050-2
Dou, H., Byrne, P.M., 1996. Dynamic response of single piles and soil-pile interaction. Can. Geotech. J. 33, 80–96. https://doi.org/10.1139/t96-025
Duncan, J.M., Chang, C.-Y., 1970. Nonlinear Analysis of Stress and Strain in Soils. J. Soil Mech. Found. Div. 96, 1629–1653.
El Naggar, M.H., Novak, M., 1996. Nonlinear analysis for dynamic lateral pile response. Soil Dyn. Earthq. Eng. 15, 233–244. https://doi.org/10.1016/0267-7261(95)00049-6
Eurocode EC8, 1998. Calcul des structures pour leur résistance aux séismes - Partie 5 : fondations, ouvrages de soutènement et aspects géotechniques.
Garnier, J., Pecker, A., 1999. Use of Centrifuge Tests for the Validation of Innovative Concepts in Foundation Engineering.
Gazetas, G., 1991. Foundation Engineering Handbook, Chapter 15. Fang H-Y (ed.), van Nostrand Reinhold: New York.
Gazetas, G., 1984. Seismic response of end-bearing single piles. Int. J. Soil Dyn. Earthq. Eng. 3, 82–93. https://doi.org/10.1016/0261-7277(84)90003-2
Gazetas, G., Mylonakis, G., 1998. Seismic soil-structure interaction: New evidence and emerging issues, in: Geotechnical Earthquake Engineering and Soil Dynamics. Geo-Institute ASCE Conference, Seattle, USA, pp. 1119–1174.
Giannakos, S., Gerolymos, N., Gazetas, G., 2012. Cyclic lateral response of piles in dry sand: Finite element modeling and validation. Comput. Geotech. 44, 116–131. https://doi.org/10.1016/j.compgeo.2012.03.013
Girout, R., 2014. Prise en compte des géosynthétiques de renforcement dans les mécanismes de transfert de charge d'un matelas granulaire sur inclusions rigides : Modélisation physique et numérique. (PhD Thesis). Centrale Nantes.
Goh, S.H., Zhang, L., 2017. Estimation of Peak Acceleration and Bending Moment for Pile-Raft Systems Embedded in Soft Clay Subjected to Far-Field Seismic Excitation. J. Geotech. Geoenvironmental Eng. 143, 04017082. https://doi.org/10.1061/(ASCE)GT.1943-5606.0001779
Guide AFPS/CFMS, 2013. Procédés d'amélioration et de renforcement des sols sous actions sismiques.

Han, J., Gabr, M.A., 2002. Numerical Analysis of Geosynthetic-Reinforced and Pile-Supported Earth Platforms over Soft Soil. J. Geotech. Geoenvironmental Eng. 128, 44–53. https://doi.org/10.1061/(ASCE)1090-0241(2002)128:1(44)
Hatem, A., 2009. Comportement en zone sismique des inclusions rigides: Analyse de l'interaction sol-inclusion-matelas de répartition-structure. (These de doctorat). Université des Sciences et Technologies de Lille, France.
Hazzar, L., Hussien, M.N., Karray, M., 2017. Influence of vertical loads on lateral response of pile foundations in sands and clays. J. Rock Mech. Geotech. Eng. 9, 291–304. https://doi.org/10.1016/j.jrmge.2016.09.002
Hetenyi, M., 1946. Beams on Elastic Foundations. The University of Michigan Press.
Hill, R., 1950. The Mathematical Theory of Plasticity, Clarendon. Oxford, 613, 614.
Hokmabadi, A.S., Fatahi, B., 2016. Influence of Foundation Type on Seismic Performance of Buildings Considering Soil–Structure Interaction. Int. J. Struct. Stab. Dyn. 16, 1550043. https://doi.org/10.1142/S0219455415500431
Hudson, M., Idriss, I.M., Beikae, M., 1994. QUAD4M – A computer program to evaluate the seismic response of soil structures using finite element procedures and incorporating a compliant base. Cent. Geotech. Model. Dept Civ. Environ. Eng. UC Davis.
Idriss, I.M., Lysmer, J., Hwang, R., Seed, H.B., 1975. A computer program for evaluating the seismic response of soil structures by variable damping finite element procedures. University of California, Berkeley, pp. 73–16.
Ishihara, K., 1996. Soil Behavior in Earthquake Geotechnics. Oxford Engineering Science Series.
Itasca, 2022. FLAC 3D Version 7.0, Online Manual.
Jakrapiyanun, W., 2002. Physical modeling of dynamics soil-foundation-structure-interaction using a laminar container. (PHD Thesis). University of California, San Diego.
Jenck, O., Dias, D., Kastner, R., 2005. Soft Ground Improvement by Vertical Rigid Piles Two-Dimensional Physical Modelling and Comparison with Current Design Methods. Soils Found. 45, 15–30. https://doi.org/10.3208/sandf.45.15
Jennings, K., Naughton, P.J., 2012. Similitude Conditions Modeling Geosynthetic-Reinforced Piled Embankments Using FEM and FDM Techniques. Int. Sch. Res. Not. 2012, 1–16. https://doi.org/10.5402/2012/251726
Kausel, E., Whitman, R.V., Morray, J.P., Elsabee, F., 1978. The spring method for embedded foundations. Nucl. Eng. Des. 48, 377–392. https://doi.org/10.1016/0029-5493(78)90085-7
Kaynia, A.M., 1982. Dynamic stiffness and seismic response of pile groups (PHD Thesis). Cambridge, Massachusetts: Department of Civil Engineering.
Kempfert, H.G., 2003. Ground improvement methods with special emphasis on column-type techniques. Presented at the VERMEER P. A., SCHWEIGER H., KARSTUNEN M., CUDNY M. Eds. Proc. of the Int. Workshop on Geotechnics of Soft Soils - Theory and Practice, 17-19 septembre 2003, Noordwijkerhout, Pays-bas. Essen : Verlag Glückauf, pp. 101–112.
Kokusho, T., Yoshida, Y., Esashi, Y., 1982. Dynamic Properties of Soft Clay for Wide Strain Range. Soils Found. 22, 1–18. https://doi.org/10.3208/sandf1972.22.4_1
Koltuniuk, R., Percell, P., Mills-Bria, B., 2013. State-of-practice for the nonlinear analysis of concrete dams. Bureau of Reclamation.
Kourkoulis, R., Gelagoti, F., Anastasopoulos, I., 2012a. Hybrid Method for Analysis and Design of Slope Stabilizing Piles. J. Geotech. Geoenvironmental Eng. 138, 1–14. https://doi.org/10.1061/(ASCE)GT.1943-5606.0000546
Kourkoulis, R., Gelagoti, F., Anastasopoulos, I., Gazetas, G., 2012b. Hybrid Method for Analysis and Design of Slope Stabilizing Piles. J. Geotech. Geoenvironmental Eng. 138.
Kramer, S., 1996. Geotechnical earthquake engineering., Prentice-Hall 1st edition. ed. New Jersey, United States of America.
Kuhlemeyer, R.L., Lysmer, J., 1973. Finite Element Method Accuracy for Wave Propagation Problems. J. Soil Mech. Found. Div. 99, 421–427.
Kumar, A., Choudhury, D., Katzenbach, R., 2016. Effect of Earthquake on Combined Pile–Raft Foundation. Int. J. Geomech. 16, 04016013. https://doi.org/10.1061/(ASCE)GM.1943-5622.0000637

Kwok, A.O.L., Stewart, J.P., Hashash, Y.M.A., Matasovic, N., Pyke, R., Wang, Z., Yang, Z., 2007. Use of Exact Solutions of Wave Propagation Problems to Guide Implementation of Nonlinear Seismic Ground Response Analysis Procedures. J. Geotech. Geoenvironmental Eng. 133, 1385–1398. https://doi.org/10.1061/(ASCE)1090-0241(2007)133:11(1385)

Lade, P.V., 2005. Overview of Constitutive Models for Soils. In Soil constitutive models: Evaluation, selection, and calibration, 1–34.

Liausu, Ph., Pezot, B., 2001. Reinforcement of soft soils by means of controlled modulus columns. Presented at the XVth International Conference of Soil Mechanics and Geotechnical Engineering (ICSMGE), Istanbul, Turkey, pp. 1613–1618.

Lila, M., 2021. Etude expérimentale et numérique du comportement hydromécanique des sols résiduels tropicaux : application à la modélisation sismique d'un barrage en remblai aux Antilles (These de doctorat). Université Aix-Marseille.

Liu, H.L., Ng, C.W.W., Fei, K., 2007. Performance of a Geogrid-Reinforced and Pile-Supported Highway Embankment over Soft Clay: Case Study. J. Geotech. Geoenvironmental Eng. 133, 1483–1493. https://doi.org/10.1061/(ASCE)1090-0241(2007)133:12(1483)

Liu, H.S., Chen, k. J., 1991. Test on Behavior of Pile Foundation in Liquefiable Soils. Presented at the Second International Conference on Recent Advances in Geotechnical Earthquake Engineering & Soil Dynamics, St. Louis, pp. 233–235.

Lopez Jimenez, G.A.L., 2019. Static and Dynamic behaviour of pile supported structures in soft soil (PHD Thesis). Université Grenoble Alpes.

Lu, X., Li, P., Chen, B., Chen, Y., 2005. Computer simulation of the dynamic layered soil-pile-structure interaction system. Can. Geotech. J. 42, 742–751.

Lu, X., Li, P., Chen, Y., Chen, B., 2004. Shaking Table Model Testing on Dynamic Soil-Structure-Interaction System. Presented at the 13th World Conference on Earthquake Engineering, Vancouver, B.C., Canada, p. 194.

Lysmer, J., Kuhlemeyer, L., 1969. Finite Dynamic Model for Infinite Media. J. Eng. Mech. Div. ASCE 95 859-878.

Maheshwari, B.K., Truman, K.Z., El Naggar, M.H., Gould, P.L., 2004. Three-dimensional nonlinear analysis for seismic soil–pile-structure interaction. Soil Dyn. Earthq. Eng. 24, 343–356. https://doi.org/10.1016/j.soildyn.2004.01.001

Mandel, J., 1962. Essais sur modèle réduits en mécanique des terrains. Etude des conditions de similitude. Rev Ind Minérale 273–295.

Mánica, M., Ovando, E., Botero, E., 2014. Assessment of damping models in FLAC. Comput. Geotech. 59, 12–20. https://doi.org/10.1016/j.compgeo.2014.02.007

Mánica Malcom, M.Á., Ovando-Shelley, E., Botero Jaramillo, E., 2016. Numerical Study of the Seismic Behavior of Rigid Inclusions in Soft Mexico City Clay. J. Earthq. Eng. 20, 447–475. https://doi.org/10.1080/13632469.2015.1085462

Mayoral, J.M., 2006. Effect of layered clay deposits on the seismic behavior of a rigid inclusion. Proceedings of the Symposium of Rigid Inclusions in Difficult Subsoil Conditions, ISSMGE TC36, Sociedad Mexicana de Mecanica de Suelos. pp. 11–12.

Messioud, S., Okyay, U.S., Sbartai, B., Dias, D., 2016. Dynamic Response of Pile Reinforced Soils and Piled Foundations. Geotech. Geol. Eng. 34, 789–805. https://doi.org/10.1007/s10706-016-0003-0

Meymand, P.J., 1998. Shaking table scale model tests of nonlinear soil-pile-superstructure interaction in soft clay. University of California, Berkeley.

Mezeh, R., Sadek, M., Hage Chehade, F., Mroueh, H., 2018. Adaptive meshing scheme for prediction of high-speed moving loads induced ground vibrations. Comput. Geotech. 100, 188–202. https://doi.org/10.1016/j.compgeo.2018.03.014

Miura, F., 2002. Some typical Examples of Damage to Pile Foundation by the 1995 Hyogoken Nambu earthquake. Presented at the International Workshop on Micropiles - IWM, Venice, Italy.

Nghiem, H., Nien-Yin, C., 2008. Soil-structure interaction effects of high rise buildings. Presented at the 6th International Conference on Case Histories in Geotechnical Engineering, pp. 11–16.

Nikolaou, S., Mylonakis, G., Gazetas, G., Tazoh, T., 2001. Kinematic pile bending during earthquakes: analysis and field measurements. Géotechnique 51, 425–440. https://doi.org/10.1680/geot.2001.51.5.425

Novak, M., Aboul-Ella, F., 1978. Impedance Functions of Piles in Layered Media. J. Eng. Mech. Div. 104, 643–661. https://doi.org/10.1061/JMCEA3.0002366
Nunez, M.A., Briançon, L., Dias, D., 2013. Analyses of a pile-supported embankment over soft clay: Full-scale experiment, analytical and numerical approaches. Eng. Geol. 153, 53–67. https://doi.org/10.1016/j.enggeo.2012.11.006
OKYAY, U.S., 2015. Sols renforcés par inclusions rigides: etude expérimentale et numérique des transferts de charge. Ed. Univ. Eur.
Okyay, U.S., Dias, D., Billion, P., Vandeputte, D., Courtois, A., 2012. Impedance Functions of Slab Foundations with Rigid Piles. Geotech. Geol. Eng. 30, 1013–1024. https://doi.org/10.1007/s10706-012-9523-4
Okyay, U.S., Dias, D., Thorel, L., Rault, G., 2014. Centrifuge Modeling of a Pile-Supported Granular Earth-Platform. J. Geotech. Geoenvironmental Eng. 140, 1–12.
Park, D., Hashash, Y.M.A., 2004. Soil damping formulation in nonlinear time domain site response analysis. J. Earthq. Eng. 8, 249–274. https://doi.org/10.1142/S1363246904001420
Paultre, P., 2018. Dynamique des structures : application aux ouvrages de génie civil. Troisième édition. – éd. Montréal : Presses internationales Polytechnique.
Pecker, A., 1984. Dynamique des sols. Presse, ENPC, Paris, France.
Pecker, A., Salencon, J., 1999. Ground Reinforcement in Seismic Aeras. Presented at the Soil Mech. and Geotech. Eng., Iguasu, pp. 799–808.
Pecker, A., Teyssandier, J.P., 1998. Seismic design for the foundations of the rion antirion bridge. Proc. Inst. Civ. Eng. - Geotech. Eng. 131, 4–11. https://doi.org/10.1680/igeng.1998.30001
Phillips, C., Hashash, Y.M.A., 2009. Damping formulation for nonlinear 1D site response analyses. Soil Dyn. Earthq. Eng. 29, 1143–1158. https://doi.org/10.1016/j.soildyn.2009.01.004
Pitilakis, D., Dietz, M., Wood, D.M., Clouteau, D., Modaressi, A., 2008. Numerical simulation of dynamic soil–structure interaction in shaking table testing. Soil Dyn. Earthq. Eng. 28, 453–467. https://doi.org/10.1016/j.soildyn.2007.07.011
Rangel-Núñez, J.L., Gómez-Bernal1, A., Aguirre-González, J., Sordo-Zabay, E., Ibarra-Razo, E., 2008. Dynamic response of soft soil deposits improved with rigid inclusions. Presented at the 14th World Conference on Earthquake Engineering (14WCEE), pp. 1–8.
Rathje, E.M., Bray, J.D., 2001. One- and two-dimensional seismic analysis of solid-waste landfills. Can. Geotech. J. 38, 850–862. https://doi.org/10.1139/t01-009
Romo, M.P., 1995. Clay Behavior, Ground Response and Soil-Structure Interaction Studies in Mexico City. Int. Conf. Recent Adv. Geotech. Earthq. Eng. Soil Dyn. 1039–1051.
Rovithis, E.N., Pitilakis, K.D., Mylonakis, G.E., 2009. Seismic analysis of coupled soil-pile-structure systems leading to the definition of a pseudo-natural SSI frequency. Soil Dyn. Earthq. Eng. 29, 1005–1015. https://doi.org/10.1016/j.soildyn.2008.11.005
Sadek, M., 2003. Etude numérique du comportement des micropieux sous chargement sismique: Analyse de l'effet de groupe et de l'inclinaison (These de doctorat). Université des sciences et technologies de Lille.
Sadek, M., Shahrour, I., 2004. A three dimensional embedded beam element for reinforced geomaterials. Int. J. Numer. Anal. Methods Geomech. 28, 931–946. https://doi.org/10.1002/nag.357
Semblat, J.F., Pecker, A., 2009. Waves and vibrations in soils: earthquakes, traffic, shocks, construction works. IUSS Press, Pavia.
Shahrour, I., Alsaleh, H., Souli, M., 2012. 3D elastoplastic analysis of the seismic performance of inclined micropiles. Comput. Geotech. 39, 1–7. https://doi.org/10.1016/j.compgeo.2011.08.006
Shahrour, I., Ousta, R., Chung, Y.S., 2000. Modélisation Tridimensionnelle du Comportement Sismique des Sols Renforcés par Micropieux. Presented at the 3ème Coll. int. "Prédiction et Réduction de l`aléa Sismique," Algerie.
Shahrour, I., Sadek, M., Ousta, R., 2001. Seismic Behavior of Micropiles: Used as Foundation Support Elements: Three-Dimensional Finite Element Analysis. Transp. Res. Rec. J. Transp. Res. Board 1772, 84–90. https://doi.org/10.3141/1772-10
Sieffert, J.-, Cevaer, F., 1992. MANUEL DES FONCTIONS D'IMPEDANCE - FONDATIONS SUPERFICIELLES. Ouest ed. Presses Académiques.

Sreerama, K., 1993. Dynamic pile-soil-pile interaction using model tests under simulated earthquakes. (PHD Thesis). University of Missouri-Rolla.
Suwal, S., Pagliaroli, P., Lanzo, G., 2014. Comparative study of 1D codes for Site Response Analyses. Int. J. Landslide Environ. 2, 24–31.
Terzaghi, K., 1943. Theoretical soil mechanics. N. Y. John Wiley Sons.
Tsai, C.-C., Park, D., Chen, C.-W., 2014. Selection of the optimal frequencies of viscous damping formulation in nonlinear time-domain site response analysis. Soil Dyn. Earthq. Eng. 67, 353–358. https://doi.org/10.1016/j.soildyn.2014.10.026
Van Nguyen, Q., Fatahi, B., Hokmabadi, A.S., 2017. Influence of Size and Load-Bearing Mechanism of Piles on Seismic Performance of Buildings Considering Soil–Pile–Structure Interaction. Int. J. Geomech. 17, 04017007. https://doi.org/10.1061/(ASCE)GM.1943-5622.0000869
Vucetic, M., Dobry, R., 1991. Effect of Soil Plasticity on Cyclic Response. J. Geotech. Eng. 117, 89–107. https://doi.org/10.1061/(ASCE)0733-9410(1991)117:1(89)
Watanabe, K., Pisanò, F., Jeremić, B., 2017. Discretization effects in the finite element simulation of seismic waves in elastic and elastic-plastic media. Eng. Comput. 33, 519–545. https://doi.org/10.1007/s00366-016-0488-4
Wilson, D.W., 1998. Soil-pile-superstructure interaction in liquefying sand and soft clay. University of California at Davis.
Winkler, E., 1876. Die Lehre von der Elastizität und Festigkeit. Verlag, 182.
Wolf, J.P., 1988. Soil-Structure Interaction Analysis in time domain. Prentice Hall N. J. Englewood Cliffs.
Wolf, J.P., 1985. Dynamic Soil-Structure Interaction. Prentice-Hall Ed N. J. Englewood Cliffs.
Woodward, P.K., Griffiths, D.V., 1996. Influence of viscous damping in the dynamic analysis of an earth dam using simple constitutive models. Comput. Geotech. 19, 245–263. https://doi.org/10.1016/0266-352X(96)00002-X
Wotherspoon, L.M., 2006. Three dimensional pile finite element modelling using OpenSees. Presented at the NZSEE Conference.
Wu, G., Finn, W., 1997. Dynamic nonlinear analysis of pile foundations using finite element method in the time domain. Can. Geotech. J. 34, 44–52. https://doi.org/10.1139/t96-088
Xu, R., Fatahi, B., 2018. Effects of Pile Group Configuration on the Seismic Response of Buildings Considering Soil-Pile-Structure Interaction. Proc. GeoShanghai 2018 Int. Conf. Adv. Soil Dyn. Found. Eng. 279–287. https://doi.org/10.1007/978-981-13-0131-5_31
Zhang, J., Jenck, O., Dias, D., 2022. 3D Numerical Analysis of a Single Footing on Soft Soil Reinforced by Rigid Inclusions. Int. J. Geomech.